NOVEL INVESTIGATIONS TO CLASSIFY FETAL GROWTH RESTRICTION IN OVINE MODELS OF REPRODUCTIVE HEALTH

A Dissertation

by

COLLEEN ANNE LAMBO

Submitted to the Office of Graduate and Professional Studies of
Texas A&M University
in partial fulfillment of the requirements for the degree of

DOCTOR OF PHILOSOPHY

Chair of Committee,	Shannon E. Washburn
Committee Members,	Fuller W. Bazer
	J. Jill Heatley
	Larry J. Suva
Head of Department,	Larry J. Suva

December 2020

Major Subject: Biomedical Sciences

ABSTRACT

Placental compromise or malnutrition during pregnancy are known risk factors for fetal growth restriction (FGR), causing developmental changes in offspring that can have lifelong health implications in many species. The ewe is a valuable model for human gestational research regarding FGR, as well as an agricultural resource that is also afflicted by FGR. This one-health mission necessarily prioritizes the needs of animal and medical researchers alike. Medical journals have called for a focus on placental pathophysiology, reflecting that 60% of FGR cases in humans are idiopathic, and inconsistently overlapping pathophysiology and varied severity appear to be at play in those with known causes. Focusing on individual etiopathologies has made a significant impact on the field but may represent a missed opportunity to identify underlying commonalities, particularly the progression of placental insufficiency. To address these concerns, we developed a novel surgical procedure to allow placental sampling in early pregnancy without halting gestation, providing evidence of early placental compromise to be compared with subsequent fetal or offspring health. Sham, control, and test ewes fared well through surgery and recovery, and the removal of a singular and central placentome was determined to be achievable in this model. We also studied uterine and fetal tissue blood flow in a nutrient restriction model of FGR. Maternal hemodynamics were not affected. Fetal weights were variable, while fetal organ weights followed “brain sparing” growth patterns. Renal and pancreatic tissue blood flow was lower in undernourished ewes. Cerebral and cardiac blood flow correlated positively with fetal weight. Finally, we assessed serum concentrations of anti-Müllerian hormone in ewes through estrous and

controlled ovarian stimulation to establish baselines and comparisons for FGR research and improved industry sheep production. Anti-Müllerian hormone concentrations at various time points were correlated with ovarian response to stimulation. However, variability was too high to rely on singular samples, and ewe baselines need to be better established before measurements of anti-Müllerian hormone can be a valuable resource for sheep. These results will offer new tools and knowledge of the pathophysiologic changes behind FGR, as well as the hormonal events relevant to our top one-health model.

ACKNOWLEDGEMENTS

I am incredibly grateful for my committee chair, Dr. Washburn, and my committee members, Dr. Bazer, Dr. Heatley, and Dr. Suva, for their guidance and support throughout the course of this project. The support and instruction from Dr. Hinrichs as my AFF advisor was also sincerely appreciated.

I am indebted to my colleagues and friends, and my Zoom study group, without whom I would not have survived the late nights and apocalyptic times. Thank you all for your love and support!

CONTRIBUTORS AND FUNDING SOURCES

Contributors

This work was supervised by a dissertation committee consisting of Dr. Washburn and Dr. Suva (Department of Veterinary Physiology and Pharmacology), and Dr. Heatley (Department of Small Animal Clinical Sciences), all within the College of Veterinary Medicine & Biomedical Sciences, and Dr. Bazer (Department of Animal Science).

Surgical procedures depicted in Chapter 3 were conducted by Dr. Washburn as lead surgeon with Dr. Lambo assisting. Ms. Padgett from Dr. Washburn's lab was integral in surgical preparations.

The analyses depicted in Chapter 4 were conducted in part by Dr. Jacques of Applied Biosciences.

All other work conducted for the dissertation was completed by Dr. Lambo in collaboration with Dr Satterfield's research team in the Department of Animal Sciences.

Funding Sources

Graduate study was supported by an R01 grant from the Eunice Kennedy Shriver National Institute of Child Health and Human Development (grant number NIH 1R01HD080658-01A1). The analyses depicted in Chapter 4 were made possible through a Department of Animal Science Mini-Grant. The contents are solely the responsibility of the author and do not necessarily represent the official views of the National Institute of Health.

NOMENCLATURE

AE	All ewes
AFC	Antral follicle count
AGA	Appropriate for gestational age
AI	Artificial insemination
AMH	Anti-Müllerian hormone
ANOVA	Analysis of variance
BAT	Brown adipose tissue
BF	Blood flow
BP	Blood pressure
C	Control group
CIDR	Controlled internal drug release
CL	Corpus luteum
COS	Controlled ovarian stimulation
CQ	Control variables when compared to quartiles
CV	Coefficient of variation
d1	Serum sample prior to 1st day of COS injections
d3	Serum sample prior to 3rd day of COS injections
dAI	Serum sample prior to AI
dET	Serum sample prior to ET
DOHaD	Developmental origins of health and disease
EL	Ewe lamb group

ELH	Ewe lambs above 1.1 ng/ml cutoff
ELISA	Enzyme-linked immunosorbent assay
ELL	Ewe lambs below 1.1 ng/ml cutoff
ET	Embryo transfer
FGR	Fetal growth restriction
fMAP	Fetal mean arterial pressure
FSH	Follicle-stimulating hormone
GD	Gestational day
GWG	Gestational weight gain
HR	Heart rate
IM	Intramuscular
IUGR	Intrauterine growth restriction
IV	Intravenous
LD	Longissimus dorsi muscle
LQ	Lower quartile of fetal weights
ME	Mature ewe group
MEH	Mature ewes above 0.4 ng/ml cutoff
MEL	Mature ewes below 0.4 ng/ml cutoff
mHR	Maternal heart rate
mMAP	Maternal mean arterial pressure
mPP	Maternal pulse pressure
mS/D	Maternal systolic to diastolic ratio
NR	Nutrient restricted

NRC	National Research Council
NT	Neural tube
OR	Ovarian response
PGF2α	Prostaglandin F2α
PI	Ponderal index
Quart	Quartile comparison - ANOVA
ROC	Receiver-operating characteristic
SD	Standard deviation
SEM	Standard error of the mean
SGA	Small for gestational age
SH	Sham
Trt	Treatment comparison – using Student’s t-test
UABF	Uterine artery blood flow
UQ	Upper quartile of fetal weights
WHO	World Health Organization

TABLE OF CONTENTS

Page

LIST OF FIGURES

Page

LIST OF TABLES

Page

1. INTRODUCTION

1.1. Overview

Links between fetal undernutrition, small fetuses, and lifelong risks of cardiovascular disease and diabetes in humans were first described by Barker et al. [1] in a series of retrospective studies from periods of famine experienced in the Netherlands and England. Their observations, based primarily on fetal size and maturity at birth, revealed that small for gestational age (SGA; in the lowest 10th percentile for gestational age) fetuses were at greater risk for neonatal morbidity and mortality as well as lifetime health implications [2]. A further study of these principles led to the discovery of fetal growth restriction (FGR), which refers to pathological influences on a fetus that restrict it from reaching its genetic growth potential [3, 4]. The generally smaller size of FGR offspring led to the tendency to presume all SGA fetuses are growth restricted [5, 6]. Many [3, 4, 7, 8] human studies caution against failing to distinguish SGA from FGR, as treatments to reduce the impacts of FGR might be harmful to healthy fetuses that are constitutionally small [9, 10].

Malnutrition, multiple fetuses, high altitude, chronic disease and substance abuse such as smoking are some of the factors known to cause FGR. Experimental conditions including carunculectomy, hypoxia, heat stress, and uterine blood flow restriction can produce FGR through placental compromise in animal models. It is believed that placental responses are not only similar despite the differences in environmental factors, but physiologically more relevant to the fetal impact [11]. Treatment of FGR should therefore focus on the underlying pathology, as focusing on etiologies ignores intricate

commonalities and maternal contributions [4, 12]. Research using sheep as an animal model of pregnancy has made progress in finding explanations, but the distinction between FGR and SGA remains essential for every species. Three experiments were intended to recategorize sheep model research outcomes to increase their informative value regarding pregnancy and fetal growth.

1.2. Fetal growth restriction

1.2.1. Nomenclature

In the early stages of developmental origins of health and disease (DOHaD) research, low birthweight (< 2500 g) was the primary factor of concern. Most studies concurred with correlations between low birthweight and a higher risk of cardiovascular, endocrine, and metabolic diseases in adult life [13]. Other risk factors, included maternal weight and body condition at conception [14], maternal and paternal stature, maternal history of prior small offspring, and low birthweight of the mother herself [13, 15]. Mounting evidence led to the realization that low birthweight was overly general since it erroneously grouped premature offspring with offspring that developed to term but were born small and restricted fetuses [16]. Authors began using the term SGA to clarify the distinctions, and the work continues to create tailored fetal growth charts to appropriately categorize SGA based on gender, nationality, and hereditary potential [10]. With the concept of fetal or intrauterine growth restriction (IUGR) introduced as the link between lifelong disease risks and low fetal weight, the terms became synonymous with SGA for a time [17]. Some literature even defined IUGR as referring to the lower 10th percentile of fetal weights [18, 19]. The oversight was exposed when scientists noted that 50–70% [8] of SGA infants were constitutionally small because their stature was a genetic expectation

rather than the outcome or expression of a significant pathology (Figure 1-1) [12]. Additionally, the SGA categorization excludes instances of FGR that did not impact overall weight or occurred in constitutionally large fetuses (while remaining appropriate for gestational age; AGA) [20]. Despite continuous cautions about the inaccuracy of using birthweight to define FGR [12, 16, 21], the literature is still impacted by casual use and misclassification of FGR, which also means that many studies use low fetal weights as primary endpoints [5, 22], despite intending to evaluate evidence for FGR.

1.2.2. Pathophysiology

In early gestation, maternal efforts are focused on placental development to provide optimal nutrient exchange. Distal uterine and spiral arteries undergo drastic remodeling through trophoblastic invasion, which leads to exponential increases in uteroplacental circulation [23]. This acts in concert with an exponential increase in uterine artery blood flow. Traditionally, capillary development within the larger spiral arteries and caruncles allows for greater capillary flow rates, which decrease vascular resistance, and allow for higher rates of flow proximally, within the uterine artery [23, 24]. Compromise to this process will result in reduced maternal blood flow, and subsequent reductions in placental growth and transfer of nutrients to the fetus.

Chassen and Jansson theorize that compromised blood flow cannot explain the reduction in nutrient transfer in all situations, and that the placenta is communicating with the fetus and dam and functioning to partition available nutrients accordingly. In a variety of in vitro and in vivo studies, activity and expression of amino acid transporters including system A, system β, and system, have been decreased in FGR [11]. Subsequently, reduced fetal levels of amino acids have been seen with NR [25], protein restriction [26] and in

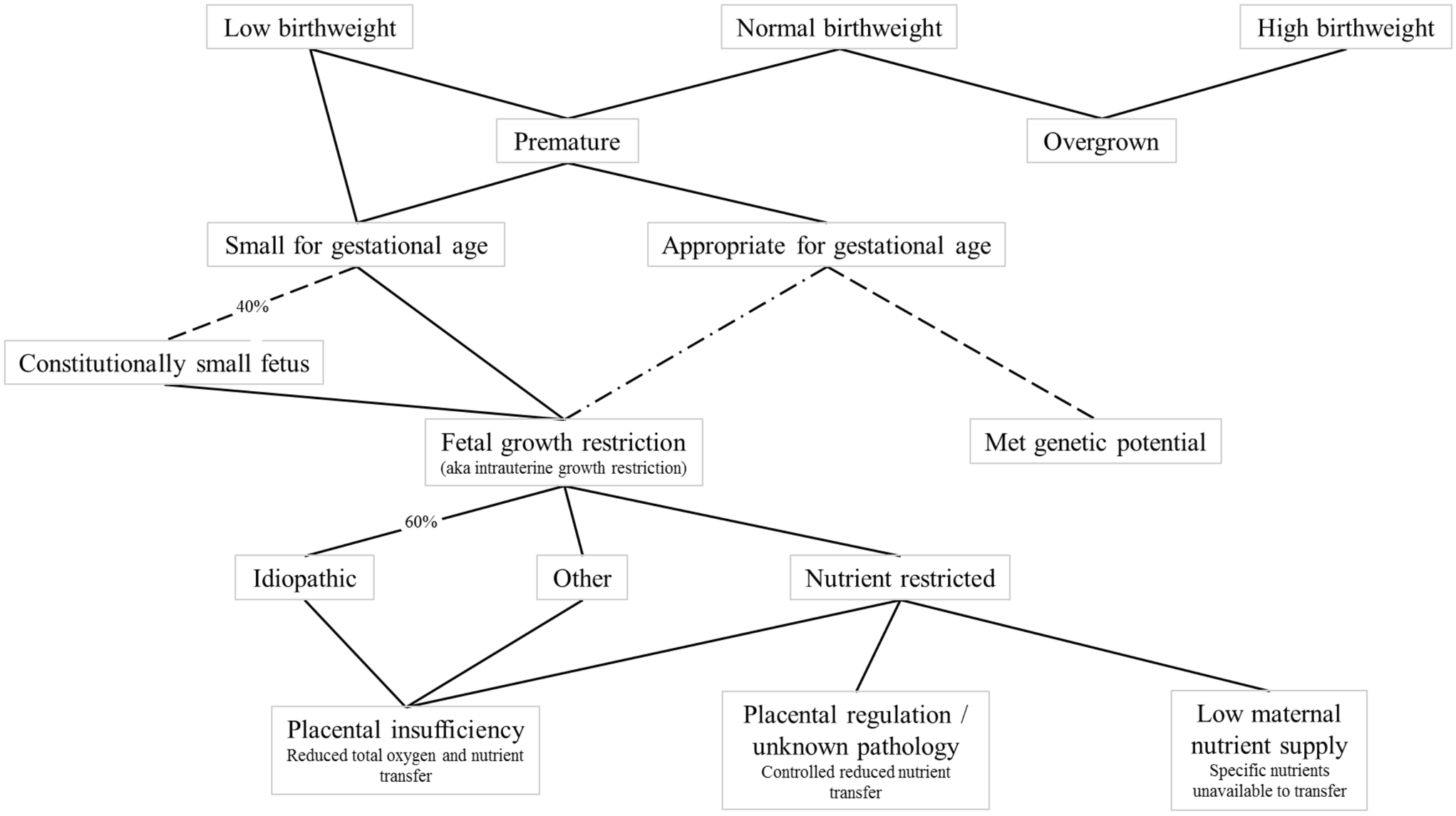

Figure 1-1: Flow chart of fetal growth terminology with human statistical occurrence. Birth weights can be high (not discussed in this paper), normal, or low (<2500g) in humans. Low birthweight infants may have been born prematurely and be an appropriate weight for their gestational age (AGA), or small for their gestational age (SGA), whether born prematurely or not. Approximately 40% of SGA infants are constitutionally small, indicating that their genetic growth potential was met, and they are most likely symmetrically small (dashed line). The remaining 60% of SGA infants may have been fetal growth restricted (FGR) through idiopathic, nutrient restricted (NR), or other causes. Idiopathic and other main causes are believed to act primarily through a placental insufficiency, whereas nutrient restriction may impact the fetus due to a simple lack of maternal supply or regulatory efforts of the placenta to alter nutrient transporters, or it may cause a placental insufficiency. Appropriate for gestational age infants may still be FGR (usually asymmetrical growth, represented by the dot/dash line), either by not affecting global infant size or through a size restriction that was not severe enough to meet the lower 10th percentile.

human FGR [27]. Oxygen is the likely exception to this, and fetal delivery is expected to be entirely dependent on blood flow and tissue thickness [11], although the placenta may participate by lowering its oxidative metabolism and direct uptake of oxygen [28]. Glucose does rely on placental transporters, although the gradient between dam and fetus is consistently maintained, making it unlikely that the transporters are limiting delivery [28, 29]. The fetus may lower its demand, increase catabolic activities, and/or drastically increase gluconeogenesis efforts to offset the reduced supply though. Increased liver size, which was not seen in our model, is occasionally contributed to larger abdominal circumferences, and believed to be linked to gluconeogenesis which the fetus normally does not participate in on a notable scale [28].

An FGR fetus is presumed to have responded physiologically and protectively to reduced nutrient and oxygen availability [12]. The initiating cause of FGR may be acute or chronic, and the timing and duration of the restriction will variably alter the fetal response based on organogenesis and stage of fetal growth. For example, maternal malnutrition in the first trimester is linked with greater risks of fetal cardiovascular disease, while in the third trimester, malnutrition is more likely to affect fetal weight and adiposity [21]. Most FGR is the result of a placental insufficiency compromising the transport of nutrients and oxygen to the fetus. The fetus responds to hypoxemia and hypoglycemia in a "brain sparing" pattern, whereby the blood supply is preferentially shunted toward the brain, adrenals, heart, and placenta, subsequently compromising the development of organs such as the pancreas, skeletal muscle, and kidneys [10, 12]. This combination has also been referred to as the "thrifty phenotype" hypothesis [17, 30]. While some facets are becoming

better understood, much of the pathophysiology behind the "thrifty phenotype" hypothesis remains elusive [12].

Curiously, the "protected" organs might not fare much better than neglected organs. Hypertrophic and elasticity changes have been observed in the heart and blood vessels as they respond to increased afterload and pumping rate caused by redistribution of flow [31]. With a drastic enough insult, cardiac function resulting from this diversion can become irreversibly and terminally compromised [32]. Evidence of cognitive dysfunction has also been linked to signs of FGR [12]. Lower systemic flow can reduce liver size, as well as muscle and fat mass, resulting in a thinner fetus with a comparatively large head [10, 33]. This growth pattern has been referred to as "asymmetrical SGA" [4, 10]. Symmetrical SGA, the counterpart, is indicative of a constitutionally small fetus [12], although some researchers theorize that symmetrical SGA may also occur when FGR is extreme or early and the fetus fails to adapt [4], which further emphasizes the need for credible distinctions between SGA and FGR.

1.2.3. Diagnostic guidelines for FGR

Doctors report difficulty with the lack of diagnostic criteria and intervention options for patients and their FGR babies [12]. A panel of 56 expert scientists in the field was gathered to debate on fetal measures of interest and determine a standardized method for categorizing FGR [34]. In clinical research, while fetal weight is still occasionally used as a proxy for evidence of FGR [35], most scientists are testing new measurement standards [36] or using more stringent weight percentiles [37].

As discussed, the lowest 10th percentile of fetal weights has a poor positive predictive value for FGR, however, studies have indicated that the lower the weight

percentile used, the greater the likelihood of FGR [8]. Many groups have chosen a cutoff of at least 2 standard deviations (SD)s below the control mean to more accurately identify FGR, but it should be noted that this practice risks missing more large FGR cases [16]. Fetuses in the lower 3rd percentile based on fetal weight (equivalent to below 2 SD) [38], experience exponential increases in morbidity and mortality regardless of pathology [10]. Milovanovic et al. demonstrated that even fetuses in the < 2 SD population exhibit a difference in morbidities that can differentiate FGR from constitutionally small babies [37].

Asymmetrical fetal growth is a primary indicator of FGR, and commonly used as a diagnostic tool [12]. Measurement of abdominal and cerebral circumference and the ratio between the two through ultrasound can be early indications of asymmetry in humans [7]. Practitioners recommend monitoring the rate of changes in these and other size parameters through specific stages of gestation with regular ultrasound testing. Any slowing of growth between time points compared with normative growth curves can indicate a period of FGR [21]. Mild or relative forms of FGR may not be associated with asymmetrical growth, and can be more challenging to diagnose [39].

Due to the shunting of blood, coronary blood flow can increase enough to be detectable via Doppler earlier in gestation in FGR fetuses than in healthy fetuses [40, 41], and reversed end-diastolic blood flow may occur in the umbilical artery [42]. Doppler assessment of coronary and umbilical blood flow has potentially high positive predictive value when timed correctly, but similar to the weight cutoffs, this procedure may miss many larger FGR fetuses [12, 41].

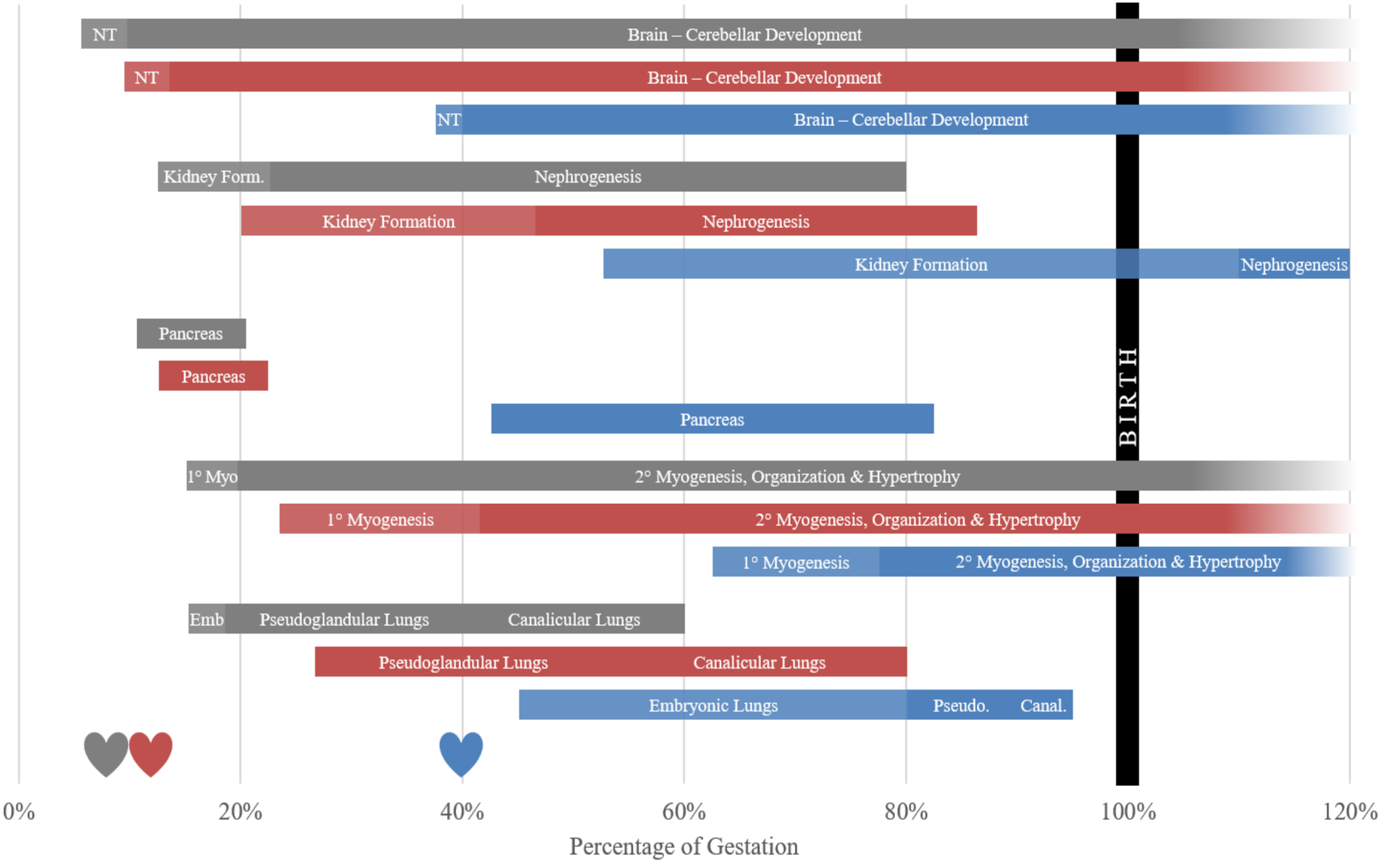

Figure 1-2: Timeline of fetal organogenesis based on percent of gestation in the human, sheep, and mouse. Developmentally critical windows represent times when organs are most susceptible to insult, albeit they can be compromised outside of these windows. The sheep (red) timeline is a closer approximation for the human (gray) timeline than that for mice (blue) that are born precocially and have experienced 40% of the gestation when the neural tube (NT) forms. Hearts in the figure represent detectable presence of a heartbeat. (Reprinted with permission, from Sandoval et al., 2020) [46]

Combinations of these measures are in use and being tested in an effort to diagnose and study FGR more accurately. A fetal weight or an abdominal circumference in the lower 3rd percentile are the top criteria in the group-developed categorization system, with supplementary evidence being unnecessary if either is present [34]. Fetal ultrasound staging is common, with increased frequency assigned when circumferential ratios or blood flow shifts cause concern. Clinically, it is important to diagnose early, increase monitoring as appropriate, and possibly intervene to improve fetal development. It is common to begin by assessing risk factors; however, FGR may be idiopathic in over 60% of the cases [43], at which point, monitoring for effects of FGR might be the best option.

1.3. The ewe as a model for gestational research

Fetal growth restriction can be studied using animal models where factors associated with impairment are applied in early- to mid-pregnancy. Because human studies of a similar nature would be unethical, animal models have proven invaluable, revealing many molecular and physiological pathways to FGR. The ewe has been an excellent resource for this research, partly due to a larger fetal size, which is similar to that for humans at parturition, and the ability to instrument the fetus during gestation [44, 45]. In comparison with rodent models, which are desirable due to a shared placental type, the length of gestation and the phases of organogenesis are better approximated by sheep (Figure 1-2) [46, 47]. Sheep are also easier and less expensive to house and maintain than cattle or non-human primates. For FGR, there are sheep models of vascular occlusion, high-altitude stress, heat stress, carunculectomy, and over- and undernutrition [48]. Researchers theorize there are shared trajectories for the maternal response to these insults, and creation of FGR conditions, and the seemingly uniform fetal response to FGR [11, 49,

50]. The comparative value of the nutritional models is the ability to encourage FGR without a costly and invasive surgical intervention.

1.4. Nutrient restriction in a sheep model of FGR

1.4.1. High variability in nutrient restriction research

The nutrient restricted (NR) ewe model is one of the most applicable to human health concerns. Considering poor-quality Western diets, morning sickness, adolescent pregnancy, poverty, and famine, experimentally limiting nutrients fed to a pregnant ewe has undeniable real-world application potential [16]. However, NR ewes produce an astonishingly wide array of fetal phenotypes [51], and due to the high percentage of relative and/or symmetric fetal responses, some texts do not include NR as a potential cause of FGR [12, 52]. Unsurprisingly, discrepancies may result from the pervasive classification challenges, with some studies that report simple averages not drawing the same conclusions as others looking at the phenotypic range in the offspring following treatments [53–55]. Researchers have reported that adolescent ewes respond more drastically to NR than mature ewes [16], thin ewes respond worse than obese ewes [56], and dietary shifts are more disruptive than consistency in diets [57]. The severity and timing of NR also have an impact on how the fetus and placenta respond. Rumball et al. compared NR in a group of lab-adapted ewes to a flock of ewes that spent generations on poor pasture [57]. The authors demonstrated that maternal familiarity with nutrient scarcity prevented fetal compromise through placental adaptations. Wallace acknowledged the importance of age, condition, parity, and weight-matched study subjects, in part due to the impact of these factors [58].

In addition to the more mild study results, work with severely undernourished adult sheep (diets were 30–40% that of control diets) showed a 17% reduction in uterine blood flow if the dietary insult occurred during mid-gestation, or a 20–33% reduction in uterine blood flow if the nutritional insult occurred in late gestation [28, 59, 60]. Similarly, a 40% reduction in dietary intake beginning in early gestation results in a reduction in umbilical blood flow and increased arterial indices of resistance [26, 61]. With the possible range in fetal responses from healthy to severe compromise, the earlier belief that there is a common pathophysiology for FGR seems inaccurate.

1.4.2. How is the placenta involved in maternal malnutrition?

Unlike overnutrition models, nutrient deficiency models are not perceived to act through primary compromise of the placenta, and it has been claimed that they limit the fetus through nutrient deficiency alone [58, 62]. It is more likely that nutrient deprivation has a multifactorial impact on fetal growth. Studies have shown compromised placental weights, uterine and placental blood flows, and capillary development in response to NR [11, 63, 64], which deserves notice.

Nutrient intake in the first third of pregnancy impacts the placenta the most [58]. When severe or early maternal malnutrition causes a placental insufficiency beyond the extensive functional reserve capacity, it can have a compound impact on the fetus, beyond the low maternal nutrient supply (Figure 1-1). Results from NR studies may contain graded instances of relative FGR, as well as both idiopathic and malnutrition-associated absolute FGR, in addition to the omnipresent variations resulting from differences in potential fetal size, all of which may or may not be impacted by individual maternal factors. If the desired outcome from these studies is to detect common pathologies that

may be mitigated in human healthcare (and agricultural) settings, categorizing NR outcomes by the placental and nutrient transfer deficiencies would offer a greater benefit to science than limiting research to find a commonality among them.

In ewes, placental growth and development are exponential prior to gestational day 50, and maternal conditioning and nutrition at conception and within the first trimester are critical to placental and subsequent fetal health [57, 65]. Placental effects resulting from NR can be less severe than in other animal models and can respond to realimentation [58, 64, 66], while fetal effects can also be minor compared to absolute FGR and not linked with placental mass to the same degree. In some instances, however, greater degrees of placental and fetal compromise are involved [62]. Carr et al. reported that 52% of the offspring in their obese adolescent ewe model consistently fell < 2 SD below the control mean [36]. Nevertheless, restriction to that degree in the undernutrition model is variable from 3–70% of study subjects (preliminary studies) [58, 67]. Researchers have noted that this is part of the spectral or graded response in most NR challenges. Burrage et al. have shown that this graded response is negatively correlated with the risk of cardiovascular changes [68], similar to the increasing risk of heart disease with decreasing fetal size in humans [69]. The cardiac and other phenotypes seen with this trend are similar to those of absolute FGR, but severity decreases as fetal weight increases. If a scaled relationship does exist in the test subjects, it is important to focus on that effect in the interpretation of results. When investigating a graded response, interest arises regarding the differences between the ewe that fails to support fetal growth potential and the more robust or adapted ewe that partitions nutrients for complete fetal or superior placental growth [13, 51]. Studies have demonstrated that thin, adolescent, and poorly adapted ewes have a more

drastic response to NR [57, 70]. This response is likely a combination of dam genetics and severe environmental conditions resulting in placental insufficiency in a NR model.

While the medical field is anxious to define absolute FGR, and to identify and mitigate the causes [9, 10, 55], the risk of human cardiac and metabolic disease also increases with decreasing birthweight [68], making the graded responses of the NR model valuable even if most malnourished infants are unlikely to meet the criteria for absolute FGR.

A primary difference between FGR caused by placental insufficiency and relative FGR is the provision of oxygen to the fetus. In instances of placental compromise, both oxygen and nutrient delivery are limited. A high-altitude sheep model might experience fetal hypoxemia, and a NR model might cause a fetal nutrient deficiency alone [54, 71]. Camm et al. demonstrated that hypoxemia impacted rat fetuses differently than malnutrition [71], in contrast to some researchers who showed that hypoglycemia activated the same fetal aortic chemoreceptors, integral to the brain sparing response, as hypoxemia [68]. The potentially divergent pathophysiologies would again be valuable to recognize independently.

1.4.3. Severity of FGR

It may seem counterintuitive to imply that the key to using the sheep model to explain FGR is to accurately identify FGR in the model. Sibley et al. discussed the importance of placental phenotypes to the trajectory of FGR [72], and this association has been confirmed in sheep [51, 73]. Although aspects of FGR cannot ethically be tested in humans, they can be tested using sheep as the animal model. For instance, it is possible to remove a single placentome from a ewe in mid-gestation while allowing the pregnancy to

continue to term. Studying the histoarchitecture of the placentome at mid-gestation can provide insight into the density of capillaries, efficiency of nutrient transfer, and early response to insult, as well as to establish a maternal baseline before applying a challenge. It is also possible to instrument the uterine artery with a flow probe at the same time to obtain correlative data about uterine blood flow to placentomes that increases exponentially as gestation continues. Current research is examining AMH as a possible biomarker to predict FGR [74–76]. In animal models for FGR research, sampling fetal tissue is possible and may provide insight into FGR [77]. Considering that the brain sparing response to fetal stress is linked to a redistribution of blood flow, a differential in blood flow is likely among fetal tissues that is greater in cases of absolute FGR versus lesser degrees of AGA relative to FGR [78]. Results from NR studies include graded instances of relative FGR, as well as both idiopathic and malnutrition-associated absolute FGR. There is a need to investigate unique patterns of fetal blood flow in fetuses to determine if maternal hemodynamics and placental changes are caused by malnutrition and provide insight to specific interventions to mitigate FGR [55, 65].

1.5. Tools for categorizing FGR

1.5.1. General objective

The objective of these studies is to identify mechanisms through which placental and fetal pathologies can be better classified in ovine models in which gestation is compromised.

1.5.2. Placentomectomy

Placental insufficiency is a primary determinant for FGR [16, 31]. Idiopathic FGR occurs in dams that are constitutionally predisposed to poor placental development. Most

environmentally induced FGR has direct effects on placental development that consequently limit oxygen and nutrient supply to the fetus [31]. Malnutrition may impact placental growth, especially in severe and early instances of restriction. If it were possible to preview placental health at early or mid-gestation, such a tool could provide definitive insight into the fetal health trajectory. While samples of placentomes have been investigated at nearly every stage of gestation, such study required terminating the pregnancies [79]. Assessing placental health without termination of the pregnancy would be ideal, relating placental findings to future phenotypical changes in the fetus. Through a novel surgical procedure in a sheep model, a placentome was removed in mid-gestation, which was then compare to fetal outcomes at later gestational time points.

1.5.3. Uterine artery and fetal organ blood flow

Reduced maternal uteroplacental blood delivery is a primary factor in FGR, but in NR, a reduced concentration of nutrients in the blood may be responsible. While Luther et al. used a NR ewe model to identify reduced capillary area density within the maternal caruncle, indirectly implying that blood flow through the caruncle was reduced [64], not all research has shown a reduction in uterine blood flow following NR [80]. Measuring uterine artery blood flow in a NR model will better define the compromised placental delivery of nutrients to the pregnant uterus and delineate how it translates into fetal development. Blood flow was also measured within fetal organs to determine the origin of organ dysfunction. Evaluating these changes in a ewe model allowed comparisons of overall changes in relation to treatment and differences within the NR group that may indicate “rescue” of the fetus or evidence of compromise despite the apparently appropriate size of the fetus. As recent studies have called for [2, 64, 81], this study investigated the

hemodynamic changes that might be responsible for compromises in placental and fetal metabolism, fetal hemodynamics, and complex interactions of diet on resilience and placental adaptation affecting fetal health. It was hypothesized that maternal NR will result in reduced uterine artery blood flow, cotyledonary tissue blood flow, and angiogenesis and blood flow within fetal organs, correlated to fetal size. Awareness of graded changes from relative FGR on additional measurable aspects of fetal and maternal health can be used to identify FGR in future studies. There is a described need to investigate unique patterns of fetal blood flow in fetuses to determine if maternal hemodynamics and placental changes are caused by malnutrition and provide insight to specific interventions to mitigate FGR [55, 65].

1.5.4. Anti-Müllerian hormone

Anti-Müllerian hormone (AMH) is of interest to human and animal fertility specialists as it is predictive of ovarian follicular reserve and response to controlled ovarian stimulation protocols [82, 83]. Due to a link between FGR offspring and reduced ovarian follicular reserve, AMH has become a recent focus in FGR research [74]. Mothers who were born SGA are more likely to have SGA babies [8]; therefore, scientists have begun studying whether AMH concentrations can identify dams at risk of having SGA offspring or if it can be used as a diagnostic measure of FGR postpartum. For example, restricted rat pups had lower follicle counts in a hypoxic model [84] and a uterine artery ligation model. Concentrations of AMH were tested in the latter and showed a tendency toward lower values in FGR pups [75]. Similarly, AMH was lower in NR heifers, which also showed lower ovarian reserve, elevated blood pressures, and enlarged aortas, despite no change in birthweight [76]. However, in a human study of short girls born SGA [85] and adolescent

girls exposed to smoking mothers or FGR, AMH concentrations were unaffected [74]. Prior to investigating this connection in sheep models, establishing baseline values for AMH in ewes would be necessary.

Variations in circulating concentrations of AMH exist among individual ewes and breeds of ewes, as well as with nutritional status, age, and disease states. Intense and persistent disagreements are prevalent in AMH research studies. Concentrations of AMH are considered infallible, with minimal fluctuations through estrous cycles or times of the year, and therefore can be sampled a single time for assessments of reproductive potential [86, 87]. Testing has been complicated for AMH, with a ELISA kits from an assortment of manufacturers, with bias between both the methods and the centers where testing is performed [88]. While many research groups have published dramatic and clinically relevant shifts in AMH [89–91], and incongruencies between test kits [92], the narrative continues to project high value and low variation [93], which is assuredly misleading to clinicians. Prior to any efforts to identify a link between AMH and FGR, baseline values and changes associated with the estrous cycle and pregnancy must be determined for sheep. By sampling ewes at multiple time points in a year, including during anestrus and throughout an entire estrous cycle, intended to determine how collection timing may impact AMH results.

1.6. References

1. Barker DJ, Osmond C, Simmonds SJ, Wield GA. The relation of small head circumference and thinness at birth to death from cardiovascular disease in adult life. *BMJ* 1993; **306**:422–426.

2. Irvine KM, Bligh LN, Kumar S. Association between the fetal cerebroplacental ratio and biomarkers of hypoxia and angiogenesis in the maternal circulation at term. *Eur J Obstet Gyn R B* 2020; **245**:198–204.

3. Easter SR, Eckert LO, Boghossian N, Spencer R, Oteng-Ntim E, Ioannou C, Patwardhan M, Harrison MS, Khalil A, Gravett M, Goldenberg R, McKelvey A, et al. Fetal growth restriction: Case definition & guidelines for data collection, analysis, and presentation of immunization safety data. *Vaccine* 2017; **35**:6546–6554.

4. VandenBosche RC, Kirchner JT. Intrauterine Growth Retardation. *Am Fam Physician* 1998; **58**:1384–1390.

5. Sawant LD, Venkat S. Comparative Analysis of Normal versus Fetal Growth Restriction in Pregnancy: The Significance of Maternal Body Mass Index, Nutritional Status, Anemia, and Ultrasonography Screening. *Int J Reprod Med* 2013:6.

6. Jazwiec PA, Li X, Matushewski B, Richardson BS, Sloboda DM. Fetal Growth Restriction Is Associated With Decreased Number of Ovarian Follicles and Impaired Follicle Growth in Young Adult Guinea Pig Offspring. *Reprod Sci* 2019; **26**:1557–1567.

7. Kahn BF, Hobbins JC, Galan HL. Intrauterine Growth Restriction. In: Gibbs RS, Danforth DN (eds.), *Danforth's obstetrics and gynecology*, 10th ed. London: Lippincott Williams & Wilkins; 2008.

8. Royal College of Obstetricians and Gynaecologists. *The Investigation and Management of the Small-for-Gestational-Age Fetus*. Green-top Guidelines 31. London: RCOG; 2014.

9. Capros H, Scoricova I, Mihalcean L. Intrauterine Growth Restriction: Contemporary Issues In Diagnosis And Management. *Mold Med J* 2017; **60**:26–30.

10. Cunningham FG (ed.). *Williams Obstetrics*, 25th ed. New York: McGraw-Hill Medical; 2014.

11. Chassen S, Jansson T. Complex, coordinated and highly regulated changes in placental signaling and nutrient transport capacity in IUGR. *Biochim Biophys Acta Mol Basis Dis* 2020; **1866**.

12. Ross MG, Mansano RZ. Fetal Growth Restriction: Medscape Reference: Drugs, Diseases and Procedures. Emedicine.medscape.com/article/261226-overview. Accessed 13 February 2020.

13. Barker DJ, Godfrey KM, Gluckman PD, Harding JE, Owens JA, Robinson JS. Fetal nutrition and cardiovascular disease in adult life. *The Lancet* 1993; **341**:938–941.

14. Edwards LJ, McMillen IC. Periconceptional nutrition programs development of the cardiovascular system in the fetal sheep. *Am J Physiol Regul Integr Comp Physiol* 2002; **283**:R669-679.

15. Sharp GC, Lawlor DA, Richardson SS. It's the mother!: How assumptions about the causal primacy of maternal effects influence research on the developmental origins of health and disease. *Soc Sci Med* 2018; **213**:20–27.

16. Simmons R. Abnormalities of Fetal Growth. In: Gleason CA, Juul SE (eds.), *Avery's diseases of the newborn*. Philadelphia: Elsevier; 2018:61–69.

17. Sharma D, Shastri S, Sharma P. Intrauterine Growth Restriction: Antenatal and Postnatal Aspects. *Clin Med Insights Pediatr* 2016; **10**:67–83.

18. Miller SL, Huppi PS, Mallard C. The consequences of fetal growth restriction on brain structure and neurodevelopmental outcome. *J Physiol* 2016; **594**:807–823.

19. Bujold E, Roberge S, Lacasse Y, Bureau M, Audibert F, Marcoux S, Forest J-C, Giguère Y. Prevention of preeclampsia and intrauterine growth restriction with aspirin started in early pregnancy: a meta-analysis. *Obstet Gynecol* 2010; **116**:402–414.

20. Mayer C, Joseph KS. Fetal growth: a review of terms, concepts and issues relevant to obstetrics. *Ultrasound Obstet Gynecol* 2013; **41**:136–145.

21. Hemachandra AH, Klebanoff MA. Use of serial ultrasound to identify periods of fetal growth restriction in relation to neonatal anthropometry. *Am J Hum Biol* 2006; **18**:791–797.

22. Mohammad N, Sohaila A, Rabbani U, Ahmed S, Ahmed S, Ali SR. Maternal Predictors of Intrauterine Growth Retardation. *J Coll Physicians Surg Pak* 2018; **28**:681–685.

23. Konje JC, Howarth ES, Kaufmann P, Taylor DJ. Longitudinal quantification of uterine artery blood volume flow changes during gestation in pregnancies complicated by intrauterine growth restriction. *BJOG* 2003; **110**:301–305.

24. Borowicz PP, Arnold DR, Johnson ML, Grazul-Bilska AT, Redmer DA, Reynolds LP. Placental Growth Throughout the Last Two Thirds of Pregnancy in Sheep: Vascular Development and Angiogenic Factor Expression. *Biol Reprod* 2007; **76**:259–267.

25. Edwards AK, McKnight SM, Askelson K, McKnight JR, Dunlap KA, Satterfield MC. Adaptive responses to maternal nutrient restriction alter placental transport in ewes. *Placenta* 2020; **96**:1–9.

26. Lekatz LA, Swanson TJ, Camacho LE, van Emon ML, Schauer CS, Maddock Carlin KR, Hammer CJ, Lemley CO, Vonnahme KA. Maternal metabolizable protein restriction during late gestation on uterine and umbilical blood flows and maternal and fetal amino acid concentrations near term in sheep. *Anim Reprod Sci* 2015; **158**:115–125.

27. Belkacemi L, Nelson DM, Desai M, Ross MG. Maternal undernutrition influences placental-fetal development. *Biol Reprod* 2010; **83**:325–331.

28. Chandler KD, Leury BJ, Bird AR, Bell AW. Effects of undernutrition and exercise during late pregnancy on uterine, fetal and uteroplacental metabolism in the ewe. *Br J Nutr* 1985; **53**:625–635.

29. Symonds ME, Dellschaft N, Pope M, Birtwistle M, Alagal R, Keisler D, Budge H. Developmental programming, adiposity, and reproduction in ruminants. *Theriogenology* 2016; **86**:120–129.

30. George LA, Zhang L, Tuersunjiang N, Ma Y, Long NM, Uthlaut AB, Smith DT, Nathanielsz PW, Ford SP. Early maternal undernutrition programs increased feed intake, altered glucose metabolism and insulin secretion, and liver function in aged female offspring. *Am J Physiol Regul Integr Comp Physiol* 2012; **302**:R795-804.

31. Malhotra A, Allison BJ, Castillo-Melendez M, Jenkin G, Polglase GR, Miller SL. Neonatal Morbidities of Fetal Growth Restriction: Pathophysiology and Impact. *Front Endocrinol* 2019; **10**.

32. Aditya I, Tat V, Sawana A, Mohamed A, Tuffner R, Mondal T. Use of Doppler velocimetry in diagnosis and prognosis of intrauterine growth restriction (IUGR): A Review. *J Neonatal Perinatal Med* 2016; **9**:117–126.

33. Giussani DA. The fetal brain sparing response to hypoxia: physiological mechanisms. *J Physiol* 2016; **594**:1215–1230.

34. Verfaille V, Jonge A de, Mokkink L, Westerneng M, van der Horst H, Jellema P, Franx A. Multidisciplinary consensus on screening for, diagnosis and management of fetal growth restriction in the Netherlands. *BMC Pregnancy Childbirth* 2017; **17**:353–370.

35. Cnattingius S, Kramer MS, Norman M, Ludvigsson JF, Fang F, Lu D. Investigating fetal growth restriction and perinatal risks in appropriate for gestational age infants: using cohort and within-sibling analyses. *BJOG* 2019; **126**:842–850.

36. Carr DJ, Aitken RP, Milne JS, David AL, Wallace JM. Fetoplacental biometry and umbilical artery Doppler velocimetry in the overnourished adolescent model of fetal growth restriction. *Am J Obstet Gynecol* 2012; **207**:141.e6–15.

37. Milovanovic I, Njuieyon F, Deghmoun S, Chevenne D, Levy-Marchal C, Beltrand J. Innate small babies are metabolically healthy children. *J Clin Endocrinol Metab* 2012; **97**:4407–4413.

38. Bozzola M, Meazza C. Growth Velocity Curves: What They Are and How to Use Them. In: Preedy VR (ed.), *Handbook of Growth and Growth Monitoring in Health and Disease*. New York: Springer New York; 2012:2999–3011.

39. Sun L, Marini D, Saini B, Schrauben E, Macgowan CK, Seed M. Understanding Fetal Hemodynamics Using Cardiovascular Magnetic Resonance Imaging. *Fetal Diagn Ther* 2020; **47**:354–362.

40. Gordijn SJ, Beune IM, Thilaganathan B, Papageorghiou A, Baschat AA, Baker PN, Silver RM, Wynia K, Ganzevoort W. Consensus definition of fetal growth restriction: a Delphi procedure. *Ultrasound Obstet Gynecol* 2016; **48**:333–339.

41. Baschat AA, Gembruch U, Gortner L, Reiss I, Weiner CP, Harman CR. Coronary artery blood flow visualization signifies hemodynamic deterioration in growth-restricted fetuses. *Ultrasound Obstet Gynecol* 2000; **16**:425–431.

42. Burton GJ, Jauniaux E. Pathophysiology of placental-derived fetal growth restriction. *Am J Obstet Gynecol* 2018; **218**:S745-S761.

43. Ghidini A. Idiopathic fetal growth restriction: a pathophysiologic approach. *Obstet Gynecol Surv* 1996; **51**:376–382.

44. Wallace JM, Aitken RP, Milne JS, Hay WW. Nutritionally mediated placental growth restriction in the growing adolescent: consequences for the fetus. *Biol Reprod* 2004; **71**:1055–1062.

45. Washburn SE, Tress U, Lunde ER, Chen W-JA, Cudd TA. The role of cortisol in chronic binge alcohol-induced cerebellar injury: Ovine model. *Alcohol* 2013; **47**:53–61.

46. Sandoval C, Lambo CA, Carey Satterfield M. Redirecting Fetal Programming: Evidence of Interventions that May Be A Tool for Health. *OBM Genet* 2018; **2**.

47. Wallace JM, Luther JS, Milne JS, Aitken RP, Redmer DA, Reynolds LP, Hay WW. Nutritional modulation of adolescent pregnancy outcome - a review. *Placenta* 2006; **27**:61-68.

48. Wallace JM, Regnault TRH, Limesand SW, Hay WW, Anthony RV. Investigating the causes of low birth weight in contrasting ovine paradigms. *J Physiol* 2005; **565**:19–26.

49. Denisenko O, Lin B, Louey S, Thornburg K, Bomsztyk K, Bagby S. Maternal malnutrition and placental insufficiency induce global downregulation of gene expression in fetal kidneys. *J Dev Orig Health Dis* 2011; **2**:124–133.

50. Giussani DA. The vulnerable developing brain. *Proc Natl Acad Sci U S A* 2011; **108**:2641–2642.

51. Jobgen WS, Ford SP, Jobgen SC, Feng CP, Hess BW, Nathanielsz PW, Li P, Wu G. Baggs ewes adapt to maternal undernutrition and maintain conceptus growth by maintaining fetal plasma concentrations of amino acids. *J Anim Sci* 2008; **86**:820–826.

52. Fox H, Sebire NJ. *Pathology of the placenta*, 3rd ed. Edinburgh: Saunders Elsevier; 2007.

53. Vonnahme KA, Hess BW, Hansen TR, McCormick RJ, Rule DC, Moss GE, Murdoch WJ, Nijland MJ, Skinner DC, Nathanielsz PW, Ford SP. Maternal undernutrition from early- to mid-gestation leads to growth retardation, cardiac ventricular hypertrophy, and increased liver weight in the fetal sheep. *Biol Reprod* 2003; **69**:133–140.

54. Armitage JA, Khan IY, Taylor PD, Nathanielsz PW, Poston L. Developmental programming of the metabolic syndrome by maternal nutritional imbalance: how strong is the evidence from experimental models in mammals? *J Physiol* 2004; **561**:355–377.

55. Burrage DM, Braddick L, Cleal JK, Costello P, Noakes DE, Hanson MA, Green LR. The late gestation fetal cardiovascular response to hypoglycaemia is modified by prior peri-implantation undernutrition in sheep. *J Physiol* 2009; **587**:611–624.

56. Wallace JM, Milne JS, Adam CL, Aitken RP. Impact of donor and recipient adiposity on placental and fetal growth in adolescent sheep. *Reprod Suppl* 2017; **153**:381–394.

57. Rumball CWH, Bloomfield FH, Oliver MH, Harding JE. Different periods of periconceptional undernutrition have different effects on growth, metabolic and endocrine status in fetal sheep. *Pediatr Res* 2009; **66**:605–613.

58. Wallace JM. Young Maternal Age, Body Composition and Gestational Intake Impact Pregnancy Outcome: Translational Perspectives. In: Green LR, Hester RL (eds.), *Parental Obesity: Intergenerational Programming and Consequences*. New York: Springer New York; 2016.

59. Reynolds LP, Caton JS, Redmer DA, Grazul-Bilska AT, Vonnahme KA, Borowicz PP, Luther JS, Wallace JM, Wu G, Spencer TE. Evidence for altered placental blood flow and vascularity in compromised pregnancies. *J Physiol* 2006; **572**:51–58.

60. Newnham JP, Kelly RW, Patterson L, James I. The influence of maternal undernutrition in ovine twin pregnancy on fetal growth and Doppler flow-velocity waveforms. *J Dev Physiol* 1991; **16**:277–282.

61. Lemley CO, Meyer AM, Camacho LE, Neville TL, Newman DJ, Caton JS, Vonnahme KA. Melatonin supplementation alters uteroplacental hemodynamics and fetal development in an ovine model of intrauterine growth restriction. *Am J Physiol Regul Integr Comp Physiol* 2012; **302**:R454-467.

62. Wallace JM. Competition for nutrients in pregnant adolescents: consequences for maternal, conceptus and offspring endocrine systems. *J Endocrinol* 2019; **242**:T1-19.

63. Lang U, Baker R, Khoury J, Clark KE. Fetal umbilical vascular response to chronic reductions in uteroplacental blood flow in late-term sheep. *Am J Obstet Gynecol* 2002; **187**:178–186.

64. Luther JS, Milne J, Aitken RP, Matsuzaki M, Reynolds LP, Redmer DA, Wallace JM. Placental growth, angiogenic gene expression, and vascular development in undernourished adolescent sheep. *Biol Reprod* 2007; **77**:351–357.

65. Oliver MH, Hawkins P, Harding JE. Periconceptional undernutrition alters growth trajectory and metabolic and endocrine responses to fasting in late-gestation fetal sheep. *Pediatr Res* 2005; **57**:591–598.

66. Vonnahme KA, Neville TL, Perry GA, Redmer DA, Reynolds LP, Caton JS. Maternal dietary intake alters organ mass and endocrine and metabolic profiles in pregnant ewe lambs. *Anim Reprod Sci* 2013; **141**:131–141.

67. Lambo CA, Edwards AK, Bazer FW, Dunlap K, Satterfield MC. Development of a surgical procedure for removal of a placentome from a pregnant ewe during gestation. *J Anim Sci Biotechnol* 2020; **11**:48–55.

68. Burrage D, Green LR, Moss TJM, Sloboda DM, Nitsos I, Newnham JP, Hanson MA. The carotid bodies influence growth responses to moderate maternal undernutrition in late-gestation fetal sheep. *BJOG* 2008; **115**:261–268.

69. World Health Organization. Promoting optimal fetal development, report of a technical consultation. *WHO Technical Report Series* 2006.

70. Goldstein RF, Abell SK, Ranasinha S, Misso M, Boyle JA, Black MH, Li N, Hu G, Corrado F, Rode L, Kim YJ, Haugen M, et al. Association of Gestational Weight Gain With Maternal and Infant Outcomes: A Systematic Review and Meta-analysis. *JAMA* 2017; **317**:2207–2225.

71. Camm EJ, Hansell JA, Kane AD, Herrera EA, Lewis C, Wong S, Morrell NW, Giussani DA. Partial contributions of developmental hypoxia and undernutrition to prenatal alterations in somatic growth and cardiovascular structure and function. *Am J Obstet Gynecol* 2010; **203**:495.e24-34.

72. Sibley CP, Turner MA, Cetin I, Ayuk P, Boyd CAR, D'Souza SW, Glazier JD, Greenwood SL, Jansson T, Powell T. Placental phenotypes of intrauterine growth. *Pediatr Res* 2005; **58**:827–832.

73. Osgerby JC, Wathes DC, Howard D, Gadd TS. The effect of maternal undernutrition on the placental growth trajectory and the uterine insulin-like growth factor axis in the pregnant ewe. *J Endocrinol* 2004; **182**:89–103.

74. Hart R, Sloboda DM, Doherty DA, Norman RJ, Atkinson HC, Newnham JP, Dickinson JE, Hickey M. Prenatal determinants of uterine volume and ovarian reserve in adolescence. *J Clin Endocrinol Metab* 2009; **94**:4931–4937.

75. Pampanini V, Jahnukainen K, Sahlin L, Germani D, Puglianiello A, Cianfarani S, Söder O. Impact of uteroplacental insufficiency on ovarian follicular pool in the rat. *Reprod Biol Endocrinol* 2019; **17**:10.

76. Mossa F, Jimenez-Krassel F, Scheetz D, Weber-Nielsen M, Evans ACO, Ireland JJ. Anti-Müllerian Hormone (AMH) and fertility management in agricultural species. *Reprod Suppl* 2017; **154**:R1-11.

77. Kwon H, Ford SP, Bazer FW, Spencer TE, Nathanielsz PW, Nijland MJ, Hess BW, Wu G. Maternal nutrient restriction reduces concentrations of amino acids and polyamines in ovine maternal and fetal plasma and fetal fluids. *Biol Reprod* 2004; **71**:901–908.

78. Jansen AH, Belik J, Ioffe S, Chernick V. Control of organ blood flow in fetal sheep during normoxia and hypoxia. *Am J Physiol* 1989; **257**:H1132-1139.

79. Reynolds LP, Borowicz PP, Vonnahme KA, Johnson ML, Grazul-Bilska AT, Wallace JM, Caton JS, Redmer DA. Animal models of placental angiogenesis. *Placenta* 2005; **26**:689–708.

80. Rumball C, Bloomfield FH, Harding JE. Cardiovascular Adaptations to Pregnancy in Sheep and Effects of Periconceptional Undernutrition. *Placenta* 2008; **29**:89–94.

81. Summers AF, Scholljegerdes EJ. Developmental Resiliency: In Utero Adaption to Environmental Stimuli. *Vet Clin North Am Food Anim* 2019; **35**:365–378.

82. Rico C, Fabre S, Médigue C, Di Clemente N, Clément F, Bontoux M, Touzé J-L, Dupont M, Briant E, Rémy B, Beckers J-F, Monniaux D. Anti-mullerian hormone is an endocrine marker of ovarian gonadotropin-responsive follicles and can help to predict superovulatory responses in the cow. *Biol Reprod* 2009; **80**:50–59.

83. Nelson SM, Iliodromiti S, Fleming R, Anderson R, McConnachie A, Messow C-M. Reference range for the antimüllerian hormone Generation II assay: a population study of 10,984 women, with comparison to the established Diagnostics Systems Laboratory nomogram. *Fertil Steril* 2014; **101**:523–529.

84. Aiken CE, Tarry-Adkins JL, Spiroski A-M, Nuzzo AM, Ashmore TJ, Rolfo A, Sutherland MJ, Camm EJ, Giussani DA, Ozanne SE. Chronic gestational hypoxia accelerates ovarian aging and lowers ovarian reserve in next-generation adult rats. *FASEB J* 2019; **33**:7758–7766.

85. Lem AJ, Boonstra VH, Renes JS, Breukhoven PE, Jong FH de, Laven JS, Hokken-Koelega ACS. Anti-Mullerian hormone in short girls born small for gestational age and the effect of growth hormone treatment. *Hum Reprod* 2011; **26**:898–903.

86. Fushimi Y, Monniaux D, Takagi M. Efficacy of a single measurement of plasma anti-Müllerian hormone concentration for ovum pick-up donor selection of Japanese Black heifers in herd breeding programs. *J Reprod Dev* 2019; **65**:369–374.

87. Hehenkamp WJK, Looman CWN, Themmen APN, Jong FH de, te Velde ER, Broekmans FJM. Anti-Müllerian hormone levels in the spontaneous menstrual cycle do not show substantial fluctuation. *J Clin Endocrinol Metab* 2006; **91**:4057–4063.

88. Ferguson J, Hockley J, Rigsby P, Burns C. Establishment of a WHO Reference Reagent for anti-Mullerian hormone. *Reprod Biol Endocrinol* 2020; **18**:86–96.

89. Alward KJ, Bohlen JF. Overview of Anti-Müllerian hormone (AMH) and association with fertility in female cattle. *Reprod Domest Anim* 2020; **55**:3–10.

90. Hadlow N, Brown SJ, Habib A, Wardrop R, Joseph J, Gillett M, Maguire R, Conradie J. Quantifying the intraindividual variation of antimüllerian hormone in the ovarian cycle. *Fertil Steril* 2016; **106**:1230–1237.

91. Waheeb RS. Changes in Serum Levels of Anti-Mullerian Hormone and Ovarian Steroids in Barki Sheep during Follicular and Early Luteal Phase of Estrous Cycle. *Pak Vet J* 2017; **37**:421-426.

92. Iliodromiti S, Anderson RA, Nelson SM. Technical and performance characteristics of anti-Müllerian hormone and antral follicle count as biomarkers of ovarian response. *Hum Reprod Update* 2015; **21**:698–710.

93. Umer S, Zhao SJ, Sammad A, Sahlu BW, Yunwei P, Zhu H. AMH: Could It Be Used as A Biomarker for Fertility and Superovulation in Domestic Animals? *Genes* 2019; **10**.

2. DEVELOPMENT OF A SURGICAL PROCEDURE FOR REMOVAL OF A PLACENTOME FROM A PREGNANT EWE DURING GESTATION*

2.1. Overview

Background: In recent decades, there has been a growing interest in the impact of insults during pregnancy on postnatal health and disease. It is known that changes in placental development can impact fetal growth and subsequent susceptibility to adult onset diseases; however, a method to collect sufficient placental tissues for both histological and gene expression analyses during gestation without compromising the pregnancy has not been described. The ewe is an established biomedical model for the study of fetal development. Due to its cotyledonary placental type, the sheep has potential for surgical removal of materno-fetal exchange tissues, i.e., placentomes. A novel surgical procedure was developed in well-fed control ewes to excise a single placentome at mid-gestation.

Results: A follow-up study was performed in a cohort of nutrient restricted ewes to investigate rapid placental changes in response to undernutrition. The surgery averaged 19 min, and there were no viability differences between control and sham ewes. Nutrient restricted (NR) fetuses were smaller than controls (C; 4.7 ± 0.1 vs 5.6 ± 0.2 kg; $p < 0.05$), with greater dam weight loss (-32.4 ± 1.3 vs 14.2 ± 2.2 kg; $p < 0.01$), and smaller

Conclusions: With this technique, gestational studies in the sheep model will provide insight into the onset and complexity of changes in gene expression in

* Reprinted with permission from Development of a surgical procedure for removal of a placentome from a pregnant ewe during gestation. By Lambo, C.A., Edwards, A.K., Bazer, F.W., Dunlap, K.A., Satterfield, M.C., 2020. *J Animal Sci Biotechnol;* **11**, Copyright [2020] by Colleen Lambo et al. License is available at: https://creativecommons.org/licenses/by/4.0. Modifications were made to article formatting.

placentomes resulting from undernutrition (as described in our study), overnutrition, alcohol or substance abuse, and environmental or disease factors of relevance and concern regarding the reproductive health and developmental origins of health and disease in humans and in animals.

2.2. Introduction

For the past half century, researchers have performed terminal procedures on ruminants to investigate placentome development and its impacts on fetal growth and health [1]. More recent studies have delved into gene expression in placentomes in early stages of gestation with similar goals [2, 3]. Acquisition of information from early and pivotal stages of placental development will advance our understanding of factors that are required for or are detrimental to optimal fetal growth and maturation. The draw-back for any terminal procedures, however, is an inability to correlate placentome growth in early- to mid-gestation with fetal development at term, or, optimally, to morbidity, mortality, and efficiency of growth and development of the resulting offspring. Non-terminal investigations have sought to evaluate parameters of placental and placentome growth and development using Doppler blood flow methods [4, 5], but placentome sampling during gestation without compromising fetal-placental development has not been reported. For the purposes of this communication, placentome will refer to entire discrete regions of interdigitating fetal (cotyledon) and maternal (caruncle) tissues [6].

The ewe has been hailed as a valuable research model for studies relevant to human pregnancy [7, 8]; therefore, knowledge of placental/fetal interactions and how treatments or diseases impact them is critical for understanding, diagnosing, and preventing, causes and effects of deleterious events in placental development which occurs during early- to

mid-gestation. Medical concerns regarding intrauterine growth restriction (IUGR), fetal alcohol syndrome, environmental toxins and pollutants, and other conditions associated with compromised pregnancy are lifelong medical issues that need to be assessed and understood from the earliest stages of gestational programming. Many of the described experimental insults produce spectral phenotypes, which can perhaps best be understood by retrospectively comparing the phenotype to the conditions that existed during early stages of fetal-placental development and before the phenotype of the live offspring is established. A non-terminal surgical technique that allows for sampling of placentomes from a pregnant ewe would provide critical knowledge related to gene-environmental interactions affecting fetal-placental development during gestation and how those interactions impact lifelong health of that offspring.

One area in which research with ewes has proven to be of benefit for human healthcare concerns is that of IUGR, or low birth-weight infants. Our laboratory has developed a nutrient restricted (NR) sheep model for studying IUGR risks in humans [9, 10]. As a proof of concept, initial trials with this novel surgical procedure were performed with ewes in which either a placentome was removed (placentomectomy) or a sham-surgery was performed. A second study tested the efficacy of the surgical approach in our established NR ewe model.

2.3. Materials & methods

2.3.1. Animals and experimental protocols

All experimental and surgical procedures were compliant with and approved by the Institutional Animal Care and Use Committee of Texas A&M University (IACUC #2016-0078).

Embryos were generated from superovulated Hampshire ewes (n = 37), of similar body weight and frame size, utilizing semen from four half-sibling rams [11]. Single grade-1 embryos were transferred into 100 synchronized Hampshire ewes, of similar body size and body condition, to generate singleton pregnancies with minimal fetal and maternal phenotypic variation. Pregnant ewes were identified using abdominal ultrasound on gestational day (GD) 28. Ewes were weighed, isolated into individual concrete pens, and fed 100% of their nutritional requirement in a fully pelleted ration, based on body weight, for a one-week acclimation period. Ewes were then randomly divided into treatment groups, with 40 ewes fed a restricted diet (50% National Research Council; NRC; beginning on GD 35; NR), and 13 fed 100% NRC. The NR ewes and 9 of the 100% ewes (C) were subject to a full placentomectomy surgeries. The remaining 4 ewes underwent a sham surgical procedure (SH). All ewes were weighed weekly, and diets adjusted according to body weight and requirements based on stage of gestation according to NRC guidelines.

2.3.2. Surgical protocol

Ewes were fasted for 24 h prior to surgery. On GD 70, subjects were anesthetized using mask-delivered isoflurane until a surgical plane of anesthesia was achieved. Abdomens were clipped, shaved, and prepped using betadine and a 70% alcohol solution. Ioban drapes (3M Inc., Maplewood, MN, USA) were applied over the abdomen. A 10–15cm ventral mid-line incision was made into the abdomen. Uterine horns were palpated, and the distal end of the gravid uterine horn was exteriorized (Figure 2-1a) for aspiration of allantoic fluid. Fluid was collected using a 20G needle and a 5cc syringe. Next, a placentome on the antimesometrial portion of the uterus was selected, near the conceptus,

but distal to the edge of the amniotic sac. Identification of placentome type was not attempted prior to removal, but an effort was made to select one of representative size. An incision was made into the uterine wall at the proximal end of the placentome using a #10 scalpel blade.

In placentomectomy subjects, the remaining interplacentomal endometrial tissue was manually separated and the placentome was exteriorized (Figure 2-1b). Curved mosquito hemostats were gently manipulated to pass beneath the chorioallantois (Figure 2-1c), containing the vasculature to the selected placentome. A length of 2-0 vicryl was placed into the hemostats and pulled through to ligate around the blood vessels in the

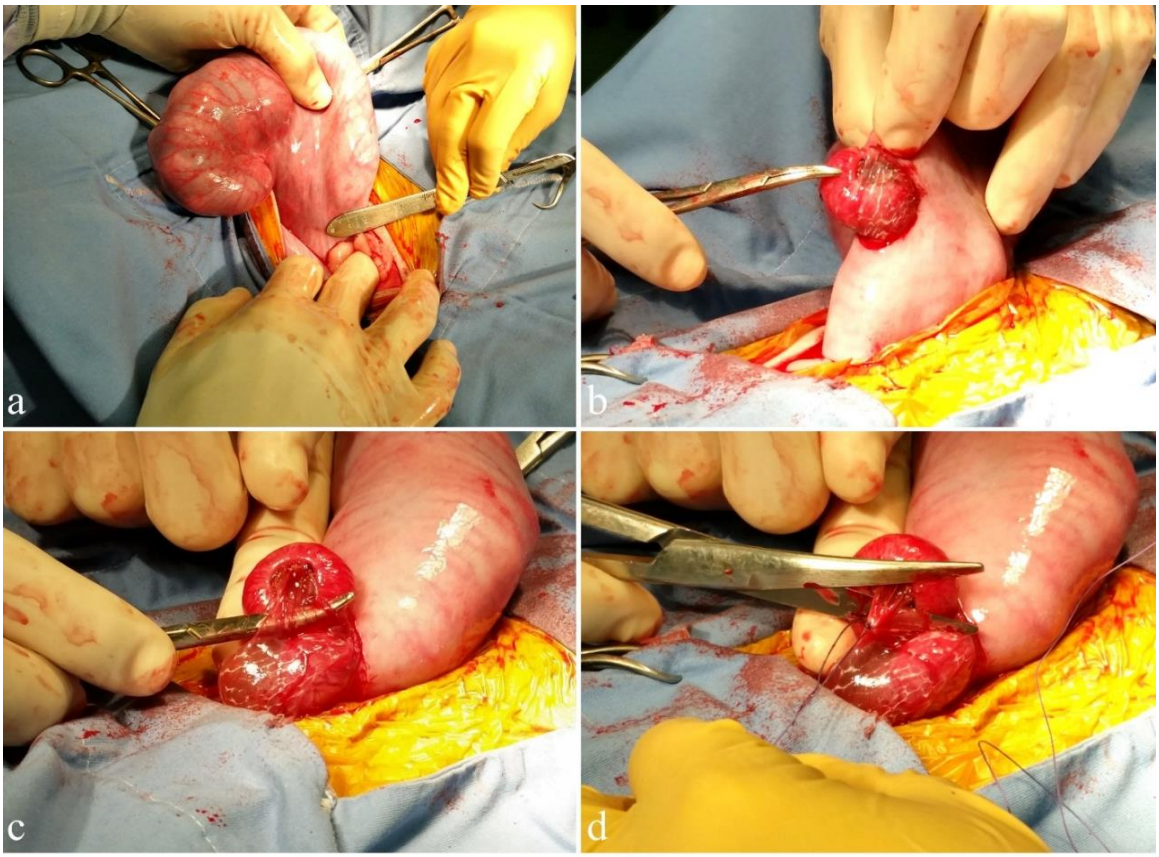

Figure 2-1: Surgical entry into uterus and separation of fetal tissues from placentome. (a) The gravid uterine horn was exteriorized, and a placentome was identified just distal to the amniotic sac, and then (b) gently exteriorized through a scalpel incision. (c) The chorioallantois was isolated using hemostats and following ligation (d) the isolated membranes were transected.

chorioallantois. Curved blunt-blunts were used to transect the tissue between the placentome and the ligature (Figure 2-1d). A 2 cm tapered needle, threaded with one folded strand of 2-0 vicryl, was then passed through the placentome stalk (Figure 2-2a). The threaded end of the suture was cut, resulting in 2 strands of suture passing through the stalk. Strands were used to ligate both sides of the stalk (Figure 2-2b). The stalk was then transected between the ligatures and the placentome, and the preparation observed to ensure that there was no bleeding (Figure 2-2c).

Four sham-operated ewes were subjected to an identical surgical protocol which concluded with the initial incision through the uterine wall. The placentomes were not exteriorized or removed, and the uterine incisions were closed as described.

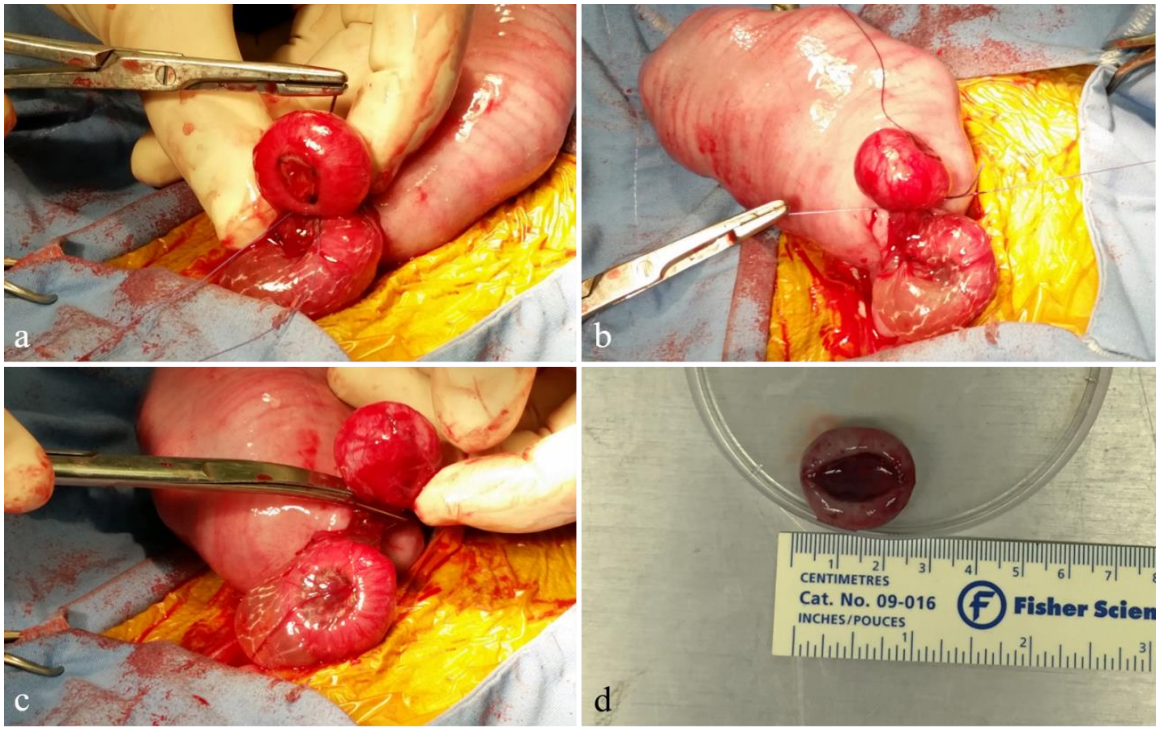

Figure 2-2: Surgical separation of the maternal tissues from the placentome. (a) A modified transfixational suture was placed on the placentome stalk by passing a doubled length of suture through the stalk (b) and tying a ligature on both sides of the stalk. (c) The stalk of the placentome was transected and the stump was observed for bleeding. (d) Excised gestational day 70 placentome.

In all ewes (placentomectomy and sham animals), the uterine incision was closed with 2-0 vicryl in a simple continuous pattern incorporating the submucosa, myometrium, and perimetrium (Figure 2-3a). Warm 5% glycerol-saline was used to cleanse the uterine surface before the uterus was replaced into the abdominal cavity. The linea alba was closed using catgut in a Ford-Interlocking suture pattern. Subcutaneous fat was closed with catgut in a simple continuous pattern, and wound clips were used to close the skin incision. Ewes were held in a recovery area for 24 h before being returned to their original pens. Approximate average surgical time was 19 minutes from first incision to body wall closure. Anesthesia recordings were made every 5 minutes during the procedure, with an approximate cut and close time marked, and this data was extrapolated for an average. Excised placentomes (Figure 2-2d) were weighed and processed according to desired study protocols.

2.3.3. Necropsy

Ewes were necropsied on GD 135. Surgical incisions (Figure 2-3b) were evaluated at the time of necropsy, and additional fetal and maternal tissue samples were collected.

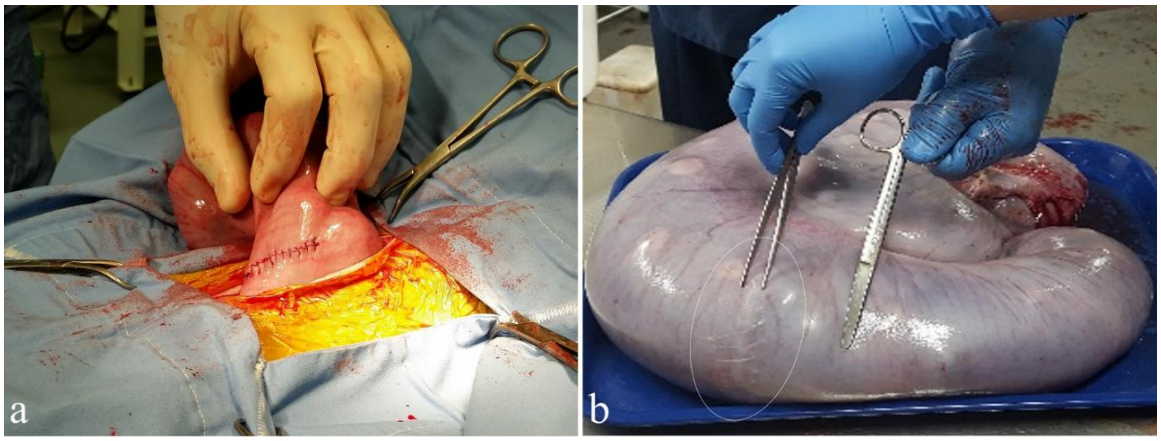

Figure 2-3: Post-operative uterine incision healing. (a) The uterine wall was closed with a simple continuous pattern. (b) Healing of uterine wall incision at the time of necropsy. Forceps are pointing at the incision site, which is also circled and the blunt-blunts indicate the distal edge of the amniotic sac.

Removed placentomes were counted and collectively weighed. Select central A-type placentomes were processed as desired for study purposes.

2.3.4. Statistical analysis

Fetal and placentome weights and counts were compared between SH, C, and NR groups by analysis of variance using SPSS Statistics 26 software (IBM, Armonk, NY, USA). All results are represented as mean ± standard error of the mean. A p-value of < 0.05 was considered significant.

2.4. Results

2.4.1. Wellness and measured outcomes were not different between control and sham ewes

There was no difference ($p = 0.31$) in fetal weights between C ewes and SH ewes (Figure 2-4). No complications from the procedure were observed in well-fed ewes. One C ewe produced a fetus with skeletal deformities and was removed from the study. From the time that pregnancies were confirmed on GD 28, all ewes in the C and SH groups maintained their pregnancies until the time of necropsy. Placentome numbers, weights, amniotic and allantoic fluid volumes, and maternal weight gain did not differ between C and SH ewes ($p > 0.24$; Table 2-1). While surgical incisions were made just beyond the edge of the amnion, at the time of necropsy the amnion had grown beyond the incision site in all subjects. Surgical time from incision to closure averaged 19 minutes. Evaluation of all surgical incisions showed complete healing. Regional placentomes were similar in appearance, size, and shape to those located distal to the incision.

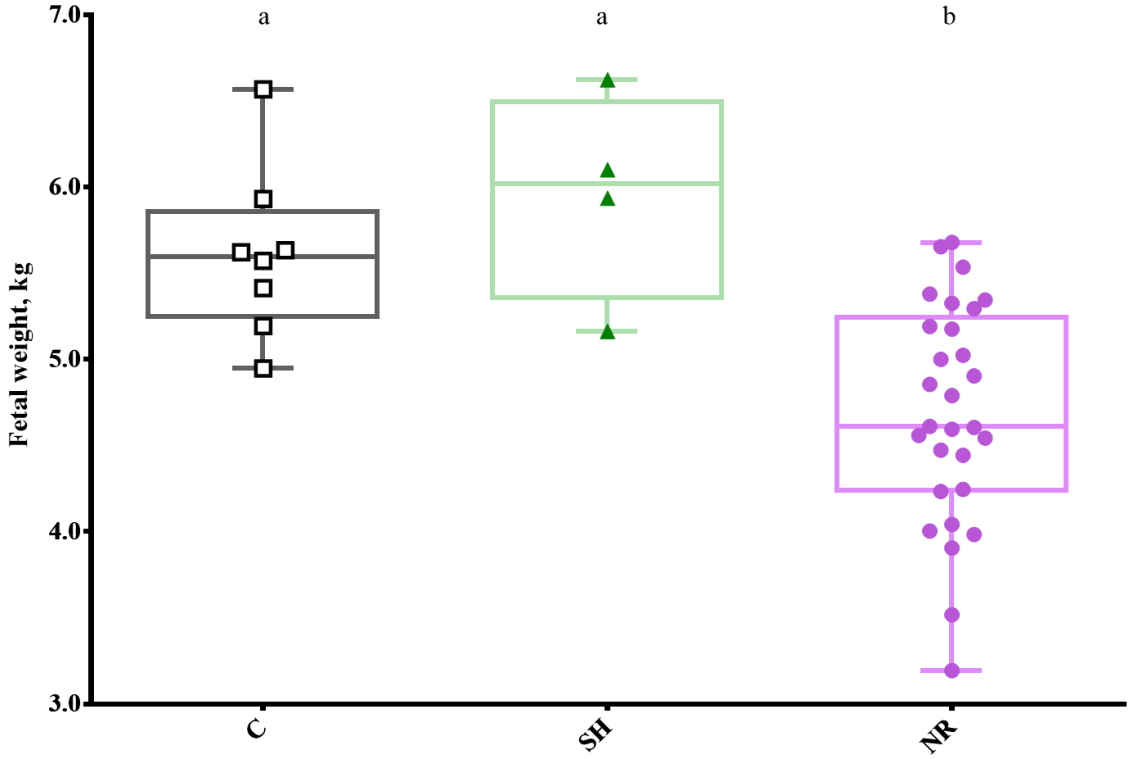

Figure 2-4: GD 135 fetal weights by treatment group. Fetal weights were not different between control and sham ewes ($p > 0.05$). Fetal weights for nutrient restricted ewes were lower than for control ($p < 0.05$).

2.4.2. Nutrient restriction predictably impacted the treatment population

One NR ewe aborted 3 days post-operatively. It was noted at the time of surgery that she had little amniotic fluid, minimal vasculature, a small fetus, and was likely losing her pregnancy. Respiratory issues were noted in one ewe and she was treated with antibiotics but expired 4 days post-operatively. Nine additional NR ewes died or were euthanized in late gestation for reasons unrelated to the surgery. Fetal weights and crown-rump lengths for NR ewes were lower than those for fetuses from C ewes (4.7 ± 0.1 vs 5.6 ± 0.2 kg; 60.3 ± 0.6 vs 64.1 ± 0.9 cm; $p < 0.05$; Figure 2-4), but ponderal indexes were not (PI = [fetal weight (g) x 100] / [fetal length (cm)]^3; 2.1 ± 0.0 vs 2.1 ± 0.0). Weights of single placentomes were not different for ewes in the C (12.0 ± 1.2 g) and NR (10.6 ± 0.6 g)

groups ($p > 0.3$). Total placentome weight determined at necropsy was lower in NR ewes (546.2 ± 43.3 C vs 440.4 ± 21.9 g NR; $p < 0.05$; Table 2-1). Placentome numbers did not vary between treatment groups (80.9 ± 6.1 C vs 78.1 ± 3.0 NR; $p > 0.30$), and were within the described range of 20–150 placentomes per ewe [6]. Nutrient restricted ewes lost a significant amount of weight compared to C ewes (14.3 ± 2.2 C; -32.4 ± 1.3 kg NR; $p < 0.01$). At necropsy, amniotic and allantoic fluid volumes and colors were within the expected range from prior experiments, and did not differ between C, SH, or NR ewes ($p > 0.16$).

Table 2-1: Control and nutrient restricted ewe comparative values

Category*	C	SH	NR
Ewes pregnant (GD 28)	n = 9	n = 4	n = 41
Ewes necropsied (GD 135)	n = 8	n = 4	n = 29
Fetal weight, kg	5.6 ± 0.3[a]	6.0 ± 0.3[a]	4.7 ± 0.1[b]
CRL, cm	64.1 ± 0.9[a]	65.0 ± 1.2[a]	60.3 ± 0.6[b]
Ponderal index	2.1 ± 0.1	2.2 ± 0.0	2.1 ± 0.0
Ewe weight change, kg	14.3 ± 2.2[a]	11.3 ± 2.7[a]	-32.4 ± 1.3[b]
Single placentome wt (GD 70), g	12.0 ± 1.2	n/a	10.6 ± 0.6
Placentome wt (GD 135), g	546.2 ± 43.3[a]	635.0 ± 50.3[a]	440.4 ± 21.9[b]
Placentome number	80.9 ± 6.1	87.0 ± 5.4	78.1 ± 3.0
Amniotic fluid volume, ml	651.9 ± 69.7	640.5 ± 39.8	778.5 ± 84.2
Allantoic fluid volume, ml	545.0 ± 115.1	702.0 ± 222.3	882.6 ± 123.3

C is control fed ewes, SH is sham ewes, NR is nutrient restricted ewes, GD is gestational day, CRL is crown rump length.
Values are reported as mean ± SEM.
[a,b] Means with different letters are statistically different ($p < 0.05$).

2.5. Discussion

Collection of sufficient placental tissues for comprehensive analyses of both histological and gene expression changes in the early stages of maternal insult without compromising pregnancy has not been described. The development of such a novel

technique is a critical step in developing the necessary tools to effectively investigate developmental origins of health and disease. Nutrient restricted ewe fetuses displayed the expected spectral variations in fetal development, where some ewes produced small for gestational age fetuses, and some produced fetuses closer to the weights observed for C and SH ewes [9]. The phenomenon of spectral variation in fetal growth rates in response to maternal nutrient restriction has also been observed in cattle [12]. The surgical procedure allowed collection of placentomes to demonstrate differences in gene expression associated with size of the fetus, which is now being investigated. As removal of an entire placentome was possible, it is reasonable to believe that any research method previously validated for placentome analysis could be applied to excised placentomes as readily as a placentome collected during a GD 70 necropsy [13].

The use of a modified transfixational ligature for stalk removal ensured hemostasis at the site of removal of the placentome. The selection of a central and presumably highly functional placentome for removal was confirmed by their weight in comparison to the weight of placentomes at necropsy, as well as their location relative to the border of the amnion at the time of necropsy. We did not attempt to identify placentome type prior to removal as most placentomes should be concave or A-type on GD 70. Morphology is known to change later in gestation, but is primarily type A for the first two-thirds [6, 14]. The placentomectomy had no identifiable negative impact on fetal development in pregnant ewes when performed on GD 70. The procedure may have hastened progression of the disease in the NR ewe which died 4 days post-operatively, as well as the abortion in the ewe which lost her pregnancy 3 days post-operatively. However, the placentomectomy itself is unlikely to have caused either event.

Placentome formation in the ewe occurs within the first two-thirds of pregnancy, with growth of the placenta plateauing near GD 90. By GD 70, the placenta has essentially achieved its full weight and completed its rapid growth phase. At this time, vascular development in the caruncular and cotyledonary tissues are also entering an exponential growth phase that continues throughout the last half of pregnancy [15]. Our selection of an essential time point for placentome sampling focused on the juncture of these significant growth stages. Concerns regarding stress and uterine manipulation were also factored into the choice of gestational stage for performing the placentomectomies. Placental production of progesterone is sufficient for maintenance of pregnancy by GD 60 and compliments production of progesterone by the corpora lutea [16]. Prior to GD 60, concentrations of progesterone are protective against uterine production of luteolytic prostaglandin F2alpha (PGF2α), but manual manipulation of the uterus may cause sufficient release of PGF2α to trigger luteolysis and subsequent abortion. Minimal handling of the uterus during the placentomectomy procedure is recommended at any gestational age, especially when attempting a placentomectomy prior to GD 60.

There are potential concerns when performing this procedure. The above-mentioned risks of abortion due to uterine handling or maternal stress would compromise the potential of the longitudinal research technique to provide useful data on gene expression critical to subsequent fetal development. Failure to maintain hemostasis at the placentomectomy site, infection, anesthesia risks, and compromise to the amniotic and allantoic sacs are all considered risks of uterine surgery during gestation. Historically, carunclectomies have been performed prior to mating in the ewe model to produce IUGR fetuses. In those studies, a large percentage of caruncles were removed, which proved to

be growth-restrictive in half of the ewes [1, 17, 18]. Sheep are considered polycotyledonary, having 20–150 smaller placentomes which occupying most, but not all available uterine caruncle sites [6]. As shown by the results of the present study, the removal of one placentome during gestation did not impact fetal size, uterine manipulation did not trigger abortion at GD 70, and hemostasis at the surgical site was sufficient to maintain a healthy pregnancy.

An alternative approach to further mitigate some of the mentioned risks would be a placentome biopsy instead of a placentomectomy. Due to the interdigitating and complex nature of placentomes, a concern would then be raised regarding the representative tissue in potential biopsy sections. Hemostasis at the biopsy site would also need to be considered. In species where the uterus is not accessed as readily as in ewes, a placentome biopsy may be an alternative but suboptimal research approach at least regarding the quantity and quality of tissue collected.

The ewe is a valuable established gestational research model [2, 7, 8]. While some aspects of placentation and gestation are different from those in women, the low cost and ease of research with the ovine model have increased its appeal. Research areas span from fetoscopy studies to placentation and fetal programming studies, as evidenced in our NR treatment group. While the rodent or lagomorph models offer a seemingly more direct comparison to the hemochorial placenta of the human, the extended gestation period (21 days in the mouse, 31 days in the rabbit, 147 days in the ewe) in the ovine model provides for a better understanding of long-term developmental impacts on gestation. Similarly, the organogenesis timeline is a closer approximation for human development in the ewe than rodent or lagomorph models [19]. Placentomes have the added value of interdigitating

maternal and fetal tissue sections that allows for growth and gene expression in these areas to be evaluated separately [20], although laser capture dissection or other approaches to single cell transcriptomics may be necessary to isolate tissue types due to the microscopic interdigitation and fusion, especially if performed later in gestation [21]. Comparisons of separate tissue types would not be possible in the more invasive tissues of the human or rodent placental disk. The availability of a procedure to sample placentomes while maintaining pregnancy, adds greatly to the worth of the sheep model in human and agricultural studies.

2.6. Conclusion

The value of this technique can be most greatly realized when studying diseases that give a spectral phenotype. Placental changes can be used to predict and/or understand developmental challenges and ill-thrift in agricultural and human health research settings. Ruminant animals are the only ones that lend themselves to sampling of this nature. Given the low cost and effort involved in housing and feeding sheep, and their shorter gestation, ewes were the ideal animal in which to explore the technique for and value of placentomectomies. With a protocol and efficacy now established, the pregnant ewe stands to serve as an invaluable research model truly linking the histological and molecular signature of the placenta with subsequent penetrance of health or disease in adulthood of the same individual. Following comparisons of the tissues acquired through this pilot study, proof of the benefits of this sampling method to research will be irrefutable.

2.7. References

1. Alexander G. Studies on the placenta of the sheep (Ovis aries L.). *J Reprod Infertil* 1964; **7**:289–305.

2. Reynolds LP, Borowicz PP, Caton JS, Vonnahme KA, Luther JS, Hammer CJ, Maddock Carlin KR, Grazul-Bilska AT, Redmer DA. Developmental programming: the concept, large animal models, and the key role of uteroplacental vascular development. *J Anim Sci* 2010; **88**:E61-72.

3. Barreto R, Bressan FF, Oliveira LJ, Pereira F, Perecin F, Ambrósio CE, Meirelles FV, Miglino MA. Gene expression in placentation of farm animals: An overview of gene function during development. *Theriogenology* 2011; **76**:589–597.

4. Carr DJ, Aitken RP, Milne JS, David AL, Wallace JM. Fetoplacental biometry and umbilical artery Doppler velocimetry in the overnourished adolescent model of fetal growth restriction. *Am J Obstet Gynecol* 2012; **207**:141.e6–15.

5. Camacho LE, Lemley CO, Prezotto LD, Bauer ML, Freetly HC, Swanson KC, Vonnahme KA. Effects of maternal nutrient restriction followed by realimentation during midgestation on uterine blood flow in beef cows. *Theriogenology* 2014; **81**:1248-1256.

6. Wooding P, Burton G. *Comparative Placentation:* Structures, Functions and Evolution. Berlin, Heidelberg: Springer-Verlag Berlin Heidelberg; 2008.

7. Carter AM. Animal Models of Human Placentation – A Review. *Placenta* 2007; **28**:S41-47.

8. Grigsby P. Animal Models to Study Placental Development and Function throughout Normal and Dysfunctional Human Pregnancy. *Semin Reprod Med* 2016; **34**:11–16.

9. Satterfield MC, Dunlap KA, Keisler DH, Bazer FW, Wu G. Arginine nutrition and fetal brown adipose tissue development in nutrient-restricted sheep. *Amino Acids* 2013; **45**:489–499.

10. Satterfield MC, Bazer FW, Spencer TE, Wu G. Sildenafil Citrate Treatment Enhances Amino Acid Availability in the Conceptus and Fetal Growth in an Ovine Model of Intrauterine Growth Restriction. *J Nutr* 2010; **140**:251–258.

11. Satterfield MC, Spencer TE, others. Asynchronous embryo transfer in sheep: lack of survival in progestinized recipient ewes. *J Anim Sci Biotechnol* 2011; **2**:9–13.

12. Long NM, George LA, Uthlaut AB, Smith DT, Nijland MJ, Nathanielsz PW, Ford SP. Maternal obesity and increased nutrient intake before and during gestation in the ewe results in altered growth, adiposity, and glucose tolerance in adult offspring. *J Anim Sci* 2010; **88**:3546–3553.

13. Ott TL, Wiley AA, Bartol FF. Effects of stage of gestation and uterine ligation on ovine placentome development and glycosaminoglycans. *J Anim Sci* 1997; **75**:1053–1062.

14. Vatnick I, Schoknecht PA, Darrigrand R, Bell AW. Growth and metabolism of the placenta after unilateral fetectomy in twin pregnant ewes. *J Dev Physiol* 1991; **15**:351–356.

15. Redmer DA, Wallace JM, Reynolds LP. Effect of nutrient intake during pregnancy on fetal and placental growth and vascular development. *Domest Anim Endocrinol* 2004; **27**:199–217.

16. Al-Gubory KH, Solari A, Mirman B. Effects of luteectomy on the maintenance of pregnancy, circulating progesterone concentrations and lambing performance in sheep. *Reprod Fertil Dev* 1999; **11**:317–322.

17. Lang U, Baker R, Braems G, Zygmunt M, Künzel W, Clark K. Uterine blood flow—a determinant of fetal growth. *Eur J Obstet Gyn R B* 2003; **110**:S55-61.

18. McMillen IC, Robinson JS. Developmental origins of the metabolic syndrome: prediction, plasticity, and programming. *Physiol Rev* 2005; **85**:571–633.

19. Sandoval C, Lambo CA, Carey Satterfield M. Redirecting Fetal Programming: Evidence of Interventions that May Be A Tool for Health. *OBM Genet* 2018; **2**.

20. Reynolds LP, Borowicz PP, Vonnahme KA, Johnson ML, Grazul-Bilska AT, Wallace JM, Caton JS, Redmer DA. Animal models of placental angiogenesis. *Placenta* 2005; **26**:689–708.

21. Poulin J-F, Tasic B, Hjerling-Leffler J, Trimarchi JM, Awatramani R. Disentangling neural cell diversity using single-cell transcriptomics. *Nat Neurosci* 2016; **19**:1131–1141.

3. REDUCED BLOOD FLOW IN CARDIAC, PANCREATIC, RENAL, AND CEREBRAL TISSUES FOLLOWING MATERNAL NUTRIENT RESTRICTION IN THE FETAL LAMB.

3.1. Introduction

Severe malnutrition during pregnancy is a known risk factor for fetal growth restriction (FGR). Women can be at risk of malnutrition due to lack of access to nutrients, poor dietary options or choices, prioritization of resources to personal growth in adolescents during pregnancy, or severe nausea and low food intake due to hyperemesis gravidarum. Livestock can suffer similarly due to food scarcity in harsh environments resulting in nutrient restriction (NR) during critical periods of fetal development and growth, that have consequences on an individual's short- and long-term health, including metabolic syndrome and cardiovascular disease risks [1–3]. Therefore, research into the nature of how malnutrition impacts fetal growth and development is expected to reveal opportunities for intervention to mitigate FGR.

Decreased placental transfer of oxygen causing acute hypoxemia in late gestation triggers a 'brain sparing' response in the fetus, through which blood is preferentially shunted toward the brain and adrenal glands at the expense of peripheral organs such as the pancreas and kidneys [4]. Workload on the heart is increased, which can cause cardiac hypertrophy [2, 5, 6]. This response ensures immediate survival, but lifelong health implications result from physical or genetic adaptations to deficiencies in transport of oxygen and nutrients to the fetus. The modified phenotypes are often more detrimental than beneficial, especially in severe cases and with mismatches between the pre- and post-

natal environments [1]. There is evidence that hypoglycemia activates the same brain sparing chemoreceptors, which may be related to how this protective mechanism occurs in cases of malnutrition in which hypoxemia is not a factor [5–8].

The human, agricultural, and financial costs of FGR are high [9, 10], and research has been intensely focused on early identification and mitigation of the many known and theorized causes; such as dietary supplementation with amino acids or melatonin. Since FGR pathophysiology can lead to a range of outcomes, focusing on the specific etiology of FGR and differentiating FGR from small for gestational age (SGA) is essential to understanding mechanisms and identifying optimal treatments [4, 11–14]. Scheaffer et al. proposed that feto-placental hypoxia may occur due to maternal hypoxia, placental insufficiency, or fetal hypoxia [15]. The categories can be correlated to cause and timing of insult but may not account for FGR occurring without a primary hypoxia, or the possibility of more than one insult occurring synchronously. For instance, down-regulation of nutrient transporters in NR models led to a theory that rather than a compromise to placental blood flow (BF), maternal malnutrition or fetal demands act directly on the placental cells that control nutrient transfer and availability [13, 16]. Part of the variation in results from malnutrition studies is likely due to severe or early maternal malnutrition causing placental insufficiency that has a compound impact on the fetus [4]. Results from NR studies include graded instances of relative FGR, as well as both idiopathic and malnutrition-associated absolute FGR. There is a need to investigate unique patterns of fetal BF in fetuses to determine if maternal hemodynamics and placental changes are caused by malnutrition and provide insight to specific interventions to mitigate FGR [17, 18]. Our lab has focused on a model of relative FGR resulting from a spectrum

of fetal weights produced in NR pregnant ewes that allows for comparisons of the responses of fetuses in the lowest (LQ) and highest (UQ) quartiles within the NR cohort to control (CQ) fetuses [19, 20].

The aims of this study were (1) to evaluate maternal hemodynamic parameters in relation to NR and resulting fetal growth and development (2), and to examine the changes in BF to organs of fetuses in the highest and lowest quartiles, based on fetal weights, from NR ewes. We hypothesized that uterine arterial BF (UABF) is reduced in NR ewes resulting in reductions in BF to systemic organs, while increasing BF to the brain and heart of fetuses developing in NR ewes.

3.2. Materials & methods

3.2.1. Animals and experimental protocols

All experimental and surgical procedures were compliant with and approved by the Institutional Animal Care and Use Committee of Texas A&M University (AUP #2015-0204).

3.2.2. Experimental design

Embryos were generated from superovulated Hampshire ewes, of similar age, body weight and frame size, bred to four half-sibling rams. Single grade-1 embryos were transferred into 92 synchronized Hampshire ewes, of similar age (3–6 years), and body size, to generate singleton pregnancies to reduce fetal and maternal phenotypic variation [20]. Pregnant ewes (n = 54) were identified using abdominal ultrasound on gestational day (GD) 28. Ewes were weighed, isolated into individual concrete pens within sight of their flock mates, and fed 100% of their nutritional requirements in a pelleted ration, according to the National Research Council (NRC) recommendations [21] for a one-week

acclimation period. Ewes were randomly divided into two experimental groups on GD 35 and fed: 1) 100% NRC requirements (C; n = 11) or 2) 50% of NRC requirements (NR; n = 43). All ewes were weighed weekly, diets adjusted according to body weight, and feed consumption was monitored daily. Of the 54 pregnant ewes, 2 aborted, 5 were euthanized due to poor health, and 47 underwent the surgical procedure. Postoperatively, 6 ewes died or aborted during the 4-day recovery period. Thus, samples were collected from 41 ewes. Two fetuses died during collection period, and one did not have a patent fetal arterial catheter for microsphere infusion. Of the 38 ewes providing a complete data set, 5 were controls and 33 were NR.

3.2.3. Surgical protocol

Ewes were fasted for 24 h prior to surgery but had access to water. On GD 117, an 18 gauge, 3 inch jugular catheter was installed in each ewe and anesthesia was induced with an intravenous (IV) injection of ketamine (6.0 mg/kg body weight; Ketaset, Zoetis Animal Health, Parsippany, NJ, USA) and diazepam (0.3 mg/kg body weight; Hospira Inc., Lake Forest, IL, USA). Ewes were intubated with a cuffed endotracheal tube. Surgical anesthesia was maintained with 2–3% isoflurane (Fluriso, VetOne, Boise, Idaho) in oxygen delivered by a ventilation system (Matrx™ Model 3000, Midmark, Orchard Park, NY, USA). Heart rate, ventilation rate, oxygen saturation, and expired carbon dioxide were monitored throughout the period using a Datascope Passport® 2 monitor (Mindray, Mahwah, NJ, USA). Ewes were placed in dorsal recumbency, wool from the surgical site was removed by clipping and shaving, and skin was disinfected using betadine and a 70% alcohol solution. Procedures for surgery and instrumentation were performed as described previously [22, 23]. Briefly, a ventral midline laparotomy was performed, the uterus was

externalized and incised, and a fetal limb was exteriorized. Catheters (0.030 inch inner diameter, 0.050 inch outer diameter polyvinyl chloride tubing) were threaded into the right and left cranial tibial arteries and saphenous veins, and advanced to the level of the abdominal aorta and inferior vena cava, respectively. Catheters were secured by suturing to the skin over the tarsus of one hind limb and the amnion and uterus were closed. A 6 mm transient-time ultrasonic perivascular flow probe (Transonic Systems Inc., Ithaca, NY, USA) was then secured around the uterine artery of the gravid uterine horn. Catheters (0.050 inch inner diameter, 0.090 inch outer diameter polyvinyl chloride) were advanced from the maternal femoral artery and vein to the level of the diaphragm in the abdominal aorta and vena cava, respectively. Catheters were filled with heparinized saline, and the amniotic catheter was filled with saline. All catheters and the flow probe were passed through the abdominal wall in the high lumbar region of the ewe, where they were stored in a cloth pouch attached to the skin. Upon completion of surgery and post-operative recovery, ewes were housed within sight of flock mates in elevated indoor pens with rubber mat flooring. Post-operatively, Banamine (0.5 mg/kg intramuscularly; Merck Animal Health, North Whales, PA, USA) and enrofloxacin (2.5 mg/kg intramuscularly; Bayer, Leverkusen, Germany) were given twice daily, and diets were maintained.

3.2.4. Blood flow sample phase

Four days postoperatively, each ewe was led into a small holding pen, and the catheters and flow probe were removed from the cloth pouch. Catheters were cleaned with betadine and alcohol, the heparinized saline was removed, patency was tested, and then catheters were connected to a blood flow system to record maternal and fetal heart rates (HR), and maternal and fetal blood pressures (PowerLab 8/30, model ML870). If any of

the catheters were not patent when tested, further attempts were made throughout the sampling process, as the fetus changed position. Uterine artery BF was recorded using a Transonic TS420 Perivascular Flowmeter coupled to a PowerLab® data acquisition system (PowerLab 8/30, model ML870) and analyzed using LabChart® software (ADInstruments Inc., Colorado Springs, CO, USA). Maternal and fetal HR and BP were measured using a transducer probe connected to arterial catheters and the PowerLab system. A syringe pump was connected to a fetal arterial catheter to perform a constant rate blood sample collection at 4 ml/min. Gold microspheres (0.05 ml/kg; BioPAL, Worcester, MA, USA) were injected as a bolus into a fetal venous catheter, and sampling was continued for 2 min. Immediately after microsphere sampling, ewes were euthanized with Beuthanasia D (Merck Animal Health, Madison, NJ, USA) administered IV, and the uterus was removed for collection of the fetus and fetal organs. Absolute tissue BF measured by stable labeled microspheres was calculated using the formula;

$$\text{Blood flow (ml/min/g)} = \frac{4.0\ (\text{ml/min}) \times [\text{Microspheres in tissue}]}{\text{Tissue weight (g)} \times [\text{Microspheres in reference blood}]}$$

where 4.0 ml/min is the reference blood withdrawal rate, [Microspheres in reference blood] is DPM in reference blood, tissue weight was in grams, and [Microspheres in tissue] is DPM in the tissue sample.

3.2.5. Tissue collection

The intact uterus was weighed, and the placenta and fetus were removed. Fetal organs were removed, weighed, and finely minced for uniform sampling for microsphere evaluation. The uterus was reweighed when empty of fluids, fetus, and placentomes.

Whole blood from the constant rate collection, and tissue sections from the cerebral cortex, thymus, heart, lungs, liver, stomach, spleen, small intestine, kidney, brown adipose tissue and longissimus dorsi muscle were precisely weighed on an analytical balance, placed into specialized tubes and dehydrated in an oven at 94°C before submission to the Bio Physics Assay Laboratory (BioPAL Inc., Worchester, MA). Placentomes were dissected free of the placental membranes, weighed, counted, and then manually separated into cotyledons and caruncles, which were weighed. Fetal ponderal index was calculated as [fetal weight (g) x 100] / [fetal length (cm)]^3 [24]. Relative organ weights were calculated by dividing the organ weight (g) by fetal weight (kg).

3.2.6. Statistical analyses

Statistical analyses were performed using SPSS Statistics 26 software (IBM, Armonk, NY, USA) and Graph Pad Prism 6.05 (GraphPad Software Inc., La Jolla, CA, USA). Comparisons were assessed using Analysis of Variance when comparing CQ, UQ, and LQ or Student's t-test when comparing C and NR. Values are represented as mean ± standard error of the mean. Pearson's correlation tests were performed only within the NR treatment group. A p-value of < 0.05 was considered significant, and < 0.10 was considered as a trend toward significance. Fetal sex was not associated with fetal weight (3.2 ± 0.1 kg in 20 females, 3.4 ± 0.1 kg in 18 males, $p > 0.100$) on GD 121. Data from both sexes were, therefore, combined. Data from two NR fetuses were determined to be outliers, based on extremes of maternal or fetal weight and their data were not included in the analyses.

3.3. Results

Restricted feed intake from GD 35 to GD 121 reduced maternal weight compared to an increase maternal weight for ewes fed the control diet ($p = 0.008$; Figure 3-1), with maternal weight trajectories diverging by GD 105. Data for measures of maternal, placental, and hemodynamics for C, NR, LQ, and UQ are summarized in Table 3-1. Final maternal weights were less for LQ than CQ ewes ($p = 0.006$). Gestational weight gain (GWG) as a percentage of initial body weight was reduced ($p < 0.001$) in NR compared to C. There was no difference ($p > 0.05$) in GWG between ewes having lambs in the UQ

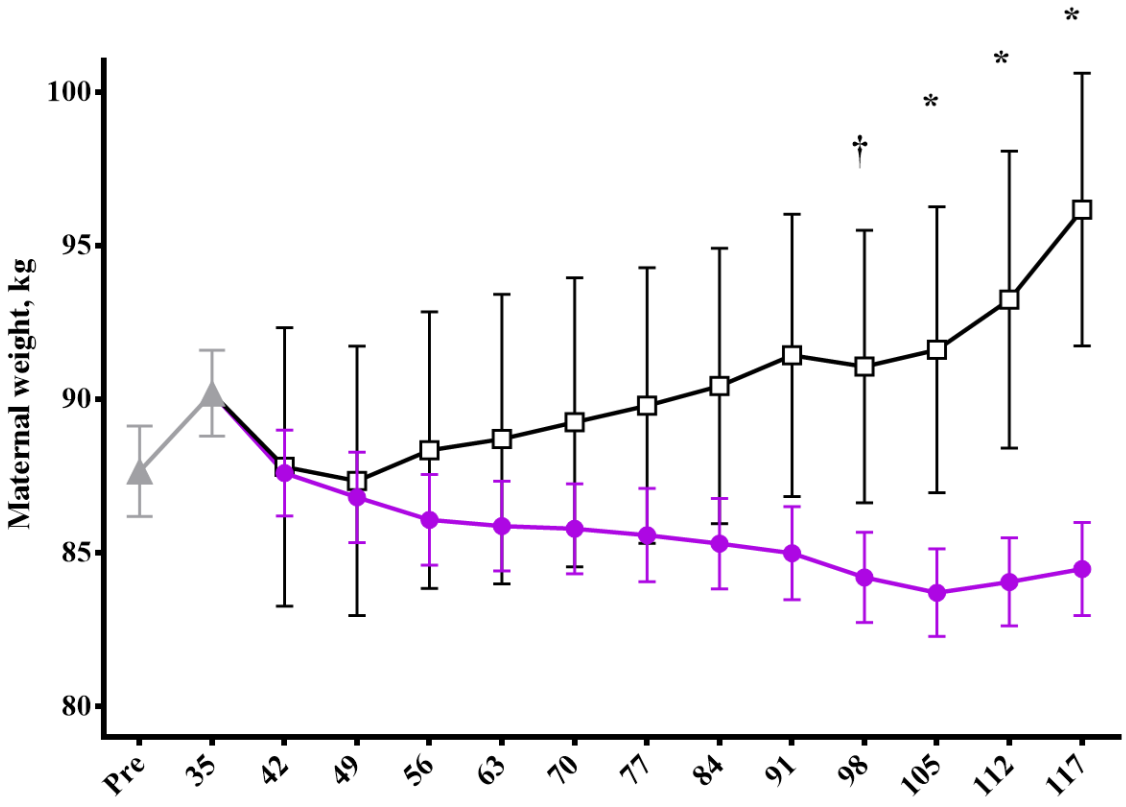

Figure 3-1: Maternal weight over time for nutrient restricted (n = 31; solid circle) and control (n = 5; open square) ewes. All ewes were weighed on GD 28, and fed a control diet for one week (n = 36; grey triangle). Nutrient restricted ewes lost weight during gestation, while the control ewes gained weight, as is expected. Weights were considered significantly different by gestational day 105. Values are reported as mean ± SEM. Means that are significantly different ($p < 0.05$) between groups are marked with an *, and those that tend toward a difference ($p < 0.1$) are marked with a †.

Table 3-1: Comparisons of maternal measures and hemodynamics between treatment groups (Trt) and quartiles (Quart).

	C/CQ (n = 5)	NR (n = 31)	LQ (n = 8)	UQ (n = 8)	p-values	
Maternal measures					**Trt**	**Quart**
GD 35, body weight kg	89.2 ± 5.1	90.4 ± 1.4	85.4 ± 3.6	93.1 ± 2.0	0.770	0.261
GD 117, body weight kg	96.2 ± 4.4[b]	84.5 ± 1.5	78.5 ± 3.6[a]	88.0 ± 2.0[ab]	0.008*	0.007*
Gestational weight gain %	8.2 ± 1.6[a]	-6.6 ± 0.5	-8.2 ± 0.8[b]	-5.6 ± 0.5[b]	<0.001*	<0.001*
Uterus, kg (empty)	1.6 ± 0.0[ab]	1.8 ± 0.1	1.5 ± 0.1[a]	1.8 ± 0.1[b]	0.198	0.019*
Placental Measures						
Placentomes, g	444.7 ± 53.0	501.9 ± 19.6	412.8 ± 30.1	507.1 ± 36.1	0.290	0.190
Placentome number	71.4 ± 6.2	74.1 ± 2.6	80.6 ± 4.0	74.6 ± 4.7	0.706	0.420
Caruncles, g	118.2 ± 19.0	113.1 ± 7.2	100.7 ± 6.1	100.1 ± 6.5	0.795	0.411
Caruncle:dam ratio	1.3 ± 0.2	1.4 ± 0.1	1.4 ± 0.1	1.2 ± 0.1	0.663	0.608
Cotyledons, g	326.5 ± 36.5	388.8 ± 16.2	312.1 ± 29.7	407.0 ± 32.2	0.156	0.095[ƒ]
Cotyledon:dam ratio	3.7 ± 0.5	5.0 ± 0.2	4.3 ± 0.4	5.0 ± 0.3	0.017*	0.096[ƒ]
Cotyledonary BF	2.2 ± 0.3	1.7 ± 0.1	1.6 ± 0.2	1.9 ± 0.3	0.113	0.234
Placenta:fetus ratio	13.3 ± 1.1	15.4 ± 0.5	14.8 ± 0.7	13.9 ± 1.0	0.137	0.522
Caruncle:fetus ratio	3.5 ± 0.5[ab]	3.5 ± 0.2	3.7 ± 0.2[a]	2.7 ± 0.2[b]	0.985	0.041*
Cotyledon:fetus ratio	9.8 ± 0.8	11.9 ± 0.4	11.2 ± 0.8	11.2 ± 0.9	0.066[ƒ]	0.508
Maternal hemodynamics						
Uterine artery BF, ml/min	467.0 ± 61.5	468.9 ± 44.2 [ṁ]	410.3 ± 57.0 [ṁ]	474.4 ± 98.2	0.986	0.841
Maternal MAP, mmHg	119.0 ± 8.6[ṅ]	104.5 ± 1.8	102.4 ± 3.6	106.9 ± 3.4	0.018*	0.092[ƒ]
Maternal S/D	1.38 ± 0.02[ab ṅ]	1.43 ± 0.04	1.46 ± 0.03[a]	1.35 ± 0.03[b]	0.673	0.033*
Maternal HR. bpm	97.3 ± 4.2	110.2 ± 3.2	109.0 ± 6.9	119.0 ± 5.3	0.126	0.081[ƒ]

Values are reported as mean ± SEM. C/CQ is the control-fed group, NR is the entire nutrient restricted group, LQ is the lower quartile of NR, UQ is the upper quartile of NR, GD is gestational day, MAP is mean arterial pressure, S/D is systolic over diastolic ratio, HR is heart rate.

[ṅ] Data available from one fewer animal.

[ṁ] Data available from two fewer animals.

[a,b,c] Means with different letters are statistically different across quartiles (CQ, LQ, UQ).

* $p < 0.05$.

[ƒ] $p < 0.10$.

Table 3-2: Comparisons of fetal organ mass and relative mass between treatment groups (Trt) and quartiles (Quart).

	C/CQ (n = 5)	NR (n = 31)	LQ (n = 8)	UQ (n = 8)	p-values	
Fetus					**Trt**	**Quart**
Sternal circumference, cm	30.3 ± 0.5[a]	30.4 ± 0.3 [ṅ]	28.8 ± 0.4[b]	31.8 ± 0.3[a]	0.920	<0.001*
Ponderal index	2.0 ± 0.1	2.0 ± 0.0	1.9 ± 0.0	2.1 ± 0.1	0.345	0.241
CRL, cm	55.2 ± 0.6[a]	54.3 ± 0.4	52.3 ± 0.5[b]	56.2 ± 0.6[a]	0.359	<0.001*
Tibial length, cm	8.9 ± 0.2	9.0 ± 0.1	8.7 ± 0.1	9.2 ± 0.1	0.452	0.091[ŧ]
Fetal hemodynamics						
Fetal MAP	61.9 ± 0.6	59.3 ± 1.7	62.4 ± 1.9	60.0 ± 1.7	0.550	0.807
Fetal S/D	1.2 ± 0.0	1.2 ± 0.0	1.2 ± 0.0	1.2 ± 0.0	0.630	0.764
Fetal HR	176.8 ± 4.5	175.0 ± 4.0	179.2 ± 4.8	174.0 ± 9.4	0.859	0.864
Brain						
Mass, g	40.9 ± 0.9	43.2 ± 0.6	42.0 ± 1.4	44.1 ± 0.9	0.142	0.159
Relative wt	12.5 ± 0.7[b]	13.4 ± 0.3	15.3 ± 0.6[a]	12.1 ± 0.25[b]	0.289	0.001*
Heart						
Mass, g	18.3 ± 1.3[a]	20.5 ± 0.4	18.3 ± 0.8[a]	22.6 ± 0.7[b]	0.073†	0.002*
Relative wt	5.5 ± 0.3[a]	6.3 ± 0.1	6.6 ± 0.2[b]	6.2 ± 0.2[ab]	0.003*	0.007*
Pancreas						
Mass, g	2.7 ± 0.2[ab]	2.8 ± 0.1 [ṅ]	2.4 ± 0.1[a]	3.0 ± 0.2[b]	0.655	0.036*
Relative wt	0.8 ± 0.1	0.8 ± 0.0	0.9 ± 0.0	0.8 ± 0.0	0.883	0.490
Kidneys						
Mass, g	18.2 ± 0.9[ab]	19.0 ± 0.5	16.3 ± 1.0[a]	20.6 ± 0.7[b]	0.545	0.007*
Relative wt	5.5 ± 0.2	5.8 ± 0.2	6.0 ± 0.5	5.7 ± 0.2	0.402	0.668
Adrenals						
Mass, g	7.6 ± 1.2	6.0 ± 0.5	6.2 ± 1.0	6.5 ± 1.0	0.215	0.691
Relative wt	0.10 ± 0.01[b]	0.11 ± 0.01	0.14 ± 0.01[a]	0.11 ± 0.01[a]	0.217	0.026*
Liver						
Mass, g	113.2 ± 6.7[ab]	117.0 ± 3.1	98.0 ± 5.6[a]	119.9 ± 3.0[b]	0.649	0.013*
Relative wt	34.2 ± 1.1	35.9 ± 0.8	35.4 ± 1.3	32.9 ± 0.8	0.404	0.267
Lungs						
Mass, g	120.8 ± 1.3[ab]	119.0 ± 3.2	108.4 ± 5.7[a]	133.1 ± 6.9[b]	0.252	0.020*
Relative wt	36.9 ± 1.7	36.6 ± 0.8	39.1 ± 0.9	36.5 ± 2.0	0.896	0.455
Spleen						
Mass, g	6.8 ± 1.5	5.5 ± 0.3	4.4 ± 0.5	5.9 ± 0.4	0.163	0.090[ŧ]
Relative wt	2.1 ± 0.4	1.7 ± 0.1	1.6 ± 0.1	1.6 ± 0.1	0.132	0.271
Thymus						
Mass, g	4.0 ± 0.4[ab]	3.8 ± 0.2	2.9 ± 0.4[a]	4.7 ± 0.5[b]	0.730	0.025*
Relative wt	1.2 ± 0.1	1.2 ± 0.1	1.0 ± 0.1	1.3 ± 0.1	0.712	0.275
BAT						
Mass, g	12.7 ± 0.4	11.5 ± 0.4	10.9 ± 0.8	12.8 ± 0.6	0.229	0.083[ŧ]
Relative wt	3.9 ± 0.2	3.5 ± 0.1	3.9 ± 0.2	3.5 ± 0.2	0.208	0.220
L.Dorsi						
Mass, g	27.0 ± 2.6[ab]	26.8 ± 0.8	22.7 ± 1.2[a]	29.1 ± 1.9[b]	0.939	0.049*
Relative wt	8.1 ± 0.4	8.2 ± 0.2	8.2 ± 0.2	7.8 ± 0.5	0.842	0.928

Values are reported as mean ± SEM. C/CQ is the control-fed group, NR is the entire nutrient restricted group, LQ is the lower quartile of NR, UQ is the upper quartile of NR, CRL is crown-rump length, MAP is mean arterial pressure, S/D is systolic over diastolic ratio, HR is heart rate.

[ṅ] Data available from one fewer animal.

[a,b,c] Means with different letters are statistically different across quartiles (CQ, LQ, UQ).

* $p < 0.05$.

[ŧ] $p < 0.10$.

Table 3-3: Pearson's correlation values for fetal tissue measures with fetal weight, fetal heart rate, maternal starting weight (GD 35), gestational weight gain (GWG %), cotyledon and caruncle weight, maternal mean arterial pressure (mMAP), and uterine artery blood flow (UABF).

	Fetal weight, kg	Fetal HR, bpm	GD 35 weight, kg	GWG %	Cotyledon weight, g	Caruncle weight, g	mMAP, mmHg[ñ]	UABF, ml/min[ñ]
Brain								
Mass, g	0.27	-0.23	0.13	0.15	0.18	0.08	0.16	-0.10
Relative wt	-0.81*	-0.02	-0.34[ŧ]	-0.23	-0.46*	-0.06	0.06	-0.14
Heart								
Mass, g	0.80*	-0.18	0.20	0.22	0.60*	0.10	-0.11	-0.07
Relative wt	-0.30	-0.11	-0.37*	-0.18	0.07	0.002	-0.29	-0.25
Pancreas								
Mass, g	0.42*	0.14	0.23	0.37*	0.18	0.37*	-0.19	0.15
Relative wt	-0.14	-0.18	-0.12	0.14	-0.27	0.11	-0.27	0.12
Kidneys								
Mass, g	0.52*	-0.12	0.46*	0.43*	0.39*	0.33ŧ	0.00	0.10
Relative wt	-0.29	-0.02	0.18	0.18	-0.08	0.23	-0.03	0.03
Adrenals								
Mass, g	0.00	0.18	-0.15	-0.19	-0.27	0.11	0.19	0.23
Relative wt	-0.51*	0.22	-0.33[ŧ]	-0.35[ŧ]	-0.49*	0.04	0.13	0.13
Liver								
Mass, g	0.62*	-0.11	0.54*	0.30	0.75*	0.32[ŧ]	-0.16	0.19
Relative wt	-0.12	-0.03	0.34[ŧ]	0.07	0.45*	0.31[ŧ]	-0.31[ŧ]	0.16
Lungs								
Mass, g	0.52*	-0.30ŧ	0.37*	0.30	0.21	-0.06	-0.14	0.05
Relative wt	-0.29	-0.21	0.04	0.03	-0.25	-0.16	-0.23	-0.02
Spleen								
Mass, g	0.51*	0.04	0.33[ŧ]	0.12	0.43*	0.09	-0.09	0.01
Relative wt	0.18	0.07	0.23	0.00	0.29	0.05	-0.14	-0.03
Thymus								
Mass, g	0.62*	-0.21	0.43*	0.20	0.41*	0.18	0.14	-0.07
Relative wt	0.39*	-0.20	0.38*	0.12	0.32[ŧ]	0.20	0.09	-0.10
BAT								
Mass, g	0.50*	-0.06	0.23	-0.06	0.20	-0.08	0.14	-0.10
Relative wt	-0.16	0.03	-0.01	-0.33[ŧ]	-0.18	-0.16	0.07	-0.15
L.Dorsi								
Mass, g	0.69*	-0.38*	0.40*	0.25	0.55*	0.20	0.23	0.06
Relative wt	0.09	-0.44*	0.18	0.05	0.28	0.19	0.24	0.02

[ñ] Data available from one fewer animal.
* $p < 0.05$.
[ŧ] $p < 0.10$.

compared to the LQ. Uterine weights were less for LQ than UQ ewes ($p = 0.019$), but there was no effect of treatment ($p = 0.198$). Placentome number, placentome weights, and caruncle and cotyledonary weights were not different between treatments or quartiles ($p \geq 0.190$). Caruncle:dam ratio was not different between treatment groups or quartiles ($p \geq 0.608$); however, the caruncle:fetus ratio was greater for LQ than UQ fetuses ($p = 0.042$). Cotyledon:dam ratio was greater for NR than C ewes ($p = 0.017$), while the cotyledon:fetus ratio was not different within groups. There were no differences in placentome:fetus ratio or cotyledonary BF due to treatment or quartile ($p \geq 0.113$).

Uterine arterial BF was not different between treatment groups or within quartiles ($p = 0.841$). Maternal mean arterial pressure (mMAP) was lower in NR ewes ($p = 0.018$), but not different among quartiles ($p = 0.092$). Maternal systolic to diastolic ratio (mS/D) was greater in LQ than UQ ewes ($p = 0.033$), but not affected by treatment ($p = 0.673$). Maternal HR was not affected by treatment or quartile ($p \geq 0.081$). Resistance index (BF change/max flow) was negatively correlated with average flow ($r(29) = -0.60$, $p = 0.001$; data not shown).

Dietary restriction did not affect fetal weight ($p = 0.824$; Figure 3-2), ponderal index, crown rump length, sternal circumference, tibial length, fetal mean arterial pressure (fMAP), systolic/diastolic ratio, or HR ($p > 0.345$; Table 3-2). Of those, fetal weight, crown rump length, and sternal circumference were less in LQ than UQ or CQ groups ($p < 0.046$). The distribution of male fetuses was uneven as there was only one male born to a control-fed ewe.

All fetal measurements and organ weights are summarized in Table 3-2. Relative fetal heart mass was greater in NR than C fetuses ($p = 0.003$), but absolute heart mass and

absolute and relative mass of other organs was not affected by diet. Absolute weights of fetal organs were greater for UQ than LQ for the pancreas, kidneys, liver, lungs, thymus, and longissimus dorsi muscle (LD; $p < 0.042$). Absolute heart weights were lighter in LQ and CQ than UQ fetuses ($p < 0.011$). For the remaining organs (brain, adrenals, spleen, and brown adipose tissue; BAT) absolute mass was not different among the quartiles ($p \geq 0.090$). Relative brain mass was greater for LQ than C and UQ fetuses ($p < 0.007$), and relative adrenal mass was greater for fetuses from LQ than C ewes ($p = 0.030$), while no other differences were detected among quartiles ($p \geq 0.220$).

All fetal organ size correlation values are provided in Table 3-3. The weights of heart, pancreas, kidneys, liver, lungs, spleen, thymus, BAT and LD mass in fetuses were

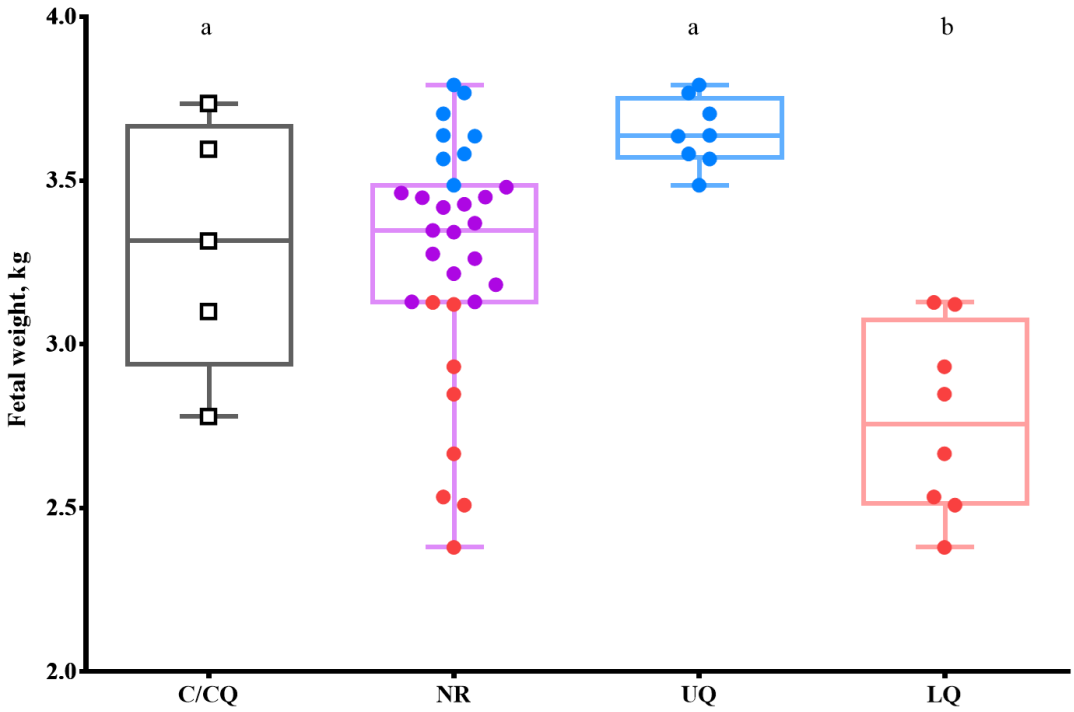

Figure 3-2: Fetal weight spectrum for all fetuses. Nutrient restricted (NR) fetuses were divided into upper (UQ) and lower (LQ) quartiles. Control (C/CQ) fetuses are shown in black squares, LQ fetuses in red circles, middle 2 quartiles in purple, and UQ fetuses in blue. LQ fetuses were significantly smaller than UQ and CQ fetuses. Control fetuses tended to be smaller than UQ fetuses. Values are reported as mean ± SEM. [a,b,c] Means with different letters are statistically significant across quartiles (CQ, LQ, UQ).

correlated with total fetal mass ($p < 0.021$). But, weights of the fetal brain and adrenal mass were not correlated with total fetal mass, ($p \geq 0.141$). In NR fetuses, the initial weight of ewes was positively correlated with kidney, liver, lung, thymus, and LD mass in fetuses ($p < 0.039$). Gestational weight gain, as a percentage of initial weight (GWG %) of ewes, was positively correlated with pancreatic and kidney mass in their fetuses ($p < 0.045$). Cotyledonary mass was positively correlated with heart, kidney, liver, spleen, thymus, and LD mass, while caruncular mass was positively correlated with pancreatic mass ($p = 0.046$). No organ mass was correlated with mMAP or UABF, but LD mass was negatively correlated with fetal HR ($p = 0.023$).

Relative brain and adrenal mass were greater in smaller fetuses ($p < 0.004$). Relative thymic mass, however, was greater in larger fetuses ($p = 0.032$). Cotyledonary mass was negatively associated with relative brain and adrenal mass ($p < 0.010$), but positively correlated with relative liver mass ($p = 0.012$). Initial body weights of ewes were negatively correlated with relative fetal heart mass ($p = 0.040$), but positively correlated with relative thymus mass ($p = 0.036$). Relative LD weight was negatively correlated with fetal HR ($p = 0.007$). Relative organ weights were not associated with GWG %, caruncle mass, mMAP, or UABF ($p \geq 0.050$). Relative heart weight was lower in NR female than male fetuses (6.1 ± 0.2 NR vs 6.3 ± 0.1 C, $p = 0.010$).

BF comparisons for fetal tissues are summarized in Table 3-4. Pancreatic and renal tissue BF were greater in fetuses from C than NR ewes ($p < 0.037$). Blood flow was not different due to treatment for other organs. Cerebral tissue from UQ fetuses had higher BF than that for LQ fetuses ($p = 0.003$). Pancreatic and cardiac tissue from CQ fetuses had higher BF than LQ ($p = 0.029$). All fetal tissue BF correlation values are summarized in

Table 3-4: Comparisons of fetal tissue blood flow (BF) between treatment groups (Trt) and quartile groups (Quart).

Fetal tissues	C/CQ (n = 5)	NR (n = 31)	LQ (n = 8)	UQ (n = 8)	p-value	
					Trt	Quart
Brain BF	1.6 ± 0.3[ab]	1.6 ± 0.2	1.1 ± 0.1[a]	2.5 ± 0.4[b]	0.885	0.004*
Heart BF	4.0 ± 0.9[a]	2.8 ± 0.2[ṅ]	2.1 ± 0.2[b]	3.4 ± 0.4[ab]	0.053[ɬ]	0.029*
Pancreas BF	1.2 ± 0.1[a]	0.8 ± 0.1	0.7 ± 0.1[b]	0.8 ± 0.1[ab]	0.020*	0.023*
Kidneys BF	2.1 ± 0.3	1.6 ± 0.1	1.5 ± 0.1	1.7 ± 0.2	0.037*	0.096[ɬ]
Adrenals BF	0.3 ± 0.0	0.4 ± 0.0[ṅ]	0.4 ± 0.0	0.4 ± 0.0	0.168	0.100
Liver BF	0.2 ± 0.1	0.2 ± 0.0[ṅ]	0.2 ± 0.0	0.3 ± 0.0	0.534	0.351
Lungs BF	1.2 ± 0.3	0.8 ± 0.1[ṁ]	0.8 ± 0.2	0.9 ± 0.4	0.828	0.761
Spleen BF	5.2 ± 0.7	3.5 ± 0.4	4.5 ± 0.6	4.0 ± 1.0	0.086[ɬ]	0.579
Thymus BF	1.5 ± 0.4	1.2 ± 0.1	1.2 ± 0.1	1.5 ± 0.2	0.221	0.426
BAT BF	1.1 ± 0.1	1.1 ± 0.1	0.9 ± 0.1	1.1 ± 0.2	0.983	0.587
L.Dorsi BF	0.2 ± 0.0	0.2 ± 0.0	0.2 ± 0.0	0.2 ± 0.1	0.551	0.902

Values are reported as mean ± SEM. C/CQ is the control-fed group, NR is the entire nutrient restricted group, LQ is the lower quartile of NR, UQ is the upper quartile of NR, BAT is brown adipose tissue, L.Dorsi is latissimus dorsi muscle.
Tissue blood flow is measured in ml/min/g.
[ṅ] Data available from one fewer animal.
[ṁ] Data available from two fewer animals.
[a,b,c] Means with different letters are statistically different across quartiles (CQ, LQ, UQ).
* $p < 0.05$.
[ɬ] $p < 0.10$.

Table 3-5: Pearson's correlation values for fetal tissue blood flow (BF) with fetal weight, fetal heart rate (HR), maternal starting weight (GD 35), gestational weight gain (GWG %), cotyledon and caruncle weight, maternal mean arterial pressure (mMAP), and uterine artery blood flow (UABF).

	Fetal weight, kg	Fetal HR, bpm	GD 35, kg	GWG %	Cotyledon weight, g	Caruncle weight, g	mMAP, mmHg[ṅ]	UABF, ml/min[ṅ]
Brain BF	0.48*	-0.34*	0.42*	0.36*	0.18	-0.18	0.11	0.07
Heart BF	0.50*	0.13	0.17	0.10	0.21	-0.11	0.39*	-0.01
Pancreas BF	0.27	0.13	0.19	0.09	0.29	0.02	0.06	-0.24
Kidneys BF	0.22	0.14	0.43*	0.10	0.24	0.15	-0.03	0.30
Adrenals BF	-0.13	0.16	0.07	0.02	-0.14	-0.48*	0.32[†]	-0.11
Liver BF	0.32[†]	0.28	0.22	0.23	0.25	-0.07	0.01	-0.10
Lungs BF	0.11	-0.33[†]	0.01	0.18	0.29	-0.02	-0.01	0.29
Spleen BF	-0.24	-0.22	0.02	-0.04	0.04	-0.32[†]	-0.07	0.01
Thymus BF	0.27	0.11	0.22	0.01	-0.08	-0.13	0.17	-0.08
BAT BF	0.08	0.42*	0.21	0.16	0.03	0.20	0.06	-0.02
L.Dorsi BF	0.10	0.35*	0.09	-0.18	0.15	-0.16	0.07	-0.29

BAT is brown adipose tissue, L.Dorsi is latissimus dorsi muscle.
Tissue blood flow is measured in ml/min/g.
n = 31
[ṅ] Data available from one fewer animal.
[m̈] Data available from two fewer animals.
* $p < 0.05$.

Table 3-6: Pearson's correlation values for hemodynamic and placental variables with fetal weight, maternal starting weight (GD 35), gestational weight gain (GWG %), maternal mean arterial pressure (mMAP), maternal pulse pressure (mPP), maternal heart rate (mHR), and uterine artery blood flow (UABF).

	Fetal weight, kg	GD 35, kg	GWG %	mMAP, mmHg[ṅ]	mPP, mmHg[ṅ]	mHR, bpm	UABF, ml/min[ṅ]
Fetal values							
Fetal weight, kg		0.40*	0.34[†]	0.09	-0.34[†]	0.24	0.07
Ponderal index	0.38*	0.04[†]	0.03	0.02	0.15	0.13	-0.01
Tibia length[ṁ], mm	0.52*	0.38*	0.30	0.27	-0.38*	0.31[†]	-0.09
Fetal hemodynamics							
Fetal MAP, mmHg	-0.08	-0.31[†]	-0.05	0.37*	-0.36*	-0.38*	0.27
Fetal PP, mmHg	-0.17	-0.16	0.09	0.44*	0.14	-0.26	0.29
Fetal heart rate, bpm	-0.13	-0.05	-0.34[†]	-0.08	-0.01	0.16	-0.39*
Uterine & placental values							
Empty uterus, kg	0.32[†]	0.39*	0.20	0.05	-0.33[†]	0.39*	0.13
Cotyledon, g	0.55*	0.42*	0.22	-0.20	-0.48*	0.33[†]	0.12
Caruncle, g	0.10	0.26	0.08	-0.25	-0.06	0.33[†]	0.41*
Cotyledon BF	0.29	0.22	0.41*	0.17	<0.00	0.15	0.08
Placentome number	-0.08	-0.03	-0.21	-0.06	-0.12	0.24	0.09
Placentome type	-0.32[†]	-0.04	0.09	-0.25	0.23	-0.16	0.15
Placental:fetal ratio	0.07	0.22	-0.17	-0.42[†]	-0.32[†]	0.33*	0.16
Cotyledon:dam ratio	0.40*	-0.03	-0.06	-0.13	-0.49*	0.21	0.05
Caruncle:dam ratio	-0.02	-0.02	-0.08	-0.21	-0.06	0.27	0.38*
Cotyledon:fetus ratio	0.14	0.25	-0.22	-0.35	-0.39*	0.30	0.04
Caruncle:fetus ratio	-0.12	0.04	0.02	-0.34*	0.00	0.21	0.31[†]

Tissue blood flow is measured in ml/min/g.
n = 31
[ṅ] Data available from one fewer animal.
[ṁ] Data available from two fewer animals.
* $p < 0.05$.
[†] $p < 0.10$.

Table 3-5. Brain BF was positively correlated with fetal weight, initial maternal weight, and GWG %, but negatively correlated with fetal HR ($p < 0.048$). Renal BF was positively correlated with initial maternal weight ($p = 0.017$), while cardiac BF was positively correlated with fetal weight and mMAP ($p < 0.031$). Fetal HR was positively correlated with BAT and LD BF ($p < 0.035$).

Fetal weight was positively correlated with GD 35 maternal weights ($p < 0.041$ and GD 117 maternal weights ($r(29) = 0.44$, $p < 0.030$). All correlation values for hemodynamic and placental variables are presented in Table 3-6. Fetal weights were positively correlated with ponderal indices, tibial length, cotyledon weight, and cotyledon:dam ratio ($p < 0.035$). Uterine and cotyledon weights were greater for ewes with greater initial body weights ($p < 0.029$), and change in maternal body weight, as a percentage was positively correlated with cotyledon tissue BF ($p = 0.024$). Length of the fetal tibia was negatively correlated with maternal pulse pressure (mPP; $p = 0.04$) and positively correlated with GD 35 maternal weight ($p = 0.041$). Fetal mean arterial pressure was positively correlated with mMAP and negatively correlated with maternal HR and maternal PP ($p < 0.048$). Fetal pulse pressure was also positively associated with mMAP ($p = 0.013$). Fetal HR was negatively associated with UABF ($p = 0.039$).

Cotyledon mass, cotyledon:dam ratio, and cotyledon:fetus ratio were negatively correlated with mPP ($p < 0.024$; Table 3-6). Maternal HR was positively correlated with uterine weight and placental:fetal ratio ($p < 0.048$). Caruncular weight and caruncle:dam ratio were positively correlated with UABF ($p < 0.042$). Caruncle:fetus ratio was negatively correlated with mMAP ($p = 0.046$).

3.4. Discussion

In this study, the range of fetal weights was greater within NR than control fed ewes, as seen previously [19, 20, 25], however few fetuses weighing less than 2 SD below the control mean were observed and there was overlap between fetuses in the LQ and CQ groups. Despite the lack of extremely small fetuses, the differentials in organ size and BF were consistent with asymmetrical FGR growth patterns. The quartile model developed by our team is ideal for this cohort, providing insight into the changes and possible pathophysiology behind relative FGR [19, 20]. For the brain and adrenals, relative weights increased while BF declined with lower fetal weights in NR ewes. Pancreatic and kidney BF were reduced by dietary restriction.

The identified changes are consistent with asymmetrical fetal growth, which is a primary indicator of and diagnostic tool for FGR [26]. Depending on the timing and severity of insult, NR results in a range of fetal responses [27]. In our study, overall fetal size was not affected significantly, which highlights the importance of looking beyond fetal weight to identify indices of FGR [17, 27, 28]. Symmetrical growth restriction has been linked to constitutionally small fetuses or global insults such as genetic errors and infectious or toxic conditions and is considered less severe than asymmetrical fetal growth [26]. Asymmetrical fetal growth is associated with a protective response from the fetus, intended to save the most vital organs, such as the brain and adrenal glands.

The brain sparing mechanism occurs after activation of the carotid chemoreceptor, which initiates vagal reductions in fetal HR, and sympathetic vasoconstriction of peripheral vessels to redirect BF to the brain [29, 30]. Researchers have demonstrated that fetal hypoxemia, secondary to placental insufficiency and/or maternal hypoxia, activates

this chemoreceptor [31]. While this may be beneficial in cases of acute hypoxia, chronic hypoxia is likely to result in asymmetrical FGR [5]. As with our model, asymmetrical FGR has been seen in a variety of NR studies [6, 32], and with demonstrably similar physiological outcomes [18, 33]. The carotid receptor is known to be involved in NR fetal growth [6], and it can respond to hypoglycemia in addition to hypoxemia [5, 8]. Many models of mid- and late-gestational NR of ewes have resulted in various degrees of hypoglycemia in the fetus and dam and/or reduced uptake of glucose by the placenta [15, 34–38]. It is likely that hypoglycemia from NR stimulates the carotid body receptor to induce a similar, but possibly slower cardiovascular response [6, 33]. Available evidence suggests that NR can elicit a redistribution of BF, causing asymmetrical fetal growth, through hypoglycemia, hypoxemia, or a combination of those two factors [4, 30]. Additionally, Chassen and Jansson theorize that the placenta can partition available nutrients by altering expression of transporters, although these global changes have not been associated with asymmetrical growth [13].

Our results add to those in which placental weights and UABF are unaffected by dietary restriction [28, 38, 39]. Conflicting results are associated with compromised placental weights, uterine and placental BF, and capillary development in response to NR in mid- to late-gestation [27, 40, 41] while others have showed a compensatory gain in placental weight [42]. Placental weight is a marker of nutrient exchange surface area [43], particularly since placental and fetal weights are typically positively correlated [39, 44]. The fetal:placental weight ratio is considered an index of placental efficiency or of FGR [43, 45, 46]. When this relationship is not maintained, and a small fetus is associated with a large placenta, human offspring have been at higher risk of adult hypertension [47]. In

some studies small placental size was more impacted by initial maternal condition than NR [45, 48, 49]. While overall placental size, and placentome portions were not impacted by diet, there were greater cotyledon:dam weight ratios in NR ewes, and cotyledonary weights were directly associated with fetal weights. Studies in which there has been reductions in caruncle [50, 51] or cotyledonary growth in NR ewes [52], or a shift to more C and D placentomes than A and B [40], imply the placenta is trying to compensate for NR.

In sheep, placentome growth is considered complete by mid-gestation, and late gestational changes are primarily increases in capillary area density [27, 53]. In the present study, cotyledonary BF was not different between treatments. Luther et al. identified reduced capillary area density within the maternal caruncle, which implied reduced caruncular BF in their NR model [54]. Our model did not result in a difference in UABF between C and NR dams, but UABF was correlated with the caruncular mass. Healthy BF and a developed vasculature are considered essential to placental nutrient transport, as there is a direct relationship between transport efficiency and UABF [32, 55, 56]. The effect of NR on UABF can be surprisingly modest and varies widely among studies, likely due to differences in severity and duration of NR [35, 57]. A decrease in BF is typically associated with an increased vascular resistance [27], which was not detected in the present study, but the anticipated negative correlation between resistance index and UABF was detected. It has been theorized that an increase in mS/D ratio may be a compensatory mechanism for low placental mass in NR ewes [58]. While we didn't observe a difference in placental weights [59], dams with LQ fetuses did have higher mS/D ratios than UQ fetuses.

Our results showed the anticipated fetal response in an FGR sheep model. Fetal weights within the NR group were variable, and the fetal growth pattern was asymmetrical, supporting a brain sparing pathophysiology. This indicates that a proportion of fetuses responded to reduced nutrients and/or oxygen supply by diverting BF to the brain as the top priority for growth/survival. This theoretically protective response comes at a high cost. Increased systemic vascular resistance directs a higher volume of blood toward the lower resistance in the cerebral vasculature. The developing systemic tissues compromised by low levels of oxygen and nutrients then receive even lower quantities of blood. Lighter organ weights from lighter fetuses are not representative of this phenomenon, but the specificity of only adrenal and brain weights not declining linearly with fetal weights, and relative weights increasing with decreasing fetal weight is highly indicative of this brain sparing mechanism.

Interestingly, with relatively large brains, yet the lowest measured cerebral tissue BF, there is an indication that the brain sparing efforts in the LQ were insufficient to protect cerebral tissue development and angiogenesis. This may indicate that the compromise was too severe, or that the theory of brain sparing is based on acute insults, not a chronic state of NR. If BF is low as a result of the brain sparing efforts, cerebral tissue angiogenesis could be a potential biomarker for relative FGR severity in terminal studies. The UQ fetuses tended to have greater BF to tissues than controls, which indicates that the efforts to increase flow to the brain were successful. Similarly, cerebral capillary density can be reduced during acute hypoxemia [29]. The redistribution hierarchy was summarized by Cohen et al. noting that cognitive function will be prioritized initially, by an increase in BF to the frontal lobes, whereas in extreme instances it will retreat further

and hyperperfuse the brainstem and basal ganglia [2]. In addition to the redistribution of flow, hypoxia decreases angiogenic protein expression, and capillary area density in the fetal brain [29], which corresponds with the reduced BF we demonstrated. In humans and other mammals there are links between low birthweight and lower mental acuity [6].

Nutrient restriction in our study caused an increase in relative heart weights. Blood flow, however, was highest in cerebral tissue of C fetuses, and lowest in LQ fetuses. Circulation to the brain is enhanced by a shift toward higher left ventricular output and lower carotid resistance, and increased flow within the ductus venosus [18], while simultaneous mechanisms reduce systemic vascular resistance and subsequently right ventricular output [9, 60]. Shuttling this pooling blood supply preferentially toward the cerebral vessels puts an extra strain on the heart. The high relative weight of LQ hearts, and the low perfusion rate may indicate that while the heart worked strenuously, it was not able to sufficiently perfuse itself, despite its hypertrophy. The relative FGR changes resulting from NR, however, can be variable, and may present differently than those linked to absolute FGR or hypoxemia [18].

The pancreas is a notable victim of the brain-sparing response, as a decrease in B-cell mass has been described for multiple FGR models [61–63], and diabetes is one of the primary concerning DOHaD sequelae [64]. Extensive remodeling of B-cells occurs during late gestation [64], so it may be assumed that susceptibility is higher with late insults. In an early NR model, where fetal blood glucose and oxygen were unchanged, pancreatic BF was not different between treatments, but variation in sample values was high [18]. Pancreatic BF was not impacted by heat stress in late gestation [65], but it was greater in FGR fetuses following carunculectomy [66]. Results from a study of mid-gestation heat

stressed ewes revealed a reduction in pancreatic islet vascularity that was more severe than the reduction in fetal weights. A corresponding reduction in hepatocyte growth factor production from pancreatic endothelial cells, and VEGFA from pancreatic β-cells likely explained the compromise, and the resulting risk of type-2 diabetes in adults that experienced FGR [67]. These results are similar to our findings, with reduced pancreatic BFs in NR fetuses. Even in the UQ, BF to the pancreas tended to be less than that for C fetuses.

The sentinel variable for FGR might be reduced BF within the renal artery. Kidneys have an autoregulatory system in adults that maintains consistent blood pressures for appropriate functions. It is theorized that this system activates in hypoxic situations, prior to the brain sparing redistribution of blood [68, 69], although, denervation at the carotid sinus prevented the decrease in renal BF [70]. The consequences appear to depend on the degree of hypoxemia, as demonstrated in ewes exposed to hypoxic episodes during late gestation [71]. Additionally, studies have shown increased flow in the fetal renal artery using doppler on NR ewes, that showed no other obvious signs of FGR, including stable renal mass [69]. In the present study, renal tissue BF decreased ~35% in NR fetuses compared to C fetuses without a reduction in mass or relative mass. With the exception of BF, the mass of the kidneys was positively correlated with fetal weight, maternal weight, GWG, and cotyledonary mass. Given the reduction in BF to the kidneys, it would be expected that the fetal kidneys would have fewer, but larger glomeruli, resulting in adult kidneys with fewer functioning nephrons, hypertension, and renal disease [69].

3.5. Conclusion

Despite the known graded response to NR, with lower fetal weights being correlated with greater severity of cardiovascular disease [26, 72], most reports in the literature recognize that fetal weight alone is a poor determinant of FGR [43]. While using lower fetal weight percentiles can increase the positive predictive value of severe FGR cases, a greater proportion of compromised AGA fetuses will not be identified using those cutoffs. The quartiles used by our group provide insight into variations of compromise caused globally in NR offspring, versus compromises that may be more severe at lower fetal weights. The correlation of fetal weight with fetal organ weights, with the exception of brain and adrenal weights, revealed that relative weights were negatively correlated with fetal weights, but not absolute weights of the organs. It was also interesting that weights of cotyledons and cotyledon:dam ratios were correlated with fetal weight, while caruncular weights were not. This same study design has consistently resulted in varied phenotypes. When performing necropsies on GD 125 and GD 135, there were higher percentages (25%) of NR fetuses below the 2SD cutoff than in the current study (<10%), and placentome weights were less for NR than C ewes [20, 25]. Dietary insults may impact the dam to a different degree depending on her age, body condition, health, prior acclimation, resilience, and duration of restriction. The level of malnutrition may then impact placental growth and angiogenesis depending on the timing and duration of the insult, and placental phenotype. Finally, the fetus may respond to hypoglycemia and nutrient deficiency and/or hypoxemia if thresholds are reached. When making so many comparisons, it is more important to identify variations in the response, which we have shown here with the quartile model.

3.6. References

1. George LA, Zhang L, Tuersunjiang N, Ma Y, Long NM, Uthlaut AB, Smith DT, Nathanielsz PW, Ford SP. Early maternal undernutrition programs increased feed intake, altered glucose metabolism and insulin secretion, and liver function in aged female offspring. *Am J Physiol Regul Integr Comp Physiol* 2012; **302**:R795-804.

2. Cohen E, Baerts W, van Bel F. Brain-Sparing in Intrauterine Growth Restriction: Considerations for the Neonatologist. *Neonatology* 2015; **108**:269–276.

3. Kuo AH, Li C, Huber HF, Clarke GD, Nathanielsz PW. Intrauterine growth restriction results in persistent vascular mismatch in adulthood: Persistent vascular mismatch in IUGR. *J Physiol* 2018; **596**:5777–5790.

4. Armitage JA, Khan IY, Taylor PD, Nathanielsz PW, Poston L. Developmental programming of the metabolic syndrome by maternal nutritional imbalance: how strong is the evidence from experimental models in mammals? *J Physiol* 2004; **561**:355–377.

5. Giussani DA. The fetal brain sparing response to hypoxia: physiological mechanisms. *J Physiol* 2016; **594**:1215–1230.

6. Burrage D, Green LR, Moss TJM, Sloboda DM, Nitsos I, Newnham JP, Hanson MA. The carotid bodies influence growth responses to moderate maternal undernutrition in late-gestation fetal sheep. *BJOG* 2008; **115**:261–268.

7. Gardner DS, Fletcher AJW, Bloomfield MR, Fowden AL, Giussani DA. Effects of prevailing hypoxaemia, acidaemia or hypoglycaemia upon the cardiovascular, endocrine and metabolic responses to acute hypoxaemia in the ovine fetus. *J Physiol* 2002; **540**:351–366.

8. Camm EJ, Hansell JA, Kane AD, Herrera EA, Lewis C, Wong S, Morrell NW, Giussani DA. Partial contributions of developmental hypoxia and undernutrition to prenatal alterations in somatic growth and cardiovascular structure and function. *Am J Obstet Gynecol* 2010; **203**:495.e24-34.

9. Malhotra A, Allison BJ, Castillo-Melendez M, Jenkin G, Polglase GR, Miller SL. Neonatal Morbidities of Fetal Growth Restriction: Pathophysiology and Impact. *Front Endocrinol* 2019; **10**.

10. Colella M, Frérot A, Novais ARB, Baud O. Neonatal and Long-Term Consequences of Fetal Growth Restriction. *Curr Pediatr Rev* 2018; **14**:212–218.

11. VandenBosche RC, Kirchner JT. Intrauterine Growth Retardation. *Am Fam Physician* 1998; **58**:1384–1390.

12. Anderson NH, Sadler LC, Stewart AW, Fyfe EM, McCowan LME. Independent risk factors for infants who are small for gestational age by customised birthweight centiles in a multi-ethnic New Zealand population. *Aust N Z J Obstet Gynaecol* 2013; **53**:136–142.

13. Chassen S, Jansson T. Complex, coordinated and highly regulated changes in placental signaling and nutrient transport capacity in IUGR. *Biochim Biophys Acta Mol Basis Dis* 2020; **1866**.

14. Cunningham FG (ed.). *Williams Obstetrics*, 25th ed. New York: McGraw-Hill Medical; 2014.

15. Anthony RV, Scheaffer AN, Wright CD, Regnault TRH. Ruminant models of prenatal growth restriction. *Reprod Suppl* 2003:183–194.

16. Gaccioli F, Lager S, Powell TL, Jansson T. Placental transport in response to altered maternal nutrition. *J Dev Orig Health Dis* 2013; **4**:101–115.

17. Oliver MH, Hawkins P, Harding JE. Periconceptional undernutrition alters growth trajectory and metabolic and endocrine responses to fasting in late-gestation fetal sheep. *Pediatr Res* 2005; **57**:591–598.

18. Burrage DM, Braddick L, Cleal JK, Costello P, Noakes DE, Hanson MA, Green LR. The late gestation fetal cardiovascular response to hypoglycaemia is modified by prior peri-implantation undernutrition in sheep. *J Physiol* 2009; **587**:611–624.

19. Sandoval C, Lambo CA, Beason K, Dunlap KA, Satterfield MC. Effect of maternal nutrient restriction on skeletal muscle mass and associated molecular pathways in SGA and Non-SGA sheep fetuses. *Domest Anim Endocrinol* 2020:106443.

20. Edwards AK, McKnight SM, Askelson K, McKnight JR, Dunlap KA, Satterfield MC. Adaptive responses to maternal nutrient restriction alter placental transport in ewes. *Placenta* 2020; **96**:1–9.

21. National Research Council. *Nutrient requirements of small ruminants: sheep, goats, cervids, and new world camelids*. Washington DC: National Academies Press; 2007.

22. Washburn SE, Sawant OB, Lunde ER, Wu G, Cudd TA. Acute alcohol exposure, acidemia or glutamine administration impacts amino acid homeostasis in ovine maternal and fetal plasma. *Amino Acids* 2013; **45**:543–554.

23. MacKay EE, Washburn KE, Padgett AL, Fajt VR, Lo C-P, Mays TP, Washburn SE. Pharmacokinetics of tulathromycin in fetal sheep and pregnant ewes. *J Vet Pharmacol Ther* 2019; **42**:373–379.

24. Lang U, Baker R, Khoury J, Clark KE. Fetal umbilical vascular response to chronic reductions in uteroplacental blood flow in late-term sheep. *Am J Obstet Gynecol* 2002; **187**:178–186.

25. Lambo CA, Edwards AK, Bazer FW, Dunlap K, Satterfield MC. Development of a surgical procedure for removal of a placentome from a pregnant ewe during gestation. *J Anim Sci Biotechnol* 2020; **11**:48–55.

26. Ross MG, Mansano RZ. Fetal Growth Restriction: Medscape Reference: Drugs, Diseases and Procedures. Emedicine.medscape.com/article/261226-overview. Accessed 13 February 2020.

27. Vonnahme KA, Lemley CO, Shukla P, O'Rourke ST. 2011 and 2012 Early Careers Achievement Awards: Placental programming: how the maternal environment can impact placental function. *J Anim Sci* 2013; **91**:2467–2480.

28. Lekatz LA, Swanson TJ, Camacho LE, van Emon ML, Schauer CS, Maddock Carlin KR, Hammer CJ, Lemley CO, Vonnahme KA. Maternal metabolizable protein restriction during late gestation on uterine and umbilical blood flows and maternal and fetal amino acid concentrations near term in sheep. *Anim Reprod Sci* 2015; **158**:115–125.

29. Nalivaeva NN, Turner AJ, Zhuravin IA. Role of Prenatal Hypoxia in Brain Development, Cognitive Functions, and Neurodegeneration. *Front Neurosci* 2018; **12**.

30. Giussani DA. The vulnerable developing brain. *Proc Natl Acad Sci U S A* 2011; **108**:2641–2642.

31. Stefopoulou M, Johnson J, Wilsgaard T, Lindgren P, Herling L, Kiserud T, Acharya G. Volume blood flow-based indices of fetal brain sparing in the second half of pregnancy: A longitudinal study. *Acta Obstet Gynecol Scand* 2020; **00**:1–11.

32. Lemley CO, Vonnahme KA. Physiology and Endocrinology Symposium: Alterations in uteroplacental hemodynamics during melatonin supplementation in sheep and cattle. *J Anim Sci* 2017; **95**:2211–2221.

33. Cleal JK, Bagby S, Hanson MA, Gardiner HM, Green LR. The effect of late gestation foetal hypoglycaemia on cardiovascular and endocrine function in sheep. *J Dev Orig Health Dis* 2010; **1**:42–49.

34. Edwards LJ, McMillen IC. Maternal undernutrition increases arterial blood pressure in the sheep fetus during late gestation. *J Physiol* 2001; **533**:561–570.

35. Chandler KD, Leury BJ, Bird AR, Bell AW. Effects of undernutrition and exercise during late pregnancy on uterine, fetal and uteroplacental metabolism in the ewe. *Br J Nutr* 1985; **53**:625–635.

36. Hoffman F, Boretto E, Vitale S, Gonzalez V, Vidal G, Pardo MF, Flores MF, Garcia F, Bagnis G, Queiroz OC, others. Maternal nutritional restriction during late gestation impairs development of the reproductive organs in both male and female lambs. *Theriogenology* 2018; **108**:331–338.

37. Lemley CO, Camacho LE, Meyer AM, Kapphahn M, Caton JS, Vonnahme KA. Dietary melatonin supplementation alters uteroplacental amino acid flux during intrauterine growth restriction in ewes. *Animal* 2013; **7**:1500–1507.

38. Vonnahme KA, Hess BW, Hansen TR, McCormick RJ, Rule DC, Moss GE, Murdoch WJ, Nijland MJ, Skinner DC, Nathanielsz PW, Ford SP. Maternal undernutrition from early- to mid-gestation leads to growth retardation, cardiac ventricular hypertrophy, and increased liver weight in the fetal sheep. *Biol Reprod* 2003; **69**:133–140.

39. Alexander G. Studies on the placenta of the sheep (Ovis aries L.). *J Reprod Infertil* 1964; **7**:289–305.

40. Osgerby JC, Wathes DC, Howard D, Gadd TS. The effect of maternal undernutrition on the placental growth trajectory and the uterine insulin-like growth factor axis in the pregnant ewe. *J Endocrinol* 2004; **182**:89–103.

41. Morriss FH, Rosenfeld CR, Crandell SS, Adcock EW. Effects of fasting on uterine blood flow and substrate uptake in sheep. *J Nutr* 1980; **110**:2433–2443.

42. McCrabb GJ, Egan AR, Hosking BJ. Maternal undernutrition during mid-pregnancy in sheep. Placental size and its relationship to calcium transfer during late pregnancy. *Br J Nutr* 1991; **65**:157–168.

43. Simmons R. Abnormalities of Fetal Growth. In: Gleason CA, Juul SE (eds.), *Avery's diseases of the newborn*. Philadelphia: Elsevier; 2018:61–69.

44. Gadd TS, Aitken RP, Wallace JM, Wathes DC. Effect of a high maternal dietary intake during mid-gestation on components of the utero-placental insulin-like growth factor (IGF) system in adolescent sheep with retarded placental development. *J Reprod Infertil* 2000; **118**:407–416.

45. Wallace JM, Milne JS, Aitken RP. Effect of weight and adiposity at conception and wide variations in gestational dietary intake on pregnancy outcome and early postnatal performance in young adolescent sheep. *Biol Reprod* 2010; **82**:320–330.

46. Ghidini A. Idiopathic fetal growth restriction: a pathophysiologic approach. *Obstet Gynecol Surv* 1996; **51**:376–382.

47. Barker DJ, Bull AR, Osmond C, Simmonds SJ. Fetal and placental size and risk of hypertension in adult life. *BMJ* 1990; **301**:259–262.

48. McCrabb GJ, Egan AR, Hosking BJ. Maternal undernutrition during mid-pregnancy in sheep: variable effects on placental growth. *J Agric Sci* 1992; **118**:127–132.

49. Vonnahme KA, Hess BW, Nijland MJ, Nathanielsz PW, Ford SP. Placentomal differentiation may compensate for maternal nutrient restriction in ewes adapted to harsh range conditions. *J Anim Sci* 2006; **84**:3451–3459.

50. Lemley CO, Meyer AM, Camacho LE, Neville TL, Newman DJ, Caton JS, Vonnahme KA. Melatonin supplementation alters uteroplacental hemodynamics and fetal development in an ovine model of intrauterine growth restriction. *Am J Physiol Regul Integr Comp Physiol* 2012; **302**:R454-467.

51. Eifert AW, Wilson ME, Vonnahme KA, Camacho LE, Borowicz PP, Redmer DA, Romero S, Dorsam S, Haring J, Lemley CO. Effect of melatonin or maternal nutrient restriction on vascularity and cell proliferation in the ovine placenta. *Anim Reprod Sci* 2015; **153**:13–21.

52. Clarke L, Heasman L, Juniper DT, Symonds ME. Maternal nutrition in early-mid gestation and placental size in sheep. *Br J Nutr* 1998; **79**:359–364.

53. Luther JS, Redmer DA, Reynolds LP, Wallace JM. Nutritional paradigms of ovine fetal growth restriction: Implications for human pregnancy. *Hum Fertil (Camb)* 2005; **8**:179–187.

54. Luther JS, Aitken RP, Milne J, Matsuzaki M, Reynolds LP, Redmer DA, Wallace JM. Maternal and fetal growth, body composition, endocrinology, and metabolic status in undernourished adolescent sheep. *Biol Reprod* 2007; **77**:343–350.

55. Vonnahme KA, Lemley CO. Programming the offspring through altered uteroplacental hemodynamics: how maternal environment impacts uterine and umbilical blood flow in cattle, sheep and pigs. *Reprod Fertil Dev* 2012; **24**:97–104.

56. Reynolds LP, Borowicz PP, Caton JS, Vonnahme KA, Luther JS, Buchanan DS, Hafez SA, Grazul-Bilska AT, Redmer DA. Uteroplacental vascular development and placental function: an update. *Int J Dev Biol* 2010; **54**:355–366.

57. Reynolds LP, Borowicz PP, Vonnahme KA, Johnson ML, Grazul-Bilska AT, Wallace JM, Caton JS, Redmer DA. Animal models of placental angiogenesis. *Placenta* 2005; **26**:689–708.

58. Kelly RW. Nutrition and placental development. In: *Proceedings of the Nutrition Society of Australia*; 1992:203–211.

59. González-Cossío T, Delgado H. Functional consequences of maternal malnutrition. *World Rev Nutr Diet* 1991; **64**:139–173.

60. Baschat AA, Gembruch U, Gortner L, Reiss I, Weiner CP, Harman CR. Coronary artery blood flow visualization signifies hemodynamic deterioration in growth-restricted fetuses. *Ultrasound Obstet Gynecol* 2000; **16**:425–431.

61. Hay WW. Recent observations on the regulation of fetal metabolism by glucose. *J Physiol* 2006; **572**:17–24.

62. Brenseke B, Prater MR, Bahamonde J, Gutierrez JC. Current thoughts on maternal nutrition and fetal programming of the metabolic syndrome. *J Pregnancy* 2013:1–13.

63. van Assche FA, Aerts L, Prins FA de. The fetal endocrine pancreas. *Eur J Obstet Gyn R B* 1984; **18**:267–272.

64. Jahan-Mihan A, Rodriguez J, Christie C, Sadeghi M, Zerbe T. The role of maternal dietary proteins in development of metabolic syndrome in offspring. *Nutrients* 2015; **7**:9185–9217.

65. Walker DW, Hale JR, Fawcett AA, Pratt NM. Cardiovascular responses to heat stress in late gestation fetal sheep. *Exp Physiol* 1995; **80**:755–766.

66. Poudel R, McMillen IC, Dunn SL, Zhang S, Morrison JL. Impact of chronic hypoxemia on blood flow to the brain, heart, and adrenal gland in the late-gestation IUGR sheep fetus. *Am J Physiol Regul Integr Comp Physiol* 2015; **308**:R151-162.

67. Rozance PJ, Anderson M, Martinez M, Fahy A, Macko AR, Kailey J, Seedorf GJ, Abman SH, Hay WW, Limesand SW. Placental insufficiency decreases pancreatic vascularity and disrupts hepatocyte growth factor signaling in the pancreatic islet endothelial cell in fetal sheep. *Diabetes* 2015; **64**:555–564.

68. Arbeille P. Fetal arterial Doppler-IUGR and hypoxia. *Eur J Obstet Gyn R B* 1997; **75**:51–53.

69. Barbero A, Porcu C, Spezzigu A, Succu S, Dattena M, Gallus M, Molle G, Naitana S, Gonzalez-Bulnes A, Berlinguer F. Changes in renal hemodynamics of undernourished fetuses appear earlier than IUGR evidences. *J Dev Orig Health Dis* 2018; **9**:338–343.

70. Green LR, Bennet L, Robson S, Hanson MA. The role of carotid chemoreceptors in the effects of hypoxia on renal blood flow in the late gestation sheep fetus. *Exp Physiol* 1997; **82**:183–192.

71. Peeters LL, Sheldon RE, Jones MD, Makowski EL, Meschia G. Blood flow to fetal organs as a function of arterial oxygen content. *Am J Obstet Gynecol* 1979; **135**:637–646.

72. Hanson MA, Gluckman PD. Developmental processes and the induction of cardiovascular function: conceptual aspects. *J Physiol* 2005; **565**:27–34.

4. A STUDY OF ANTIMULLERIAN HORMONE (AMH) IN EWES REGARDING VARIATIONS IN RESULTS FROM ASSAYS AND VARIATIONS DUE TO DAY OF THE ESTROUS CYCLE WITHIN INDIVIDUAL EWES

4.1. Introduction

Anti-Müllerian hormone (AMH), a member of the transforming growth factor-β superfamily, is produced by granulosa cells of developing follicles in females [1]. Concentrations of AMH are highest from pre-antral and antral ovarian follicles, and correlate with antral follicle counts (AFC) [2], ovarian reserve [3, 4], response to controlled ovarian stimulation (COS) [5, 6], and reproductive lifespan [7, 8] in several species. Concentrations of AMH may also correlate with fertility for humans and cattle [9–11]. The perceived production value of AMH as a fertility marker, in comparison to less consistent and predictive hormones such as follicle stimulating hormone and inhibin, led to a rapid entry of AMH to the clinical market. However, the predictive value of AMH is poor within the restrictions of the current testing methods and knowledge.

4.1.1. Physiology of AMH

Concentrations of AMH from growing follicles suppresses FSH-responsiveness and aromatase activity for producing estradiol to regulate follicular recruitment and selection [9]. After a follicle has been selected for dominance, AMH production ceases, allowing aromatase activity to increase. Remaining antral follicles stop producing AMH as they undergo atresia [10]. Concentrations of AMH increase during maturation, reaching their zenith during peak reproductive age (5 ng/ml^{1}), and subsequently declining as ovarian reserves are depleted. A lesser peak (1.5 ng/ml^{1}) of AMH concentration occurs perinatally

[12], the physiology of which is unclear [13]. Reduced AMH concentrations are common with use of hormonal contraceptives (1.9 vs 3.9 ng/ml[1]) [14] and during late pregnancy (0.5 vs 1.69 ng/ml[1]) [15], and undetectable concentrations are considered diagnostic for ovariectomy in women [7], dogs, and cats [16, 17]. Extremely high concentrations of AMH (1.9 – 26.1 vs 1.4 – 7.0 ng/ml[1]) are associated with polycystic ovarian disease [18] based on a dysregulation of AMH expression in pathologic follicles, and concentrations remain elevated as follicles grow [19]. A heritable aspect (0.28 estimate in Nellore cattle) [20] of AMH concentrations may also occur, although environmental factors could impact selection potential, including fetal growth restriction which can compromise ovarian development and may decrease AMH concentrations [21].

4.1.2. Inconsistent testing results

Although AMH concentrations appear relatively stable throughout menstrual and estrous cycles [22, 23], cyclical fluctuations could vary enough to misclassify an individual depending on timing of the sample collection [9, 24, 25]. Breed differences may be responsible for some of the variations with Bos indicus cattle having the highest concentrations of AMH, followed by other beef and then dairy breeds [9]. A lack of standard testing, and agreed unit of measurement has added to inconsistent results and interpretation of AMH values [26]. Other factors which contribute to these discrepancies include, test recalls and redesigns, sample instability, inter-laboratory variations, and assays which can differ in a non-linear manner [27]. The clinical value of AMH concentrations in women may be premature based on a lack of industry standards and sample consistency [28, 29]. Some testing concerns have been recently addressed [30]

with the development of automated kits [31] and an international standard for testing uniformity of AMH in women [32].

4.1.3. Intentions for AMH use

Assisted reproductive technologies are key to rapid advancement of desirable herd genetics, however, high drug and technical costs can make program development a high financial risk for a producer [10, 33]. Having a validated diagnostic marker for fertility could mitigate this risk. Although AMH concentrations and ova production correlate [6, 34, 35], published values for AMH concentrations in dairy cattle herds vary widely from 0.01–400 pg/ml [3, 36] to 10–3198 pg/ml [37]. This lack of consistency across studies makes diagnostic use of findings challenging, beyond creating cutoff comparisons within contemporary groups [6, 9, 33]. Regardless of testing variation, using AMH concentrations to tailor COS protocols for women [38–40] has reduced the risks of hyperstimulation, increased pregnancy rates (17.9 vs 27.7% live birth rate[1]) and reduced COS costs (averaged 29% costs reduction or $500[1,2]) [41]. Preliminary studies indicate the use of AMH concentrations to tailor COS protocols may also be successful in cattle [6, 9, 10].

4.1.4. What changes have been observed for AMH in sheep?

While much effort has been spent studying AMH in cattle, sheep have received less attention despite their high production value worldwide [1, 10].

4.1.4.1. Concentrations of AMH in ewes

Providing a fertility marker for prepubertal lambs would be a major industry boon, to select ewes early based on fertility or response to COS. Lambs sampled at 3 and 5 weeks were positively correlated with AFC and in vitro embryo production at the 5-week

time point[35]. Further, samples from ewe lambs at 3.6 months could be used to select for fertility at first mating [42]. In a longitudinal study, ewes sampled at multiple prepubertal time points had great inconsistency in concentrations of AMH, with peaks occurring in different months within the sample group. Ultimately, these studies determined that precocious sampling was not likely to be productive [34] due to the variation in ovarian maturation rates, inability to plan for sample timing, and differences between contemporary groups.

4.1.4.2. Variations in AMH during the estrous cycle in ewes

At post-pubertal time points, research has debatably linked AMH concentrations with AFC, response to COS, and fertility in ewes [1, 33, 34]. Consistent AMH concentrations throughout an estrous cycle, and between cycles would allow for repeatable results with single time point sample collection. Studies have shown this can occur [22], although proving that there can be high variation is the stronger argument [9, 25]. Waheeb et al. demonstrated that follicular phase changes in AMH concentrations may vary enough to affect repeatability of testing among individual cycling ewes [25]. They used hormonal stimulation to set up precise testing intervals pre-and post-ovulation. The lowest AMH concentrations (0.9 ng/ml) occurred two days after induction of luteolysis, which corresponded with low follicle numbers (4.0 vs 9.7) seen on ultrasound. The lowest point was dramatically different from the high mean of 11.8 ng/ml [25]. Despite these data and the contested confidence in other species, many studies with ewes cited the trusted single measure repeatability in humans and cattle, to support single time point sampling in sheep [1, 43]. To date, no study has assessed individual changes in AMH during a natural

estrous cycle in ewes, which may be important in assessing the diagnostic utility of AMH concentrations in sheep.

4.1.5. Study design

The predictive value of AMH concentrations for ewe productivity could have a major impact for livestock producers in the meat and dairy industries worldwide, promoting the selection of top producing ewes for natural and assisted reproduction success. Conversely, further evidence of testing concerns and result inconsistencies could suggest a lack of applicability for AMH concentrations in the assessment of fertility. Therefore this study aimed to **1**) determine intra-individual variation in AMH concentrations in serum to determine the value of single time point sampling and **2**) examine inter-individual differences in AMH concentrations and determine whether the differences are predictive of response to COS. Concentrations of AMH were hypothesized to have appreciable variability across an estrous cycle, in addition to points of correlation between AMH concentrations and COS response. This study contributes to efforts determining whether AMH can be used to select ovine breeding stock and when samples for AMH concentration should be collected.

4.2. Materials & methods

Animal use approval was not needed because archival serum samples from a previous Texas A&M University IACUC approved study were used (IACUC #2016-0078), in addition to serum from privately owned animals.

4.2.1. Animal data

Data were collected and evaluated from two groups of ewes. Serum was evaluated from Hampshire ewe lambs (EL; n = 21) raised on a private show stock farm (MacLennan

Club Lambs) in Byers, CO. Ewes had similar birthdates (± 1 day) and pedigree and were intended embryo donors for an embryo transfer program to improve genetic merit of the flock. The second study group included Hampshire cross mature ewes (ME; n = 37) with unknown reproductive history and ages, assessed to be older than 12 mo of age, selected from a sale barn as embryo donors for an approved research project and maintained in College Station, TX. All ewes (AE) were maintained on pasture, supplemented with pelleted diets and had *ad libitum* access to water and mineral blocks.

4.2.2. Adolescent and estrous collections

The EL were sampled at 4, 5, and 6 months of age (Figure 4-1). Beginning in September, teaser rams were introduced daily to check for heat. Each EL came into heat naturally and completed at least one estrous cycle and was then synchronized to estrus by inserting a controlled internal drug release (CIDR; progesterone; Zoetis, Parsippany, NJ, USA) intra-vaginally for 12 days. Ewe lambs displayed standing estrus 2–3 days after device removal, and blood collection began 17 days later when they again demonstrated standing estrus with a teaser ram. Blood samples were collected every evening for 18 days to ensure that data for a full estrous cycle was obtained.

4.2.3. Controlled ovarian stimulation

Baseline values for AMH concentration were determined in samples drawn from EL and ME prior to initiating COS using standard 4-day FSH protocols [44, 45]. Briefly, 10 days following insertion of a CIDR in AE, ovulatory stimulation was performed using sequentially decreasing doses of follicle-stimulating hormone (FSH), given intramuscularly (IM) twice daily for 8 injections (Folltropin; Vetoquinol, Fort Worth, TX, USA; 2.5 ml, 1.9 ml, 1.5 ml, and 1.0 ml in ME; 2.2 ml, 1.7 ml, 1.3 ml, and 0.7 ml in EL).

After the 6th injection, CIDRs were removed, and ewes were given 4 mL of Lutalyse IM (Prostaglandin; Zoetis, Parsippany, NJ, USA). The day after the final injection, AE were artificially inseminated (AI) using standard laparoscopic protocols [44]. New CIDRs were placed 3 days later to support the embryos until embryo transfer (ET; standard protocol) [44], 6 days following AI. At the time of collection, ovaries were examined laparoscopically, and all corpora lutea (CL) and follicles ≥ 2 mm diameter were recorded. Recovered embryos were counted, staged, and graded for each ewe [46]. Serum samples were collected from AE prior to COS (baseline), before the 1st and 5th FSH injections (d1, d3), prior to AI (dAI), and prior to ET (dET).

4.2.4. Sample handling

Blood samples were collected from jugular venipuncture into 5 ml BD Vacutainer SS Plus Blood Collection Tubes (Beckton Dickson, Franklin Lakes, NJ, USA), and were allowed to clot for 20 min at room temperature, then centrifuged for 10 min at 2,500 rpm. Serum was transferred into new tubes and stored at -20°C for 1–2 years. Stored serum was thawed and analyzed using the Ovine AMH enzyme-linked immunosorbent assay (ELISA) kit (AL-155; Ansh Labs, Webster, TX, USA). Samples were randomized across 20 plates and run in duplicate according to manufacturer instructions [1, 47]. The monoclonal antibodies used were 7/4A as capture and 37/7 as detection. Serially diluted standards were run in duplicate on each plate, as well as high and low controls.

4.2.5. Statistics

Statistical questions were addressed using SPSS Statistics 26 software (IBM, Armonk, NY, USA) and Graph Pad Prism 6.05 (GraphPad Software Inc., La Jolla, CA, USA). Pearson's correlation coefficients were calculated between AMH concentrations

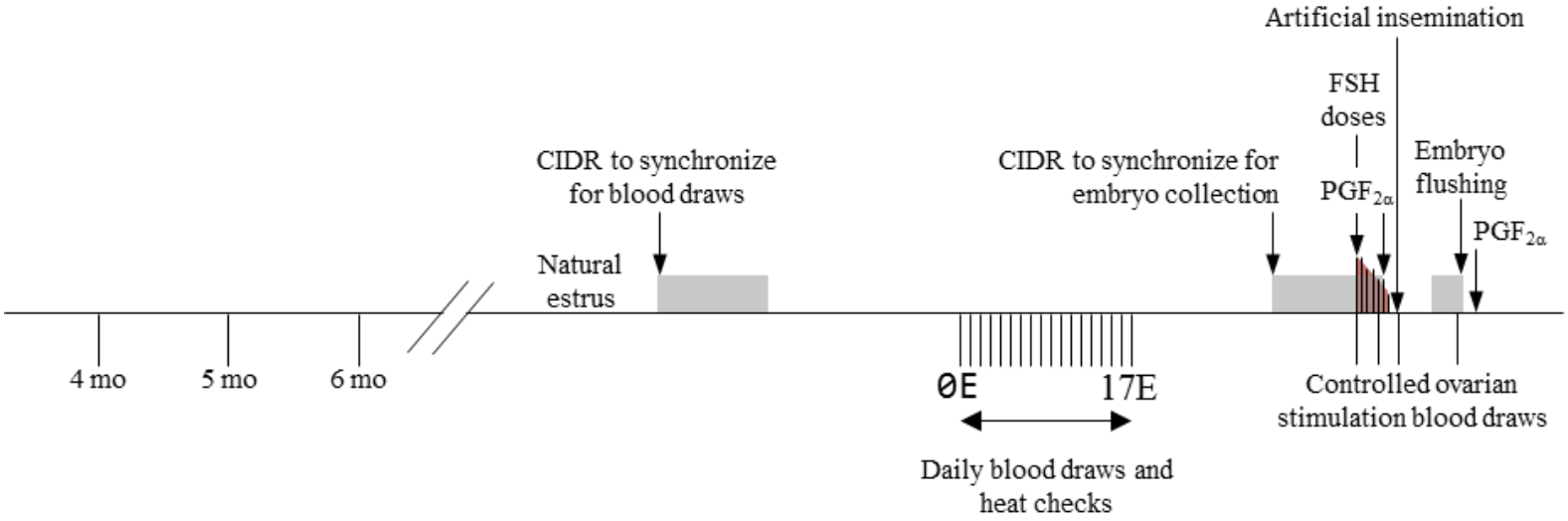

Figure 4-1: Study timeline for controlled ovarian stimulation (COS) protocol, and anti-Müllerian hormone (AMH) sample collection in ewes. Ewe lambs were sampled at 4, 5, and 6 months of age, allowed to cycle naturally in the fall, and then synchronized using a CIDR. Estrous phase sampling began 1 cycle after CIDR inserts were removed and continued from day O through day 17. Synchronization with a CIDR was repeated for controlled ovarian stimulation. Six days after CIDR insertion, lambs were given decreasing doses of FSH, injected IM twice daily for 4 days. The CIDR was then pulled and they were given an IM injection of PGF2α to induce ovulation. The morning following their final FSH injection, they were artificially inseminated, and 6 days later they were surgically flushed to collect embryos.

and ovarian response values. Comparisons between experimental groups were evaluated using a Student's t-test. One-way ANOVA with trend analysis was used to determine the effect of COS on AMH concentrations, and a Tukey post-hoc test identified significant differences based on sample day. Cut-off values for AMH were calculated using receiver-operating characteristic (ROC) analysis, with a target of at least 7 ovarian structures following COS, within each experiment group [33]. Results are reported as mean ± standard error. A p-value of ≤ 0.05 was considered significant, and < 0.10 was considered as a trend toward significance [48], based on wide variation of sample AMH concentrations.

4.3. Results

4.3.1. Sample counts

A single outlier EL was removed from calculations for AMH concentrations. From 20 EL, there were 497 samples, and from 37 ME, there were 154 samples which were assayed for AMH concentrations. Baseline samples were obtained for all ME ewes, but 3 to 14 samples were missing for the COS collection times from these ewes.

4.3.2. Assay performance

The inter-assay coefficient of variation (CV) was 47.7%. Intra-assay precision was moderate, with CVs 8.1% to 23.8% and a median of 11.7%. The r^2 values for the standard curves were 0.98–1.00. The lowest detectable AMH concentration was 0.14 ng/ml.

4.3.3. Comparison of averages between groups

Ovarian response (OR; total of ovarian corpora lutea and follicle count), collected embryos, and transferrable embryo numbers were similar between ME and EL ($p \geq 0.651$;

Table 4-1: Comparison of ovarian responsiveness between study groups and cutoff divisions

	Ewe lambs	Mature ewes	p-value
Ovarian response	8.6 ± 0.8	8.1 ± 0.7	0.651
Corpora lutea	7.8 ± 0.9	7.4 ± 0.7	0.766
Follicles	0.9 ± 0.2	0.7 ± 0.2	0.641
Embryos	5.9 ± 0.8	5.5 ± 0.8	0.786
Transferable embryos	4.5 ± 0.6	4.2 ± 0.7	0.805

	EL-Low	EL-High	p-value	ME-Low	ME-High	p-value
Ovarian response	5.3 ± 0.5	10.0 ± 0.9	0.004*	3.9 ± 0.5	10.4 ± 0.6	0.000*
Corpora lutea	4.8 ± 0.7	9.0 ± 1.0	0.019*	3.1 ± 0.4	9.8 ± 0.7	0.001*
Follicles	0.5 ± 0.3	1.0 ± 0.3	0.284	0.8 ± 0.3	0.7 ± 0.3	0.811
Embryos	3.7 ± 0.8	6.8 ± 1.0	0.083†	1.9 ± 0.3	7.5 ± 1.0	<0.001*
Transferable embryos	3.0 ± 1.0	5.1 ± 0.7	0.103	1.2 ± 0.3	5.9 ± 0.9	0.001*

Ewe lambs (EL) divided based on ROC baseline AMH cutoff value (1.1 ng/ml) for which ovarian response was ≥ 7 (EL-High), or < 7 (EL-Low)
Mature ewes (ME) divided based on ROC baseline AMH cutoff value (0.4ng/ml) for which ovarian response was ≥ 7 (ME-High), or < 7 (ME-Low)
Values are reported as mean ± SEM.
* $p < 0.05$.
† $p < 0.10$.

Table 4-1). Baseline AMH values did not differ between ME and EL ($p = 0.775$; Figure 4-2). Concentrations of AMH in serum during COS were higher in EL than ME ($p \leq 0.054$;). Coefficients of variation during COS were 43.9 ± 4.5% for EL and 62.9 ± 4.8% for ME. For EL, baseline values were positively correlated with OR and embryo counts ($p < 0.020$; Figure 4-3) and tended to be correlated positively with transferable embryos ($p = 0.097$). For ME, d1 samples were positively correlated with OR and CL counts ($p = 0.043$).

4.3.4. Cutoff values

Analysis via ROC identified optimum AMH concentrations to predict ewes with at least 7 ovarian structures in response to COS compared with those with fewer than 7 [33].

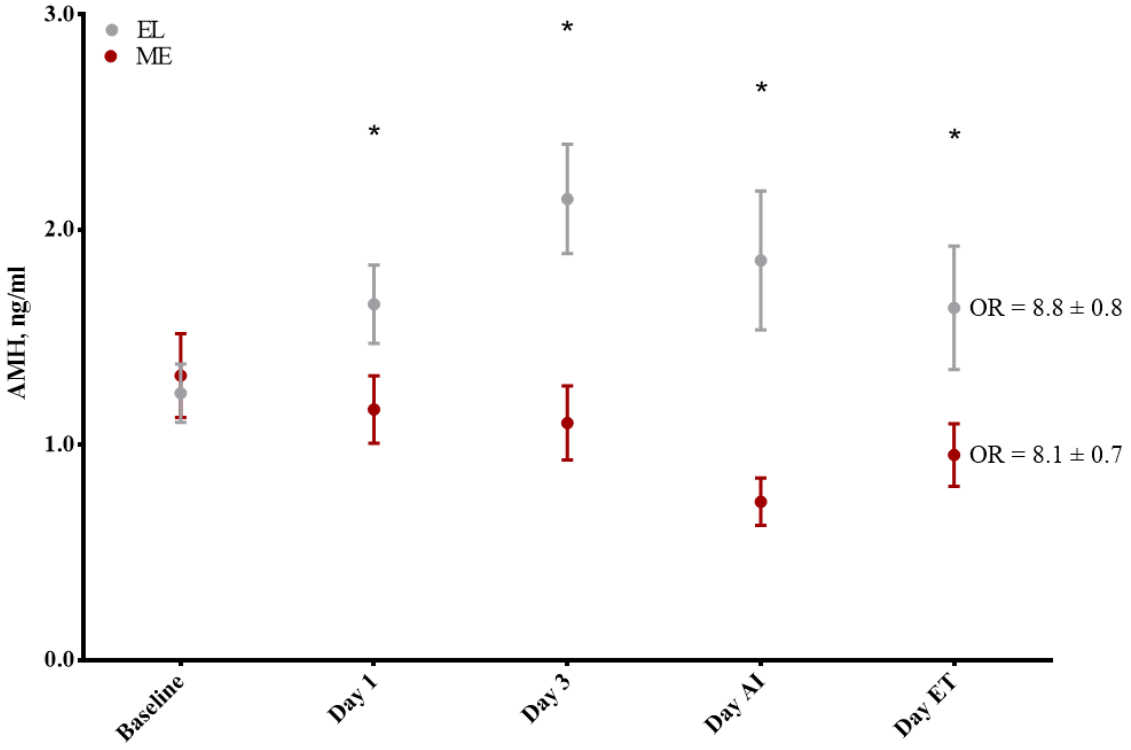

Figure 4-2: Anti-Müllerian hormone concentrations of mature ewes (ME) and ewe lambs (EL) during controlled ovarian stimulation (COS). Samples are baseline (before CIDR), at the start of COS (Day 1), midway through FSH injections (Day 3), the day of AI , and the day of ET . Significantly different ($p < 0.05$) group means are denoted *.

Optimum cutoff values were 1.1 ng/ml AMH for EL and 0.4 ng/ml AMH for ME. These cutoff values gave sensitivities of 89% and 95% with specificities of 55% and 57%, respectively.

4.3.5. Cutoff division comparisons

Concentrations of AMH from ewe lambs below their cutoff (ELL) had a lower baseline than those above the cutoff (ELH; $p < 0.001$; Figure 4-4). Serum AMH concentrations during COS did not differ between ELL and ELH ($p > 0.123$). The average ovarian responses were greater for ELH than ELL ($p = 0.028$; Table 4-1). However, ELL and ELH had comparable embryo and transferable embryo counts ($p > 0.084$).

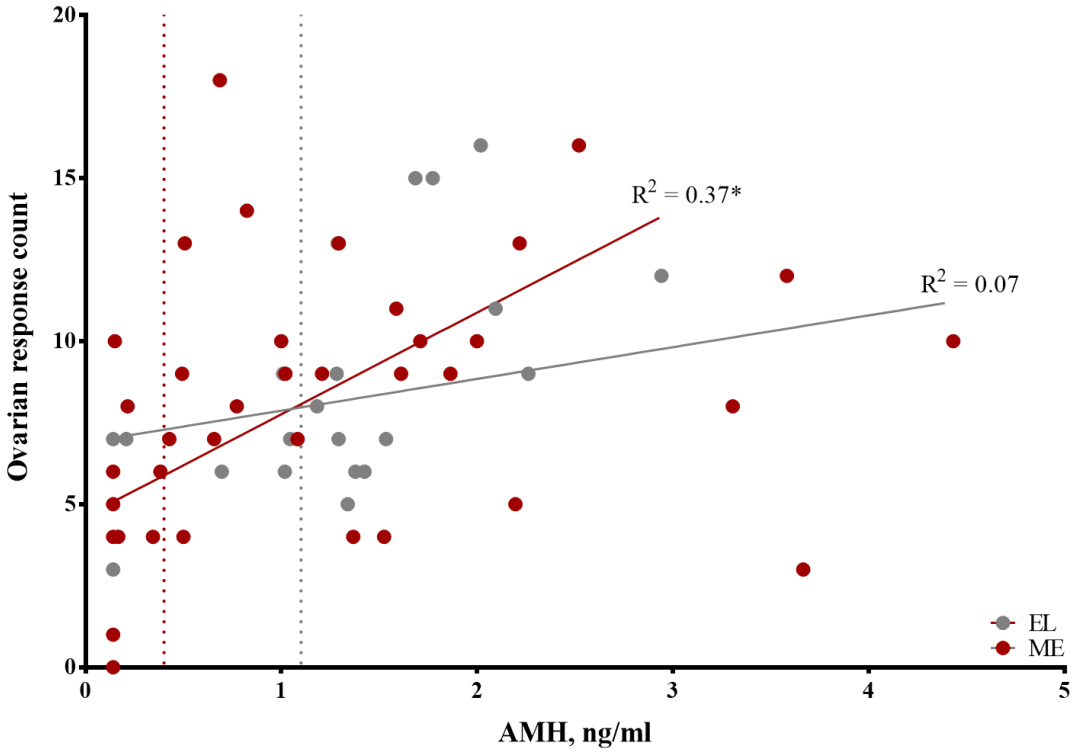

Figure 4-3: Baseline anti-Müllerian hormone (AMH) concentration correlations with ovarian response in ewe lambs and mature ewes. Cutoff values determined by ROC analysis shown with dotted lines. Significant linear correlation ($p < 0.05$) is denoted *.

Mature ewes with baseline AMH concentrations below 0.4 ng/ml (MEL) had a lower average AMH concentration than the division above the cutoff (MEH; 0.2 ± 0.0 vs 1.7 ± 0.2 ng/ml; $p < 0.001$). Concentrations of AMH throughout COS were higher or tended to be higher in MEH compared to MEL (Figure 4-4; $p < 0.063$). Ovarian response for MEH was higher than for MEL ($p < 0.001$; Table 4-1). Embryo count tended to be higher in MEH than MEL ($p = 0.076$). Follicle numbers and transferable embryo counts were comparable between MEH and MEL ($p > 0.210$).

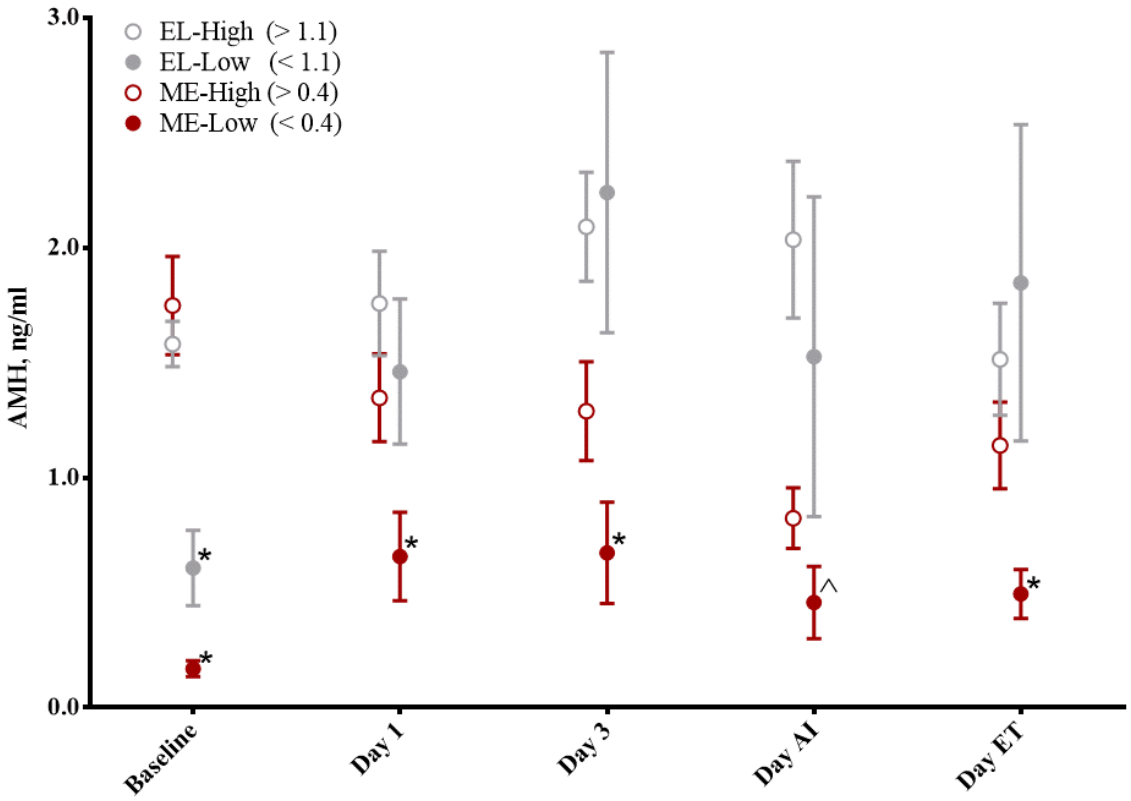

Figure 4-4: Average anti-Müllerian hormone (AMH) concentrations during controlled ovarian stimulation (COS) of mature ewes (ME) and ewe lambs (EL). Cutoff values of AMH were 0.4 ng/ml for mature ewes and 1.1 ng/ml for ewe lambs. Low values that are significantly different ($p < 0.05$) from the high value in the same cohort are marked with an *, and those that tend toward a difference ($p < 0.1$) are marked with a ^.

4.3.6. Values for AMH during the estrous cycle of ewes

Figure 4-5 shows all individual AMH concentrations from EL during an estrous cycle. High intraindividual variation occurred with an average CV of 41.0%. The variation was great enough that at least one sample measured above the baseline cutoff value in 90% (18/20) of EL, or would have changed that ewes assigned category, for at least one day during the cycle. Two ewes had low to undetectable concentrations throughout their cycle and would not have changed categories. Interestingly, concentrations of AMH for those two ewe lambs had the highest and lowest CVs (1.5%

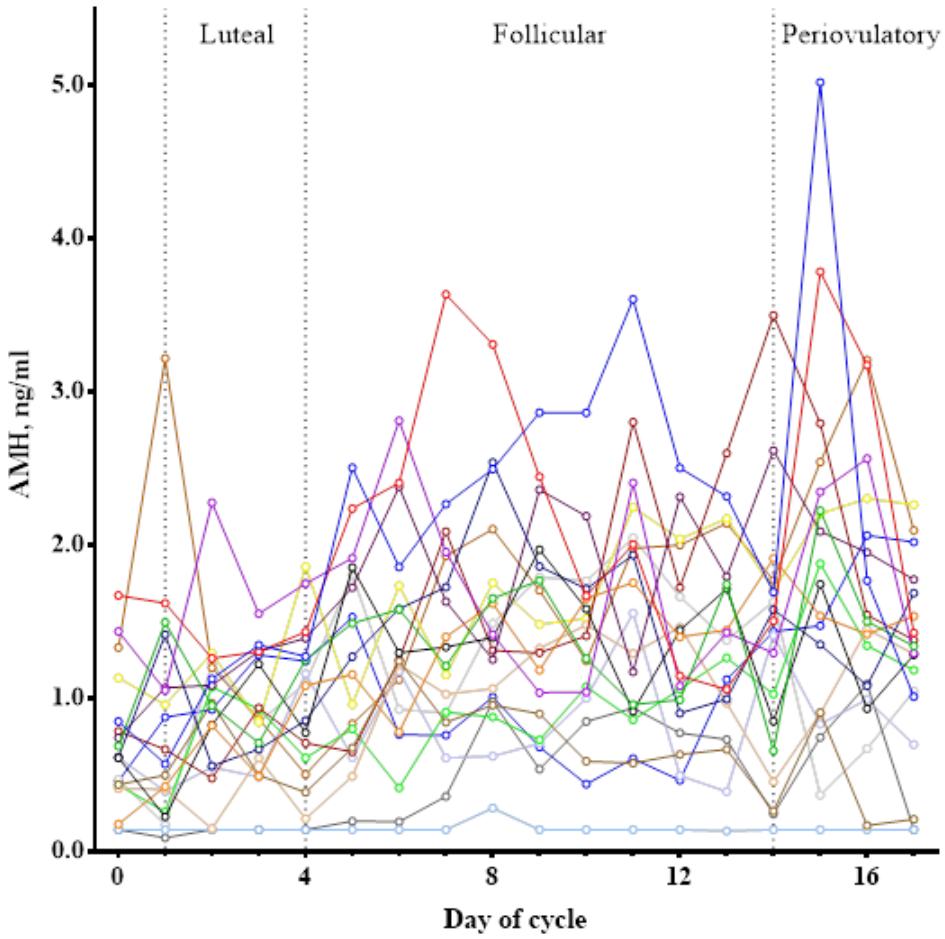

Figure 4-5: Variation of ewe lamb anti-Müllerian hormone during one estrous cycle. Each circle represents a sample. The dashed lines demarcate the phases of the estrous cycle.

and 76.0%) for their estrous cycles, and CVs were not correlated with the percentage of samples consistently above the baseline ($p = 0.562$). Average AMH concentrations were higher for ELH than ELL at multiple time points during the estrous cycle (Figure 4-6). The percentage of samples collected for the 18 days which were above the cutoff was 66.7 ± 5.6% in ELH, which was higher than 34.9 ± 14.5% in ELL ($p = 0.022$).

4.3.7. Analysis of blood samples from adolescent ewes

At 5 months of age, AMH concentrations of EL positively correlated with OR ($r(18) = 0.54$; $p = 0.030$) and tended to positively correlate with embryo count ($r(18) = 0.39$; $p = 0.093$). Concentrations of EL AMH at 6 months tended toward a positive

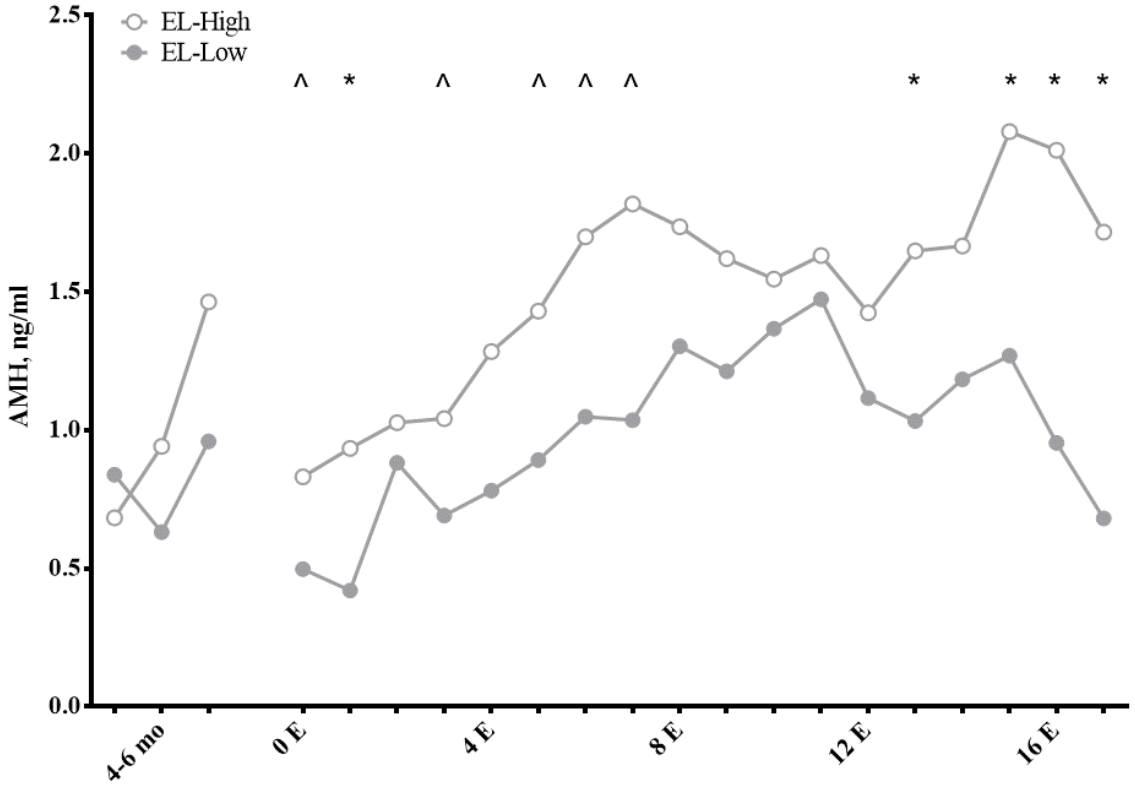

Figure 4-6: Anti-Müllerian hormone concentrations in ewe lambs at 4, 5, and 6 months of age, and during one estrous cycle. Day of standing estrus is marked 0E, and samples were collected for 18 days. Samples are divided by the cutoff value of 1.1 ng/ml. Points where means are significantly different ($p < 0.05$) between EL-High and EL-Low are marked with an *, and those that tend toward a difference ($p < 0.1$) are marked with a ^.

correlation with OR ($r(18) = 0.39$; $p = 0.092$). Concentrations of EL AMH from 4 months of age were not correlated with ovarian response or embryo counts ($p \geq 0.707$). Concentrations of AMH were undetectable in 35% of EL at 4 months of age, 15% at 5 months of age, and 5% at 6 months of age. Trends for AMH concentrations were inconsistent, with 25% of ewes having their highest values at 4 months, 10% at 5 months, and 65% at 6 months of age.

4.4. Discussion

Concentrations of AMH had enough predictive utility as a marker of fertility to occasionally show correlations with COS response, even though intraindividual and testing error variation is high. However, these correlations cannot compensate for the lack of overall baseline information determined. In EL, peaks in AMH concentrations occurred at different ages before puberty. High CVs across estrous cycles with most fluctuations severe enough to change cutoff classification for at least one day of the cycle could also limit diagnostic utility of this analyte. Further, baseline AMH concentrations for ME did not correlate with OR or embryo production, while they did for EL. Although cutoff values could be selected for baseline sample predictability of strong COS response, these AMH concentration ranges may lack sufficient robustness to translate to other test groups or to producer programs. This conclusion is supported by the incongruency of other AMH cutoff values published thus far for sheep [1, 9, 25, 49]. Based on current results and possible analysis imprecision, a deficiency in knowledge and dependable equipment to use AMH effectively for flock management remains.

4.4.1. Prepubertal variations in AMH peaks

Producers would gain the most benefit if they could assess the reproductive potential in their flock at the earliest possible age to prioritize investment in top performers. In humans and cattle, AMH concentrations increase during the prenatal period, peak around 3 months of age and then return to low baseline levels until the subjects mature [9]. In sheep, peak AMH concentrations occur at different ages [34], with a possible link to peak and low AFC [35], and rates of ovarian maturation[50]. This study's results confirm unpredictable AMH concentration peaks and high intra- and interindividual variations in AMH concentrations in EL at 4, 5, and 6 months of age. However, concentrations of AMH in serum of EL at 5 mo of age did correlate with OR. Although technically possible (though statistically not a good fit) to create cutoffs for AMH concentrations from EL at 5- and 6-mo of age to produce significant differences in OR and transferrable embryos, the findings would lack translation to other lamb populations. If EL peak in production of AMH at different rates, a single-point measure of AMH in prepubertal EL is unlikely to provide vigorous insight into future reproductive potential [34]. However, there may be a diagnostic opportunity for multiple samples over the 3–6 mo period for fertility selection from a flock.

4.4.2. Cyclical variations in AMH concentrations

Following puberty, AMH concentrations had continuing high intraindividual variations. Cyclical changes and fluctuations in AMH in blood of humans and cattle during menstrual and estrous cycles [23, 25, 51–59] create concern AMH variation could cross cut-off lines and impact clinical application of the hormone resulting in recategorizing an individual depending on when samples were collected [57–59]. With

90% of EL in this study being miscategorized depending on the sample day, chances of crossing cutoffs should be a calculated comparison in future studies to provide more insight into clinically relevant fluctuations than CVs. While using averages for results of assays to detect trends and commonalities remains valuable, individual EL AMH concentrations obtained during their estrous cycles highlight that generalized curves may fail to depict these true clinical values (Figures 4-6). Additionally, AMH concentration of EL in this study failed to follow patterns considered cyclical or responsive to the growth of follicular pools or antagonism from estradiol. Instead, AMH concentration ranges appears to be random noise for each individual. There may be no "best" day to collect samples, as the natural changes are inconsistent and seem unrelated to expected AMH fluctuations based on follicular growth and other studies [23, 25]. Hypothetically, improvements in assays and automation may yield cleaner results, implying that current concentrations are different from the true intraindividual or intracycle variation, as has been demonstrated with the automated human kits to assay AMH [30].

4.4.3. AMH response to controlled ovarian stimulation hormones

Expected declines in AMH concentrations during COS are attributed to small antral follicles being stimulated to grow into larger, less productive follicles [60, 61]. Most studies, across species and protocols, have reported a gradual decline of AMH after the initiation of COS and until the induction of ovulation [61–64]. Response to COS was examined in both cohorts of ewes, with surprisingly incongruent results. Average AMH concentrations were higher for EL than ME, with the exception of baseline samples. There was a gradual decline of AMH concentrations in ME until ovulation induction, as expected. Values for EL, on the other hand, increased after CIDR insertion and initial FSH

injections, with declines toward AI and ET. This pattern resembles the "hyperresponsive" profile of a polycystic ovary syndrome response in humans [65], which could exemplify the greater variation sometimes seen in samples from younger women [51–56], Or could be a normal physiologic process in sheep which have been selected for centuries to produce more than one lamb.

4.4.4. Testing method and quality may alter results

In the current study, intra- and inter-assay variability indicated some individual variations could have a technical origin. Testing challenges are common for measurement of AMH concentrations in humans. Ovine testing varies from studies using human kits validated for use in sheep [13, 34, 35, 42, 66], to the use of ovine-specific assays [1, 25], or modification of those ovine assays to increase sensitivity [33]. Discrepancies in published average and range values, and even units of measurement across these studies, reflects the lack of an international standard for ovine AMH measurement. Despite decades of research and extensive development and external reviews of AMH test kits, the human reproductive health industry continues to report high method and site testing biases [67, 68], which should be regarded as a cause for concern for the less-investigated sheep methods [27, 39, 69–71]. The World Health Organization (WHO) recently developed a universal standard for human AMH in order to improve agreement of kit assays and diagnostic laboratories [26, 32]. During the WHO validation process, assay results for the standard ranged from 282 ng/amp to 1157 ng/amp across 16 methods after 5 methods were excluded for lack of linearity [26, 32].

Although high inter-assay CVs is not directly related to the discussed method bias, the lack of standardization and agreement of assays may limit troubleshooting and efforts

to improve detection of AMH. Direct factors that could impact testing should also be considered. While sample handling may have caused inconsistencies in AMH concentrations in the past [72], newer kit designs have greater consistency regardless of refrigeration intervals or freeze-thaw cycles [68, 73, 74]. This enhancement may be due to newer assays use of multiple antibodies to bind epitopes of different isoforms of circulating AMH [71, 75, 76], consequently recognizing cleavage-products and active variants similarly. Inter- and intra-assay CV values for Ansh Labs' kits have been acceptable in other studies (< 8.3%) [1, 33, 77]. However, samples have not been assayed for AMH in duplicate in all sheep studies [33, 47], others have not reported CVs [47], or did not use the Ansh Labs kit [13, 35]. Based on low CVs of duplicate standards and high r^2 of the standard curves, plating and reagent errors could have contributed but are less likely to be responsible for the variation in this study than interfering sample components. Continued improvements in AMH assays may yield more reliable results to detect true variations in concentrations of AMH for an intraindividual or intracycle basis as demonstrated by the automated human kits for AMH assay [30].

4.5. Conclusion

Values for AMH concentrations were identified in each experimental group that would provide a reasonable selection tool for improved ovarian responsiveness in ewes. However, based on variations in test results, testing errors, maturation rates, and natural intraindividual fluctuations during the estrous cycle, serum AMH concentrations reported here are unlikely to translate to future studies or real-world use. Prepubertal lambs and ME from sale barns are the most critical populations to assess for reproductive potential, as these are decision points for flock management, and testing did not show promise within

either group. Applying new universal human standards to assays for ovine AMH may standardize results across labs and testing methods to improve understanding of AMH and its utility in assessing reproductive performance. Regarding the applicability of using AMH as a screening test in prepubertal or even mature ewes, the need remains to understand the relationship between AMH values and ewe reproductive performance before the results are of real value to producers.

4.6. Endnotes

[1] Representative values were selected from studies in women related to a published range [12] to provide context for the discussed changes in AMH concentrations in ewes. Due to the variation in AMH concentrations across studies, and species of interest, values chosen were not comprehensive.

[2]Calculated based on inflation rate since 2011 and currency conversion from British Pounds to US Dollars.

4.7. References

1. Acharya M, Burke JM, Ashworth AJ, Rorie RW. Relationship of Anti-Mullerian Hormone to Reproductive Traits in Katahdin Ewes Bred in Late Spring or Fall. *ARSci* 2020; **08**:48–56.

2. Hansen KR, Hodnett GM, Knowlton N, Craig LB. Correlation of ovarian reserve tests with histologically determined primordial follicle number. *Fertil Steril* 2011; **95**:170–175.

3. Rico C, Fabre S, Médigue C, Di Clemente N, Clément F, Bontoux M, Touzé J-L, Dupont M, Briant E, Rémy B, Beckers J-F, Monniaux D. Anti-mullerian hormone is an endocrine marker of ovarian gonadotropin-responsive follicles and can help to predict superovulatory responses in the cow. *Biol Reprod* 2009; **80**:50–59.

4. Nelson SM, Iliodromiti S, Fleming R, Anderson R, McConnachie A, Messow C-M. Reference range for the antimüllerian hormone Generation II assay: a population study of 10,984 women, with comparison to the established Diagnostics Systems Laboratory nomogram. *Fertil Steril* 2014; **101**:523–529.

5. Rico C, Drouilhet L, Salvetti P, Dalbiès-Tran R, Jarrier P, Touzé J-L, Pillet E, Ponsart C, Fabre S, Monniaux D. Determination of anti-Müllerian hormone concentrations in blood as a tool to select Holstein donor cows for embryo production: from the laboratory to the farm. *Reprod Fertil Dev* 2012; **24**:932–944.

6. Jaques JT, Cardoso RC, Chachere J, Sinha S, Seery R, Wilkes AA, Forrest D, Looney CR. Using Anti-Müllerian Hormone (AMH) as a Predictor of Ova Production for Bovine Embryo Transfer. *ARSci* 2020; **08**:36–47.

7. La Marca A, Leo V de, Giulini S, Orvieto R, Malmusi S, Giannella L, Volpe A. Anti-Mullerian hormone in premenopausal women and after spontaneous or surgically induced menopause. *J Soc Gynecol Investig* 2005; **12**:545–548.

8. La Marca A, Sighinolfi G, Papaleo E, Cagnacci A, Volpe A, Faddy MJ. Prediction of age at menopause from assessment of ovarian reserve may be improved by using body mass index and smoking status. *PLoS ONE* 2013; **8**:1-7.

9. Alward KJ, Bohlen JF. Overview of Anti-Müllerian hormone (AMH) and association with fertility in female cattle. *Reprod Domest Anim* 2020; **55**:3–10.

10. Daly J, Smith H, McGrice HA, Kind KL, van Wettere WHEJ. Towards Improving the Outcomes of Assisted Reproductive Technologies of Cattle and Sheep, with Particular Focus on Recipient Management. *Animals (Basel)* 2020; **10**:1–15.

11. Christou G, Dimitriadis I, Hsu JY, James K, Bormann CL, Souter I. Can anti-müllerian hormone (AMH) predict the outcome of gonadotropin induction/ intrauterine insemination (GN/IUI) cycles among infertile women? *Fertil Steril* 2018; **110**:e328.

12. Kelsey TW, Wright P, Nelson SM, Anderson RA, Wallace WHB. A validated model of serum anti-müllerian hormone from conception to menopause. *PLoS ONE* 2011; **6**:e22024.

13. Torres-Rovira L, Gonzalez-Bulnes A, Succu S, Spezzigu A, Manca ME, Leoni GG, Sanna M, Pirino S, Gallus M, Naitana S, Berlinguer F. Predictive value of antral follicle count and anti-Müllerian hormone for follicle and oocyte developmental competence during the early prepubertal period in a sheep model. *Reprod Fertil Dev* 2014; **26**:1094–1106.

14. Kallio S, Puurunen J, Ruokonen A, Vaskivuo T, Piltonen T, Tapanainen JS. Antimüllerian hormone levels decrease in women using combined contraception independently of administration route. *Fertil Steril* 2013; **99**:1305–1310.

15. Köninger A, Kauth A, Schmidt B, Schmidt M, Yerlikaya G, Kasimir-Bauer S, Kimmig R, Birdir C. Anti-Mullerian-hormone levels during pregnancy and postpartum. *Reprod Biol Endocrinol* 2013; **11**:1–9.

16. Place NJ, Hansen BS, Cheraskin J-L, Cudney SE, Flanders JA, Newmark AD, Barry B, Scarlett JM. Measurement of serum anti-Müllerian hormone concentration in female dogs and cats before and after ovariohysterectomy. *J Vet Diagn Invest* 2011; **23**:524–527.

17. Axnér E, Ström Holst B. Concentrations of anti-Müllerian hormone in the domestic cat. Relation with spay or neuter status and serum estradiol. *Theriogenology* 2015; **83**:817–821.

18. Caglar GS, Kahyaoglu I, Pabuccu R, Demirtas S, Seker R. Anti-Mullerian hormone and insulin resistance in classic phenotype lean PCOS. *Arch Gynecol Obstet* 2013; **288**:905–910.

19. Kedem A, Yung Y, Yerushalmi GM, Haas J, Maman E, Hanochi M, Hemi R, Orvieto R, Dor J, Hourvitz A. Anti Müllerian Hormone (AMH) level and expression in mural and cumulus cells in relation to age. *J Ovarian Res* 2014; **7**:113–118.

20. Grigoletto L, Santana MHA, Bressan FF, Eler JP, Nogueira MFG, Kadarmideen HN, Baruselli PS, Ferraz JBS, Brito LF. Genetic Parameters and Genome-Wide Association Studies for Anti-Müllerian Hormone Levels and Antral Follicle Populations Measured After Estrus Synchronization in Nellore Cattle. *Animals (Basel)* 2020; **10**:1185–1200.

21. Mossa F, Ireland JJ. Physiology and endocrinology symposium: Anti-Müllerian hormone: a biomarker for the ovarian reserve, ovarian function, and fertility in dairy cows. *J Anim Sci* 2019; **97**:1446–1455.

22. Fushimi Y, Monniaux D, Takagi M. Efficacy of a single measurement of plasma anti-Müllerian hormone concentration for ovum pick-up donor selection of Japanese Black heifers in herd breeding programs. *J Reprod Dev* 2019; **65**:369–374.

23. Hehenkamp WJK, Looman CWN, Themmen APN, Jong FH de, te Velde ER, Broekmans FJM. Anti-Müllerian hormone levels in the spontaneous menstrual cycle do not show substantial fluctuation. *J Clin Endocrinol Metab* 2006; **91**:4057–4063.

24. Hadlow N, Brown SJ, Habib A, Wardrop R, Joseph J, Gillett M, Maguire R, Conradie J. Quantifying the intraindividual variation of antimüllerian hormone in the ovarian cycle. *Fertil Steril* 2016; **106**:1230–1237.

25. Waheeb RS. Changes in Serum Levels of Anti-Mullerian Hormone and Ovarian Steroids in Barki Sheep during Follicular and Early Luteal Phase of Estrous Cycle. *Pak Vet J* 2017; **37**:421-426.

26. Ferguson J, Hockley J, Rigsby P, Burns C. Establishment of a WHO Reference Reagent for anti-Mullerian hormone. *Reprod Biol Endocrinol* 2020; **18**:86–96.

27. Magnusson Å, Oleröd G, Thurin-Kjellberg A, Bergh C. The correlation between AMH assays differs depending on actual AMH levels. *Hum Reprod* 2017:1-5.

28. Clark CA, Laskin CA, Cadesky K. Anti-Mullerian hormone: reality check. *Hum Reprod* 2014; **29**:184–185.

29. Fréour T, Mirallié S, Bach-Ngohou K, Denis M, Barrière P, Masson D. Measurement of serum anti-Müllerian hormone by Beckman Coulter ELISA and DSL ELISA: comparison and relevance in assisted reproduction technology (ART). *Clin Chim Acta* 2007; **375**:162–164.

30. Melado L, Lawrenz B, Sibal J, Abu E, Coughlan C, Navarro AT, Fatemi HM. Anti-müllerian Hormone During Natural Cycle Presents Significant Intra and Intercycle Variations When Measured With Fully Automated Assay. *Front Endocrinol* 2018; **9**:1–8.

31. Nelson SM, Pastuszek E, Kloss G, Malinowska I, Liss J, Lukaszuk A, Plociennik L, Lukaszuk K. Two new automated, compared with two enzyme-linked immunosorbent, antimüllerian hormone assays. *Fertil Steril* 2015; **104**:1016-1021.

32. Ferguson JM, Pépin D, Duru C, Matejtschuk P, Donahoe PK, Burns CJ. Towards international standardization of immunoassays for Müllerian inhibiting substance / anti-Müllerian hormone. *Reprod Biomed Online* 2018; **37**:631–640.

33. Pinto PHN, Balaro MFA, Souza-Fabjan JMG, Ribeiro LdS, Bragança GM, Leite CR, Arashiro EKN, Silva KdM, Da Fonseca JF, Brandão FZ. Anti-Müllerian hormone and antral follicle count are more effective for selecting ewes with good potential for in vivo embryo production than the presence of FecGE mutation or eCG pre-selection tests. *Theriogenology* 2018; **113**:146–152.

34. Lahoz BC, Alabart JL, Cocero MJ, Monniaux D, Echegoyen E, Sánchez P, Folch J. Anti-Müllerian hormone concentration in sheep and its dependence of age and independence of BMP15 genotype: An endocrine predictor to select the best donors for embryo biotechnologies. *Theriogenology* 2014; **81**:347–357.

35. McGrice H, Kelly JM, Kleemann DO, Kind KL, Hampton AJ, Hannemann P, Walker SK, van Wettere WHEJ. Plasma anti-Müllerian hormone concentration as a predictive endocrine marker for selection of donor lambs to improve success in juvenile in vitro embryo transfer programs. *Reprod Fertil Dev* 2020; **32**:383–391.

36. Souza AH, Carvalho PD, Rozner AE, Vieira LM, Hackbart KS, Bender RW, Dresch AR, Verstegen JP, Shaver RD, Wiltbank MC. Relationship between circulating anti-Müllerian hormone (AMH) and superovulatory response of high-producing dairy cows. *J Dairy Sci* 2015; **98**:169–178.

37. Ribeiro ES, Bisinotto RS, Lima FS, Greco LF, Morrison A, Kumar A, Thatcher WW, Santos JEP. Plasma anti-Müllerian hormone in adult dairy cows and associations with fertility. *J Dairy Sci* 2014; **97**:6888–6900.

38. Guzman L, Ortega-Hrepich C, Polyzos NP, Anckaert E, Verheyen G, Coucke W, Devroey P, Tournaye H, Smitz J, De Vos M. A prediction model to select PCOS patients suitable for IVM treatment based on anti-Mullerian hormone and antral follicle count. *Hum Reprod* 2013; **28**:1261–1266.

39. Yates AP, Jopling HM, Burgoyne NJ, Hayden K, Chaloner CM, Tetlow L. Paediatric reference intervals for plasma anti-Müllerian hormone: comparison of data from the Roche Elecsys assay and the Beckman Coulter Access assay using the same cohort of samples. *Ann Clin Biochem* 2019; **56**:536–547.

40. La Marca A, Sunkara SK. Individualization of controlled ovarian stimulation in IVF using ovarian reserve markers: from theory to practice. *Hum Reprod Update* 2014; **20**:124–140.

41. Yates AP, Rustamov O, Roberts SA, Lim HYN, Pemberton PW, Smith A, Nardo LG. Anti-Mullerian hormone-tailored stimulation protocols improve outcomes whilst reducing adverse effects and costs of IVF. *Hum Reprod* 2011; **26**:2353–2362.

42. Lahoz BC, Alabart JL, Monniaux D, Mermillod P, Folch J. Anti-Müllerian hormone plasma concentration in prepubertal ewe lambs as a predictor of their fertility at a young age. *BMC Vet Res* 2012; **8**.

43. Umer S, Zhao SJ, Sammad A, Sahlu BW, Yunwei P, Zhu H. AMH: Could It Be Used as A Biomarker for Fertility and Superovulation in Domestic Animals? *Genes* 2019; **10**.

44. Shipley CF, Buckrell BC, Mylne MJ, Pollard J, Hunton JR. Artificial Insemination and Embryo Transfer in Sheep. In: Youngquist RS, Threlfall WR (eds.), *Current therapy in large animal theriogenology*, 2nd ed. St. Louis: Saunders Elsevier; 2007:629–641.

45. Cognié Y, Baril G, Poulin N, Mermillod P. Current status of embryo technologies in sheep and goat. *Theriogenology* 2003; **59**:171–188.

46. Racowsky C, Vernon M, Mayer J, Ball GD, Behr B, Pomeroy KO, Wininger D, Gibbons W, Conaghan J, Stern JE. Standardization of grading embryo morphology. *J Assist Reprod Genet* 2010; **27**:437–439.

47. Smartt JA. Anti-mullerian hormone: potential association with fertility in ewes. San Angelo: Angelo State University; 2015. Masters Thesis.

48. Camacho LE, Lemley CO, Dorsam ST, Swanson KC, Vonnahme KA. Effects of maternal nutrient restriction followed by realimentation during early and mid-gestation

in beef cows. II. Placental development, umbilical blood flow, and uterine blood flow responses to diet alterations. *Theriogenology* 2018; **116**:1–11.

49. Lahoz BC, Alabart JL, Folch Pera J. Relación de la hormona Anti-Mülleriana (AMH) y la respuesta ovulatoria en corderas de tres meses con su eficiencia reproductiva en la edad adulta. [Relationship between Anti-Müllerian hormone (AMH) and the ovulatory response measured in three-month old ewe lambs with their reproductive efficiency in adulthood]. *Inf Tec Econ Agrar* 2016; **112**.

50. Torres-Rovira L, Succu S, Pasciu V, Manca ME, Gonzalez-Bulnes A, Leoni GG, Pennino MG, Spezzigu A, Gallus M, Dattena M, Monniaux D, Naitana S, et al. Postnatal pituitary and follicular activation: a revisited hypothesis in a sheep model. *Reprod Suppl* 2016; **151**:215–225.

51. La Marca A, Malmusi S, Giulini S, Tamaro LF, Orvieto R, Levratti P, Volpe A. Anti-Müllerian hormone plasma levels in spontaneous menstrual cycle and during treatment with FSH to induce ovulation. *Hum Reprod* 2004; **19**:2738–2741.

52. La Marca A, Stabile G, Artenisio AC, Volpe A. Serum anti-Mullerian hormone throughout the human menstrual cycle. *Hum Reprod* 2006; **21**:3103–3107.

53. Cook CL, Siow Y, Taylor S, Fallat ME. Serum müllerian-inhibiting substance levels during normal menstrual cycles. *Fertil Steril* 2000; **73**:859–861.

54. Tsepelidis S, Devreker F, Demeestere I, Flahaut A, Gervy C, Englert Y. Stable serum levels of anti-Müllerian hormone during the menstrual cycle: a prospective study in normo-ovulatory women. *Hum Reprod* 2007; **22**:1837–1840.

55. Sowers M, McConnell D, Gast K, Zheng H, Nan B, McCarthy JD, Randolph JF. Anti-Müllerian hormone and inhibin B variability during normal menstrual cycles. *Fertil Steril* 2010; **94**:1482–1486.

56. Overbeek A, Broekmans FJM, Hehenkamp WJ, Wijdeveld ME, van Disseldorp J, van Dulmen-den Broeder E, Lambalk CB. Intra-cycle fluctuations of anti-Müllerian hormone in normal women with a regular cycle: a re-analysis. *Reprod Biomed Online* 2012; **24**:664–669.

57. Wunder DM, Bersinger NA, Yared M, Kretschmer R, Birkhäuser MH. Statistically significant changes of antimüllerian hormone and inhibin levels during the physiologic menstrual cycle in reproductive age women. *Fertil Steril* 2008; **89**:927–933.

58. Robertson DM, Hale GE, Fraser IS, Hughes CL, Burger HG. Changes in serum antimüllerian hormone levels across the ovulatory menstrual cycle in late reproductive age. *Menopause* 2011; **18**:521–524.

59. Kissell KA, Danaher MR, Schisterman EF, Wactawski-Wende J, Ahrens KA, Schliep KC, Perkins NJ, Sjaarda LA, Weck J, Mumford SL. Biological variability in serum anti-Müllerian hormone throughout the menstrual cycle in ovulatory and sporadic anovulatory cycles in eumenorrheic women. *Hum Reprod* 2014; **29**:1764–1772.

60. Böttcher B, Tsybulyak I, Grubinger T, Wildt L, Seeber B. Dynamics of anti-Müllerian hormone during controlled ovarian stimulation. *Gynecol Endocrinol* 2014; **30**:121–125.

61. Lee JR, Kim SH, Kim SM, Jee BC, Ku S-Y, Suh CS, Choi YM, Kim JG, Moon SY. Anti-Mullerian hormone dynamics during controlled ovarian hyperstimulation and optimal timing of measurement for outcome prediction. *Hum Reprod* 2010; **25**:2597–2604.

62. Eldar-Geva T, Margalioth EJ, Gal M, Ben-Chetrit A, Algur N, Zylber-Haran E, Brooks B, Huerta M, Spitz IM. Serum anti-Mullerian hormone levels during controlled ovarian hyperstimulation in women with polycystic ovaries with and without hyperandrogenism. *Hum Reprod* 2005; **20**:1814–1819.

63. Patrelli TS, Gizzo S, Sianesi N, Levati L, Pezzuto A, Ferrari B, Bacchi Modena A. Anti-Müllerian hormone serum values and ovarian reserve: can it predict a decrease in fertility after ovarian stimulation by ART cycles? *PLoS ONE* 2012; **7**:e44571.

64. Fanchin R, Taieb J, Lozano DHM, Ducot B, Frydman R, Bouyer J. High reproducibility of serum anti-Mullerian hormone measurements suggests a multi-staged follicular secretion and strengthens its role in the assessment of ovarian follicular status. *Hum Reprod* 2005; **20**:923–927.

65. Weintraub A, Margalioth EJ, Chetrit AB, Gal M, Goldberg D, Alerhand S, Eldar-Geva T. The dynamics of serum anti-Mullerian-hormone levels during controlled ovarian hyperstimulation with GnRH-antagonist short protocol in polycystic ovary syndrome and low responders. *Eur J Obstet Gyn R B* 2014; **176**:163–167.

66. Book of abstracts. Book of abstracts. 18th International Congress on Animal Reproduction (ICAR), June 26-30, Tours (France); 2016.

67. Khader A, Lloyd SM, McConnachie A, Fleming R, Grisendi V, La Marca A, Nelson SM. External validation of anti-Müllerian hormone based prediction of live birth in assisted conception. *J Ovarian Res* 2013; **6**:3.

68. Zuvela E, Walls M, Matson P. Within-laboratory and between-laboratory variability in the measurement of anti-müllerian hormone determined within an external quality assurance scheme. *Reprod Biol* 2013; **13**:255–257.

69. Iliodromiti S, Salje B, Dewailly D, Fairburn C, Fanchin R, Fleming R, Li HWR, Lukaszuk K, Ng EHY, Pigny P, Tadros T, van Helden J, et al. Non-equivalence of anti-

Müllerian hormone automated assays-clinical implications for use as a companion diagnostic for individualised gonadotrophin dosing. *Hum Reprod* 2017; **32**:1710–1715.

70. Bonifacio M, Bradley CK, Karia S, Livingstone M, Bowman MC, McArthur SJ. The original Beckman Coulter Generation II assay significantly underestimates AMH levels compared with the revised protocol. *J Assist Reprod Genet* 2015; **32**:1691–1696.

71. Bungum L, Tagevi J, Jokubkiene L, Bungum M, Giwercman A, Macklon N, Andersen CY, Klausen TW, Tørring N, Kumar A, Skouby SO. The Impact of the Biological Variability or Assay Performance on AMH Measurements: A Prospective Cohort Study With AMH Tested on Three Analytical Assay-Platforms. *Front Endocrinol* 2018; **9**:603.

72. Rustamov O, Smith A, Roberts SA, Yates AP, Fitzgerald C, Krishnan M, Nardo LG, Pemberton PW. The measurement of anti-Müllerian hormone: a critical appraisal. *J Clin Endocrinol Metab* 2014; **99**:723–732.

73. Kumar A, Kalra B, Patel A, McDavid L, Roudebush WE. Development of a second generation anti-Müllerian hormone (AMH) ELISA. *J Immunol Methods* 2010; **362**:51–59.

74. Fleming R, Fairbairn C, Blaney C, Lucas D, Gaudoin M. Stability of AMH measurement in blood and avoidance of proteolytic changes. *Reprod Biomed Online* 2013; **26**:130–132.

75. Mamsen LS, Petersen TS, Jeppesen JV, Møllgård K, Grøndahl ML, Larsen A, Ernst E, Oxvig C, Kumar A, Kalra B, Andersen CY. Proteolytic processing of anti-Müllerian hormone differs between human fetal testes and adult ovaries. *Mol Hum Reprod* 2015; **21**:571–582.

76. McLennan IS, Pankhurst MW. Methodological considerations in measuring different AMH cleavage forms using ELISA: validity of proAMH ELISA. *Mol Hum Reprod* 2016; **22**:373.

77. Lahoz BC, Alabart JL, Cocero MJ, Monniaux D, Fabre S, Folch J. Elección de las mejores ovejas donantes de embriones mediante la determinación plasmática de su AMH (hormona anti-mülleriana). [The use of plasma anti-müllerian hormone in sheep as an endocrine marker of the ovarian response to follicle-stimulating hormone in multipleovulation embryo transfer programs]. *Reprod Fertil Dev* 2015; **27**:264.

5. CONCLUSION

5.1. Broad perspectives

These experiments highlighted the importance of broad perspectives and avoiding myopia in valuable research. The assessment of anti-Müllerian hormone (AMH), for instance, holds so much promise for livestock producers and human fertility experts, that successful projects which confirm the desired goals overshadow those which advise caution. For both fetal growth restriction (FGR) and AMH, there are broad ranges of research results so contradictory that none should be viewed in isolation. Real world examples of this might be: rejecting a client for a fertility procedure due to low AMH, without knowing to inquire if she was on hormonal contraceptives, or interpreting FGR study results for an obese subject in a similar manner to a slighter framed female, because the experimental treatments were the same. In these instances, there is little benefit to limiting physiological complexities to singular cause and effect outcomes.

The AMH literature is saturated with arguments for and against intracycle variation significance, including impassioned letters to the editor [1] and challenges to manuscript authors [2–4]. Additionally, review articles and assay critiques [5–8] pick apart the current state of AMH research. Meanwhile, singular studies on 50 cows report affirmative outcomes with little mention of a controversy [9], or repeat the claim that AMH is highly repeatable despite other evidence [10, 11]. It is likely that the high degree of interindividual difference in AMH concentrations has a strong relationship with ovarian yields and fertility, although clear and consistent results may not be realized until newer assays are validated for use in sheep. However, clinical interpretations of AMH should always be based on an understanding of factors that might impact a clients' test results.

Uterine or ovarian pathology, pregnancy, heredity, hormonal contraception, and even phases of an estrous cycle can impact AMH and cause concentrations to be inconsistent with the clinically intended assessment of fertility or COS response.

For FGR, it was important to look beyond the results from a portion of agreeable studies. Rather than determining that NR doesn't cause placental pathology, researchers conceptualized how extreme within-model fetal variation could relate back to the diet. Reductions in blood flow, placental mass, oxygen, or glucose may not occur to an appreciable level in every study but noticing when their appropriate or deficient levels relate back to the study outcome may provide new insights. In other words, recognizing when results aren't repeatable, or publications differ, is when the simple concepts of input and output erode, and the understanding of intricate pathophysiology begins.

The introduced placentomectomy technique is an ideal tool to deepen understanding of FGR beyond endpoints. Results have already identified decreased placentome volume and feto-maternal exchange area, as well as altered expression of amino acid transporters in a nutrient restriction model [12], and would be expected to provide evidence of reduced angiogenesis if treatment conditions created an insufficiency. In theory, consistent measurement of fetal glucose and oxygen levels, and placentomectomy samples could help define many of the physiological changes that cause FGR, and specifically what level of deprivation that creates for the fetus. Unfortunately, they are all slightly invasive interventions since post-partum fetal oxygen levels could be impacted by parturition. Standardization for fetal weight categories, and other fetal measures to assess could also enhance the learning objectives of the diverse groups involved in the field.

Enthusiasm and eagerness to find answers with new tools may inadvertently bypass the learning necessary to interpret them. Sharp et al. also cautioned against the maternal bias that appears ubiquitous in the field, with a resultant self-actualizing array of dam-specific studies [13]. This is a sound critique of the FGR literature, as results are typically assessed from the perspective of the intended input variables, and better efforts should be made to assess for contributions from lesser factors as well.

5.2. References

1. Clark CA, Laskin CA, Cadesky K. Anti-Mullerian hormone: reality check. *Hum Reprod* 2014; **29**:184–185.

2. McLennan IS, Pankhurst MW. Methodological considerations in measuring different AMH cleavage forms using ELISA: validity of proAMH ELISA. *Mol Hum Reprod* 2016; **22**:373.

3. van den Berg MH, Overbeek A, van Dulmen-den Broeder E, Lambalk CB. Comment on: Li HW, Wong CY, Yeung WS, Ho PC, Ng EH. Serum anti-Mullerian hormone level is not altered in women using hormonal contraceptives. Contraception 2011;83:582-5. *Contraception* 2012; **85**:519-20; author reply 520-1.

4. Roberts SA. Variability in anti-Müllerian hormone levels: a comment on Sowers et al., Anti-Müllerian hormone and inhibin B variability during normal menstrual cycles. *Fertil Steril* 2010; **94**:e59.

5. Yates AP, Jopling HM, Burgoyne NJ, Hayden K, Chaloner CM, Tetlow L. Paediatric reference intervals for plasma anti-Müllerian hormone: comparison of data from the Roche Elecsys assay and the Beckman Coulter Access assay using the same cohort of samples. *Ann Clin Biochem* 2019; **56**:536–547.

6. Iliodromiti S, Salje B, Dewailly D, Fairburn C, Fanchin R, Fleming R, Li HWR, Lukaszuk K, Ng EHY, Pigny P, Tadros T, van Helden J, et al. Non-equivalence of anti-Müllerian hormone automated assays-clinical implications for use as a companion diagnostic for individualised gonadotrophin dosing. *Hum Reprod* 2017; **32**:1710–1715.

7. Kat AC de, Broekmans FJM, van Westing AC, Lentjes E, Verschuren WMM, van der Schouw YT. A quantitative comparison of anti-Müllerian hormone measurement and its shifting boundaries between two assays. *Maturitas* 2017; **101**:12–16.

8. Pir Yagci I, Pekcan M, Polat IM, Kalender H, Macun HC. Does serum anti-Müllerian hormone levels always discriminate presence of the ovaries in adult bitches? Comparison of two ELISA kits. *Reprod Domest Anim* 2016; **51**:910–915.

9. Fushimi Y, Monniaux D, Takagi M. Efficacy of a single measurement of plasma anti-Müllerian hormone concentration for ovum pick-up donor selection of Japanese Black heifers in herd breeding programs. *J Reprod Dev* 2019; **65**:369–374.

10. Mossa F, Ireland JJ. Physiology and endocrinology symposium: Anti-Müllerian hormone: a biomarker for the ovarian reserve, ovarian function, and fertility in dairy cows. *J Anim Sci* 2019; **97**:1446–1455.

11. Tal R, Seifer DB. Ovarian reserve testing: a user's guide. *Am J Obstet Gynecol* 2017; **217**:129–140.

12. Edwards AK, McKnight SM, Askelson K, McKnight JR, Dunlap KA, Satterfield MC. Adaptive responses to maternal nutrient restriction alter placental transport in ewes. *Placenta* 2020; **96**:1–9.

13. Sharp GC, Lawlor DA, Richardson SS. It's the mother!: How assumptions about the causal primacy of maternal effects influence research on the developmental origins of health and disease. *Soc Sci Med* 2018; **213**:20–27.